Synthesis and properties of photo-crosslinked mixed-macromer networks

Erwin Zant

Synthesis and properties of photo-crosslinked mixed-macromer networks

Erwin Zant

The research described in this thesis was carried out between 2010 and 2014 in the research group Biomaterials Science and Technology at the Institute for Biomedical Technology and Technical Medicine (MIRA), University of Twente, Enschede, The Netherlands. The research was financially supported by the Netherlands Institute of Regenerative Medicine (NIRM, grant No. FES0908).

The printing of this thesis was sponsored by:

NBTE Netherlands society for Biomaterials and Tissue Engineering & PolyVation INITIATE • INNOVATE • CREATE

Synthesis and properties of photo-crosslinked mixed-macromer networks

Erwin Zant

PhD Thesis, with references and summaries in English and Dutch

University of Twente, Enschede, The Netherlands

December 2015

Printed by Gildeprint, Enschede, The Netherlands

SYNTHESIS AND PROPERTIES OF PHOTO-CROSSLINKED MIXED-MACROMER NETWORKS

PROEFSCHRIFT

ter verkrijging van
de graad van doctor aan de Universiteit Twente,
op gezag van de rector magnificus,
prof. H. Brinksma,
volgens besluit van het College voor Promoties
in het openbaar te verdedigen
op donderdag 17 december 2015 om 16:45 uur

door

Erwin Zant

geboren op 19 oktober 1983

te Nijmegen

Dit proefschrift is goedgekeurd door de promotor:

prof. dr. D.W. Grijpma

ISBN: 978-90-365-4020-9

Samenstelling promotiecommissie:

Voorzitter:	prof. dr. ir. J.W.M. Hilgenkamp
Promotor:	prof. dr. D.W. Grijpma
Leden:	prof. dr. J.F.J. Engbersen, Universiteit Twente
	prof. dr. Ir. P. Jonkheijm, Universiteit Twente
	prof. dr. J. de Boer, Universiteit Maastricht
	prof. dr. Ir. W.E. Hennink, Universiteit Utrecht
	prof. dr. L. Koole, Universiteit Maastricht

Table of contents

Chapter 1 - General introduction

General introduction to this thesis

Combinatorial chemistry can play an important role in the development of novel polymer biomaterials. A pioneering study in 1997 by Kohn and coworkers described the simultaneous synthesis of 112 different materials. Conducting multiple polycondensation reactions in parallel yielded an array of very many materials with distinct chemical and physical properties [1]. Later, the synthesis of much larger combinatorial libraries was made possible by the introduction of microarrays and high throughput analyses. Microarrays were fabricated by automated deposition of di-acrylate-functional monomers and subsequent photo-crosslinking [2]. This allowed the parallel synthesis of several hundreds of (co)polymer networks with different compositions. High throughput characterization of the prepared materials allowed researchers to find correlations between their physical properties and cell-response [3-6]. These synthetic polymeric biomaterials showed interesting biological properties, data on mechanical characteristics and biodegradability were not reported.

Combinatorial studies on biodegradable polymer blends were conducted at the National Institute of Standards and Technology (NIST). One of the first publications involved the preparation of films of a polymer blend with a gradient in poly(ε-caprolactone) (PCL) and poly(D,L-lactide) (PDLLA) composition [7]. Also, a platform to prepare combinatorial three dimensional scaffolds was developed [8]. These studies involved the selection of two polymers at a time, and combinatorial blends prepared from multiple synthetic biodegradable polymers have not been reported.

Using biodegradable macromers (oligomers functionalized with radically polymerizable end-groups) and subsequent photo-crosslinking them can also be employed in the development of new synthetic biomaterials. The combinatorial synthesis of networks based on macromers with widely differing properties may lead to the identification of new polymer biomaterials with unexpected properties.

Aim and outline of this thesis

The aim of this thesis is to develop new materials based on photo-crosslinking combinations of macromers. More specifically, mixed-macromer networks based on dimethacrylate functionalized poly(trimethylene carbonate) (PTMC-dMA), poly(D,L-lactide) (PDLLA-dMA), poly(ε-caprolactone) (PCL-dMA) and poly(ethylene glycol) (PEG-dMA) (see Figure 1) are assessed for their potential application as biomaterials in regenerative medicine.

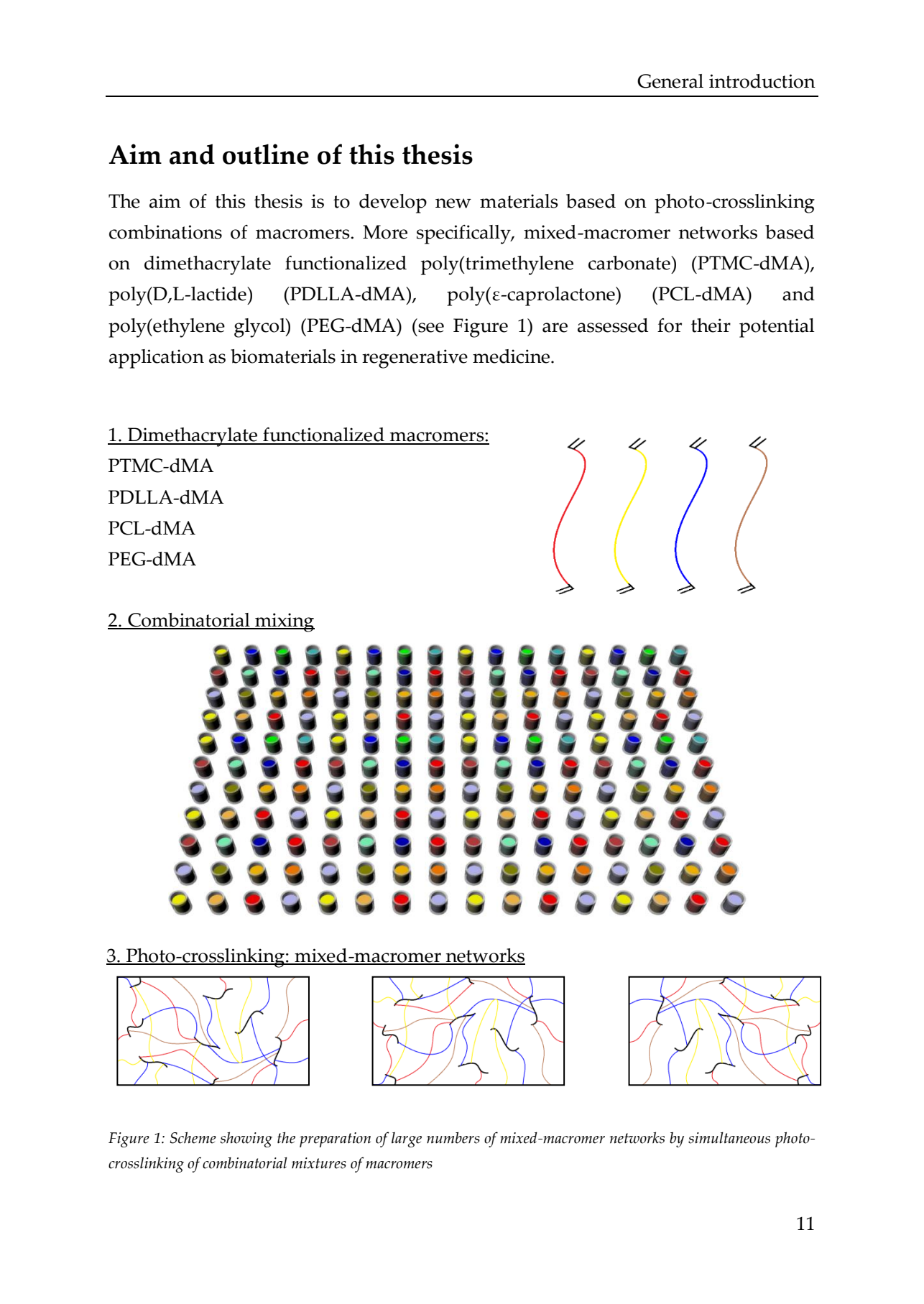

Figure 1: Scheme showing the preparation of large numbers of mixed-macromer networks by simultaneous photo-crosslinking of combinatorial mixtures of macromers

Chapter 2: An introduction on physical and chemical properties of synthetic polymers for tissue engineering is given. The principles of combinatorial chemistry and high throughput analysis are described. Some of the pioneering studies on combinatorial chemistry are highlighted and their influence on the development of new polymeric biomaterials is shown [9].

Chapter 3: Mixed-macromer networks are prepared from PTMC-dMA, PDLLA-dMA, PCL-dMA and PEG-dMA and their ability to allow the adhesion of C2C12 cells is investigated. Thermal- and mechanical characteristics of the single-macromer networks are also determined [10].

Chapter 4: Polymer networks with extraordinary high toughnesses can be prepared by crosslinking in solution. Mixed-macromer networks are prepared by mixing different macromers and crosslinking them in solution. Materials with extraordinary mechanical properties are obtained as a result of crosslinking in solution and micro-phase separation processes. Co-macromer hydrogels with very good mechanical properties are also prepared [11].

Chapter 5: A large number (255) of different well-defined mixed-macromer networks are prepared by photo-crosslinking mixtures of macromers in solution. These are subsequently examined for their ability to allow adhesion and proliferation of human mesenchymal stem cells. As a result of crosslinking mixtures of macromers with very distinct physical characteristics, the biological performance of the networks will be highly unpredictable. Most interestingly, polymer networks that showed high values of water uptake and at the same time allowed the adhesion and proliferation of stem cells are found. These synthetic hydrogels can be of particular interest in tissue engineering [12].

Chapter 6: Crystallizing a solvent into which a polymer is dissolved and subsequently removing it, can be a powerful approach to produce porous structures. By preparing combinatorial mixtures of macromers in ethylene carbonate, crystallizing the solvent, photo-crosslinking the macromers and extracting the solvent with water, we are able to simultaneously prepare large numbers of polymeric scaffolds with a very wide range of properties [13].

Chapter 7: In Chapter 6 it is shown that PCL microparticles could be incorporated into porous structures prepared from PTMC-macromers in a straightforward method. In order to investigate potential drug delivery characteristics of these microparticle-loaded scaffolds, PCL microparticles of low molecular weight, which ensures relatively rapid degradation, are produced using a double emulsion and solvent evaporation approach. Several parameters are varied to optimize the encapsulation efficiency of vitamin B12, a hydrophilic model drug.

Appendix A: Porous polymeric structures are produced using ethylene carbonate as a solvent. The structures are produced by preparing combinatorial mixtures of macromers in ethylene carbonate, crystallizing the solvent, photo-crosslinking and subsequent washing out of the crystallized solvent. The porous structures are evaluated for their cell adhesion, proliferation and infiltration characteristics using C2C12 cells.

Appendix B: Here, EC porous structures are evaluated using a new high throughput mechanical screening technique (HTMS). The results of these mechanical analyses are compared to those found by conventional testing.

In **Appendix C** a resin of mixed-macromers is formulated for application in stereolithography, a rapid prototyping technique. The resin is based on mixed-macromers, which in **Chapter 5** were shown to yield a tough hydrogel network that allowed the adhesion and proliferation of stem cells and at the same time showed a high water uptake.

References

1. Brocchini S, James K, Tangpasuthadol V, and Kohn J, A combinatorial approach for polymer design. Journal of the American Chemical Society, 1997. 119(19): p. 4553-4554.
2. Anderson DG, Levenberg S, and Langer R, Nanoliter-scale synthesis of arrayed biomaterials and application to human embryonic stem cells. Nature Biotechnology, 2004. 22(7): p. 863-866.
3. Anderson DG, Akinc A, Hossain N, and Langer R, Structure/property studies of polymeric gene delivery using a library of poly(beta-amino esters). Molecular Therapy, 2005. 11(3): p. 426-434.

4. Mei Y, Saha K, Bogatyrev SR, Yang J, Hook AL, Kalcioglu ZI, Cho S-W, Mitalipova M, Pyzocha N, Rojas F, Van Vliet KJ, Davies MC, Alexander MR, Langer R, Jaenisch R, and Anderson DG, Combinatorial development of biomaterials for clonal growth of human pluripotent stem cells. Nat Mater, 2010. 9(9): p. 768-778.
5. Urquhart AJ, Anderson DG, Taylor M, Alexander MR, Langer R, and Davies MC, High throughput surface characterisation of a combinatorial material library. Advanced Materials, 2007. 19(18): p. 2486-2491.
6. Urquhart AJ, Taylor M, Anderson DG, Langer R, Davies MC, and Alexander MR, TOF-SIMS analysis of a 576 micropatterned copolymer array to reveal surface moieties that control wettability. Analytical Chemistry, 2008. 80(1): p. 135-142.
7. Meredith JC, Sormana JL, Keselowsky BG, Garcia AJ, Tona A, Karim A, and Amis EJ, Combinatorial characterization of cell interactions with polymer surfaces. Journal of Biomedical Materials Research Part A, 2003. 66A(3): p. 483-490.
8. Simon CG, Stephens JS, Dorsey SM, and Becker ML, Fabrication of combinatorial polymer scaffold libraries. Review of Scientific Instruments, 2007. 78(7).
9. Zant E, Bosman MJ, and Grijpma DW, Physico-chemical material properties and analysis techniques relevant in high-throughput biomaterials research, Chapter 2 in Materiomics - High throughput screening of biomaterial properties. Editors: Jan de Boer and Clemens A. van Blitterswijk. 2013, Cambridge University Press. Chapter 2 of this thesis.
10. Zant E, Bosman MJ, and Grijpma DW, Combinatorial synthesis of photo-crosslinked biodegradable networks. Journal of Applied Biomaterials & Functional Materials, 2012. 10(3): p. 197-202. Chapter 3 of this thesis.
11. Zant E and Grijpma DW, Tough biodegradable mixed-macromer networks and hydrogels by photo-crosslinking in solution. Acta Biomaterialia, resubmitted after revision. Chapter 4 of this thesis
12. Zant E and Grijpma DW, Synthetic biodegradable hydrogels with excellent mechanical properties and good cell adhesion characteristics obtained by the combinatorial synthesis of photo-crosslinked networks. Biomacromolecules, submitted. Chapter 5 of this thesis.
13. Zant E, Blokzijl MM, and Grijpma DW, A combinatorial photocrosslinking method for the preparation of porous structures with widely differing properties. Macromolecular Rapid Communications, 2015. 36 (21): p. 1902-1909. DOI:10.1002/MARC.201500229. Chapter 6 of this thesis.

Chapter 2 - Combinatorial chemistry and the high throughput development of novel polymer biomaterials for tissue engineering

Erwin Zant, Mirjam J. Bosman, Dirk W. Grijpma

Physico-chemical material properties and analysis techniques relevant in high-throughput biomaterials research, Chapter 2 in Materiomics - High throughput screening of biomaterial properties. Editors: Jan de Boer and Clemens A. van Blitterswijk. 2013, Cambridge University Press.

Introduction

Chemistry is a constant factor from which the performance of most polymer biomaterials can be predicted, but this extrapolation becomes less obvious when numerous materials are mixed in huge combinatorial libraries. Therefore, researchers are increasingly involved in high throughput material research when successful correlations between biological performance and physical material properties are to be made. This accelerating trend can be extracted from many studies where high throughput technologies are successfully applied to measure physical properties and biological performance of many different polymeric biomaterials. It is known that physical properties of materials like hardness, topography and hydrophilicity are important parameters in the biological evaluation of materials, because they affect the adhesion of biological compounds which is required to allow cell-spreading, migration, proliferation and differentiation. These physical properties are naturally different for every material or combination of materials, and relate primarily to the variable properties on the chemical level (molecular structure, functional groups and degradation). Therefore, the chemistry of a biomaterial is directly contributing to its interaction with biological environments. Combinatorial chemistry and high throughput analysis is developed to accelerate the rate of experimentation in order to correlate abovementioned material properties to the biological outcome and eventually find the ultimate biomaterial.

Chemical and physical properties of polymers for tissue engineering

Building blocks (non- functional and functional units)

The properties of polymeric biomaterials on the chemical level deal with the information on the structural units, namely, what type of monomer comprises the polymer chain and whether one or more than one type of monomer (copolymer) is used. Two types of structural units can be recognized: non-functional and functional units. The non-functional units comprise the carbohydrate building blocks of the polymer chain, methylene (-CH_2-) and phenylene (-C_6H_4-) for example; in both groups the hydrogen atoms can be interchanged by other functionalities or groups. The functional structural units originate from the condensation reactions of the functional monomers (functionalized by –OH, -NH_2, -COOH, -COCl, etc.). These functional units determine the characteristic names of polymer families, such as polycarbonates, -esters, -amides, -urethanes, etc. These groups affect the thermal- and mechanical properties of polymers which largely determine their field of application. Furthermore, functional groups determine whether the polymer is prone to be affected by degradation processes like hydrolysis. This degradation process can be very useful in some polymers, which make them biodegradable and therefore applicable in medical implants, drug delivery devices [1] and tissue engineering scaffolds [2, 3].

Biodegradation

The development of biodegradable polymers has gained a lot of interest by clinicians, because it can be very useful when polymers are used as artificial implants and a second surgery is not needed. Moreover, this class of materials can lead to better recovery of the tissue and therefore is applicable in tissue engineering were tissue repair or remodeling is the goal [4]. In short, biodegradation is the chemical degradation, or backbone breakdown, of a polymer chain due to hydrolytic or enzymatic activity [5]. Therefore, only polymers with

labile structural units like esters, anhydrides, carbonates, orthoesters, and amides (Figure 1) suit the application.

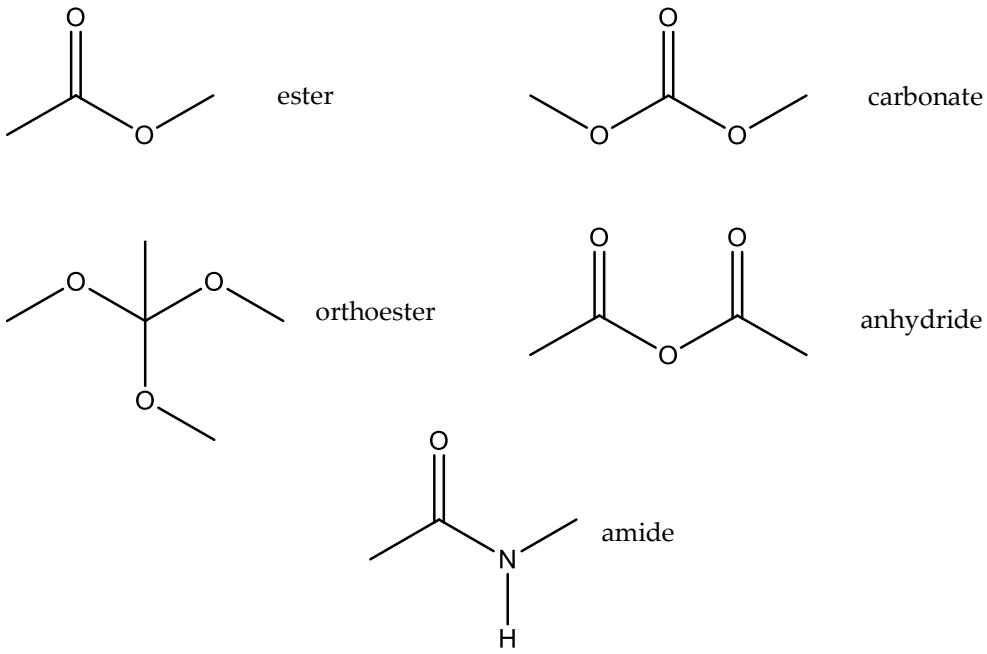

Figure 1: Structural formulas of common functional groups which are labile in biological environments and make the biodegradation of polymers possible.

Naturally derived biodegradable polymers such as collagen, glycosaminoglycans, chitosan and polyhydroxyalkanoates, representing polyamides (polypeptides), polysaccharides and polyesters respectively, have excellent biological properties and are biocompatible [6]. Their synthetic counterparts possess large scale reproducibility and can be processed into tissue engineering products in which the mechanical properties and degradation time can be controlled. Examples of synthetic polyesters are poly(glycolic acid) (PGA) and poly(lactic acid) (PLA), which are the most widely used synthetic degradable polymers in medicine . The relative hydrophilicity of PGA makes it very fast in biodegradation because the

absorption of water accelerates hydrolysis, but copolymerization with the more hydrophobic polymer PLA makes the material more suitable for a wider range of applications. Poly(ε-caprolactone) (PCL) characterizes another polyester with somewhat slower degradation than PGA and PLA, which favors its use in long term, implantable systems. To close, biodegradation is an important feature that influences the mechanical and biological properties of polymers over time and is therefore an important factor in the development of new biomaterials.

Thermal properties

The thermal properties of polymeric biomaterials are designated by two domains in the bulk of the material: the amorphous state and crystalline regions. The distribution of amorphous polymer chains in the matrix is completely random in the amorphous state (glass) and frozen in position. This phase contributes to the thermal transition from glass to rubber, the glass transition temperature (T_g), where the molecular motion in the amorphous phase of the polymer increases and becomes rubbery. Increasing the temperature of the polymer even further, the amorphous material starts to decrease in viscosity and finally flows. Where amorphous polymers are disordered structures, crystalline regions are areas where the polymer chains are highly ordered. These become mobile above the melting point (T_m) of the polymer, which is much higher than the glass transition temperature of most polymers. While increasing the temperature of semi-crystalline polymer materials, one can identify a glass phase, a rubber phase and a molten phase. Transitions between the phases lead to different mechanical properties: in the glass state (the polymer is below its glass transition temperature), the material is rigid and difficult to deform; the rubber plateau is the region above the glass transition temperature where the material is flexible and more easy to deform. Poly(trimethylene carbonate) (PTMC) is such an amorphous polymer, which has a T_g around -15°C and has no melting temperature, therefore it shows a tensile modulus (an indication of stiffness) of approximately 6 MPa at room temperature [7]. However, semi-crystalline polymers are able to maintain higher stiffnesses above the glass transition temperature, since the crystalline regions function as physical entanglements between the mobile rubber domains. This

behavior can be observed in the biodegradable polyester poly(ε-caprolactone) (PCL), the polymer has a T_g of -60°C, a T_m of 59°C and a tensile modulus of 400 MPa at room temperature [8], which is much higher than that for PTMC. Next to mechanical properties, crystallinity in the bulk also affects the morphology at the surface by increasing surface roughness, and hence can have a significant effect on biological interactions. Cells respond to this phenomenon by decreasing their proliferation rate with increasing surface roughness as was found by Washburn and coworkers [9].

Mechanical properties

Static measurements: The mechanical properties of biomaterials are of great importance, in particular in all applications where they are used as structural components. The most often determined mechanical parameter in high throughput is the elasticity modulus, which is the ratio between the stress and the applied deformation [2]. Three different modes of static deformation exist: tensile-, compression- and shear deformation. From which *E*-, *K*- and *G*-modulus are the derived moduli, respectively. The *E*-modulus or Young's modulus describes the material stiffness at small strains or the resistance of the material to reversible deformation and is defined as the initial slope of a stress-strain diagram obtained during a uni-axial tensile test as is shown in Figure 2.

In polymers, the elastic modulus mainly origins from secondary (interchain) interactions, mainly van der Waals interactions [10] and the resulting *E*-modulus of glassy polymers typically ranges from 2.5 to 3.5 GPa. Yield stress and elongation at break are two other important parameters which define the material as respectively strong or weak and brittle or tough.

Yielding, strain softening and strain hardening are processes that often occur when stress is applied on a polymer. Yield is defined as the stress at which the polymer deforms plastically and deformation is irreversible. Yielding is often followed by strain softening as the engineering deformation stress applied to the polymer decreases, strain hardening results from the resistance to deformation that often occurs subsequently. The mechanical performance of a polymer depends on its

glass transition temperature and its molecular weight and molecular weight between entanglements (which determines the entanglement density) [11].

Dynamic measurements: Polymers are viscoelastic materials, which means that they show both solid (elasticity) and fluid (flow) behavior [12]. The elasticity and flow of polymers are time dependent and can be visualized using dynamic mechanical analysis (DMA). In DMA a small force is applied on the polymer sample so that the sample is always within the reversible/elastic region of its stress-strain curve and the resulting strain is determined [13]. The applied force is sinusoidal, hence the modulus can be expresses as an in-phase component, the storage modulus, and an out of phase component, the loss modulus.

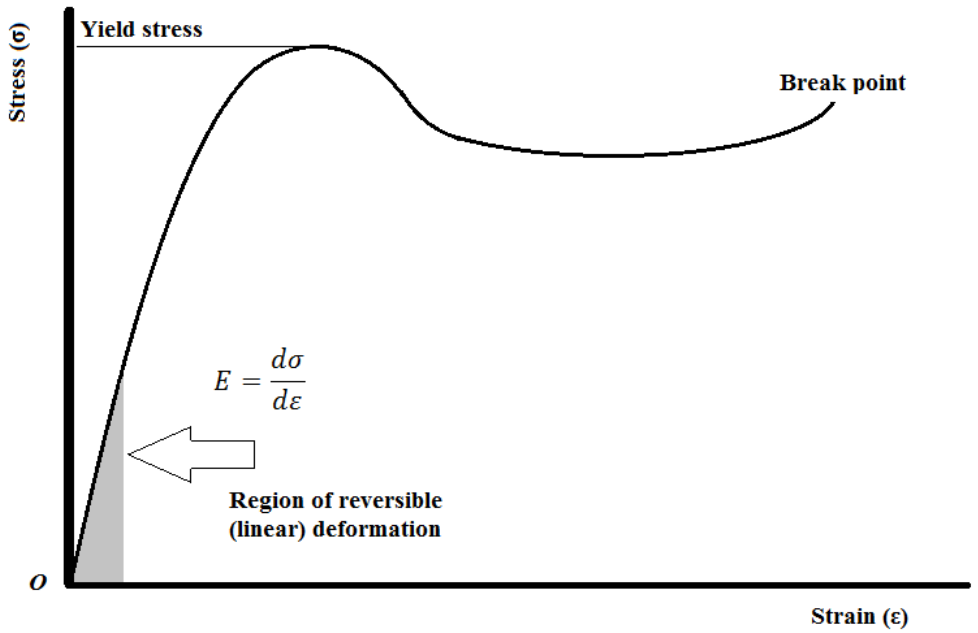

Figure 2: Tensile stress (σ) versus tensile strain (ε) of ideal thermoplastic polymers. The slope of the tensile curve in the linear deformation is a measure of the modulus or stiffness.

During the dynamic experiments, part of the material behaves elastically which comprises the in-phase component and another part in a plastic manner which causes the out of phase response. When the material is completely viscous, the

phase-shift is 90°, when the material is completely elastic the phase shift is 0°. Using DMA, the measured shift is a combination of both. To be practical in the field of (polymeric) biomaterials, DMA can be used to test materials over a broad temperature range to determine thermal transitions such as the glass transition temperature.

Hardness measurements

The material hardness is a measure of the resistance to local deformation of a material [14, 15]. The hardness of the material depends mainly on the elastic modulus of the bulk. The parameter is determined at the surface and offers a straightforward and fast evaluation method of the bulk mechanical properties of a material [16, 17]. Three methods exist to measure hardness: scratch hardness, rebound hardness and indentation hardness. Among these three, indentation, or depth sensing indentation, is the most often used technique for the analyses of polymer mechanical properties. Different polymers can have a very different material hardness values, ranging from soft gel-like materials to glasses, and different indenter geometries exist, varying from diamond pins to soft rubber spheres. Standardized methods like Shore or Rockwell hardness determination methods use fixed forces and geometries for each scale type (Shore A uses for instance a 35° hardened steel cone with diameter 1,40 mm, height 2,54 mm and the force is 8 N) which limit their applicability in high throughput screening. Instrumented micro-, ultramicro- or nanoindentation simultaneously measure the load to indent and the displacement of the probe into the surface of the material. From these two parameters, the mechanical properties of a broad range of materials can be evaluated [18].

Polymer biomaterial surface properties and cell interactions

The chemical nature of surfaces plays an important role in the performance of polymeric biomaterials. For instance, the polymer chemistry was shown to have a significant effect on the behavior of cells at the surface, as was described by Folkman and Moscona in 1978 [19]. The study concerned the seeding of cells on tissue cultured polystyrene surfaces with coatings varying in concentrations of the hydrophilic polymer poly(2-hydroxyethylmethacrylate) (pHEMA). Cell spreading was reflected by the average cell height and was found to be higher with low amounts of pHEMA. This spreading correlated with the rate of cell growth. These experiments showed that the chemical character of polymer surfaces can have important consequences for cell shape and cell proliferation characteristics. As a consequence, many researchers started to design more surface chemistries to correlate with cell function [20-23].

Surface modifications

Chemical surface modifications or the covalent immobilization of bioactive compounds onto functionalized polymer surfaces plays a key role in determining interfacial interactions between the polymeric material and biological media (such as protein solutions, cells, tissue) [4, 24]. Polystyrene substrates for tissue engineering are for instance treated by glow discharge or exposure to chemicals, such as sulfuric acid, to increase the number of charged groups at the surface, which improves cell adhesion and proliferation of many types of cells. Modification of polymeric surfaces by introducing functional groups is a chemical strategy to tune protein and cell adhesion. Several surface modification techniques have been developed to improve wetting, adhesion, and printing of polymer surfaces by introducing a variety of polar groups like amines, carboxylic acids, thiols and hydroxyls or the immobilization of proteins and peptides [25].

Another method that is widely applied is polymer grafting: a polymer is 'grown' on the surface of another polymer. In this way the desired properties of the two polymers can be combined. For instance, a polymer with good cell adhesion

properties can be grafted onto a polymer with desired mechanical and thermal properties, without significantly influencing these properties. By tuning the density and molecular weight of the grafted polymer, the desired properties can be fine-tuned for specific applications [26-28]. Polymer-cell interactions can also be tuned by incorporating specific bioactive molecules on the polymer surface, which either improve cell adhesion or prevent unspecific and/or unfavorable reactions. Heparin-based coatings are widely used for this purpose, since this molecule has proven to increase the biocompatibility of polymer surfaces *in vitro* as well as *in vivo*. Since most of the cell functions are mediated by protein-protein interactions, proteins are also often coupled to polymer surfaces in order to increase the biocompatibility. Extracellular proteins, e.g. collagen, elastin, fibrin, albumin and immunoglobulins, are the most commonly used for this application since they play a major role in cell adhesion, spreading and growth regulation [25, 29]. In addition to proteins, peptides are applied in order to enhance the stability of the bioactive molecules that are immobilized on the polymer surface. The arginine-glycine-aspartic acid (RGD) peptide is mostly used for this purpose. Growth factors can also be incorporated on the polymer surface to stimulate cell growth, proliferation and differentiation [25].

Wettability

Hydrophilicity is probably the most important parameter in cell related studies [30]. Wettable or hydrophilic surfaces have the tendency to interact with or be dissolved by water molecules. Cell adherence to surfaces is very dependent on this parameter, since cell adhesion was found to be optimal at intermediate hydrophilicity [30, 31], while proliferation increases with increasing hydrophobicity [32, 33]. Several treatments and material bulk properties influence the wettability of surfaces. For instance, increasing the number of charged groups on the surface affects wettability, because hydrogen bonding with the water is enhanced and the droplet spreads along the hydrophilic surface, resulting in a lower contact angle [25]. Cells respond to this by an increase in adhesion [30, 31]. Increased polymer crystallinity leads to increased surface roughness on a nanometer scale, which was found to optimize hydrophilicity and cell proliferation

was affected [9]. Cell adhesion is enhanced when surfaces are pretreated with proteins and protein adsorption is again depending on hydrophilicity. Therefore cell adhesion is influenced by two parameters: hydrophilicity and protein adsorption [30]. The most conventional method to assess wettability is performing water contact angle measurements. The technique is applied to measure how a water droplet spreads on a surface. As shown in Figure 3, the lower the contact angle, the more hydrophilic the surface is [34].

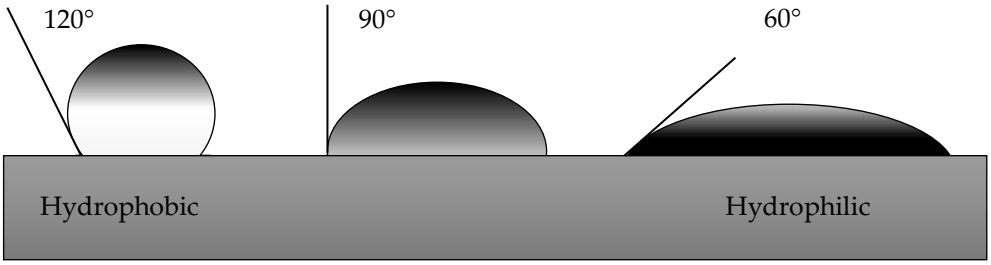

Figure 3: Water contact angle measurements. Hydrophobic surfaces show higher contact angles.

Topography

The surface morphology or topography of materials has a strong influence on the cell behavior: the response of cells (e.g. adhesion and proliferation) on patterned surfaces (nm to μm scale) is different than the behavior on smooth surfaces. For instance, results shown in the study of Riehle and coworkers demonstrate that highly ordered nanotopographies result in negligible to low cellular adhesion and osteoblastic differentiation, whereas mesenchymal stem cells on random nanotopographies exhibited a more osteoblastic morphology [35]. Research in the lab of Simon and coworkers showed that with a gradient in polymer crystallinity in poly(L-lactic acid) films, the surface roughness was affected and cell proliferation was found to be inversely correlated with the surface roughness [9]. Topography was also shown to be a driving force in a study where MC3T3-E1 cell response to dimethacrylate composites was evaluated. The used biomaterials varied in filler content, degree of methacrylate conversion, and surface roughness, hence a combinatorial testing platform was developed. Overall, the cell response

was found to depend upon multiple material properties. For instance, cell viability was highest at higher degrees of conversion, a less rough surface, and more hydrophilic regions, and was only mildly affected by filler type and content. At lower degrees of conversion the surface of the materials was rougher and more hydrophobic, and cells did not spread as well as on smooth surfaces [36].

Combinatorial chemistry and high throughput screening

As shown in the previous section, the physical properties of polymeric materials greatly influence their interaction with cells. These become variable and difficult to predict when combinations of materials are being prepared. A combinatorial experiment is one where multiple chemically divergent materials are being prepared and analyzed for key properties [37] Combinatorial chemistry is a very efficient approach to find new materials with the desired interaction, which could never be designed using conventional synthesis methods. The first polymer-related combinatorial study involved the synthesis of hundreds of different catalysts from polyallylamine [38]. The first combinatorial design concept of polymers for tissue engineering was published in 1997 by Brocchini and his colleagues [39]. By combining a selection of bifunctional monomers A and B, 112 polymers with different physical properties where obtained. The polymers where screened for their glass transition temperature and contact angle, which was later found to be of great influence on fibroblast proliferation [21].

In order to allow a rapid combinatorial experiment, high throughput techniques that enable the rapid preparation and screening of many materials at the same time, are usually involved. Combinatorial and high throughput techniques have been mostly applied in the development of inorganic materials, catalysts and drugs, but are increasingly applied in polymer science.

High throughput screening (HTS) techniques

Mostly, conventional material characterization methods lack the possibility to repeat measurements many times in a short time period. Though, other methods were developed or modified to allow rapid material characterization. Relevant and often applied high throughput techniques that are used to analyze polymer properties like topography, hydrophilicity, stiffness and chemistry are atomic force microscopy (AFM), X-ray photoelectron spectroscopy (XPS), Time-of-flight secondary ion mass spectrometry (ToF-SIMS), Fourier Transform Infrared (FTIR) / Raman spectroscopy, nanoindentation and water contact angle (WCA).

Fourier Transform Infrared (FTIR) / Raman Spectroscopy

FTIR/Raman micro spectroscopy provides an approach to determine the bulk chemical functionalities of materials [25, 32]. Upon interaction with the electromagnetic waves from the FTIR/Raman spectroscope, chemical bonds stretch, contract, and bend, causing it to absorb radiation of a defined wavenumber, which in spectroscopy is used as a unit of energy. The output describes an image of the absorption versus the wavenumber, where the wavenumber identifies a specific chemical bond. Because the technique is able to provide the chemical information in seconds, FTIR/Raman spectroscopy is widely used in high throughput analysis of combinatorial and gradient material arrays. It was for instance applied in a study of a 2D gradient specimen, where both monomer composition and degree of conversion were analyzed simultaneously, providing a qualitative analysis of the polymer chemistry [40]. The high throughput application of FTIR spectroscopy was also found to be very practical in the characterization of biodegradable polyanhydride compositions produced in a gradient like library, where a correlation with phase behavior results from optical and atomic force microscopy was performed to provide information about polymer composition, upper critical solution temperature and surface roughness [41]. Hence, FTIR can be a helpful tool to analyze libraries of materials were the composition at different positions in the library is unknown.

Nanoindentation

The most often used technique for the assessment of the mechanical properties of materials is tensile testing. However, tensile testing is not well-suited for high-throughput techniques and hence other methods for the high throughput analysis of mechanical properties have been developed. One of the most common high throughput mechanical analysis techniques is nanoindentation, which refers basically to a technique where a hardness test is performed at the nanometer scale, so only small amounts of material are required to quantify the mechanical properties [14, 17, 18]. The method is also known as depth sensing indentation, where the name already denotes the principle of operation. Both the load and the displacement of the probe into the polymer are measured simultaneously.

As an example, a schematic representation of a typical data set obtained with a Berkovich indenter is presented in Figure 4.

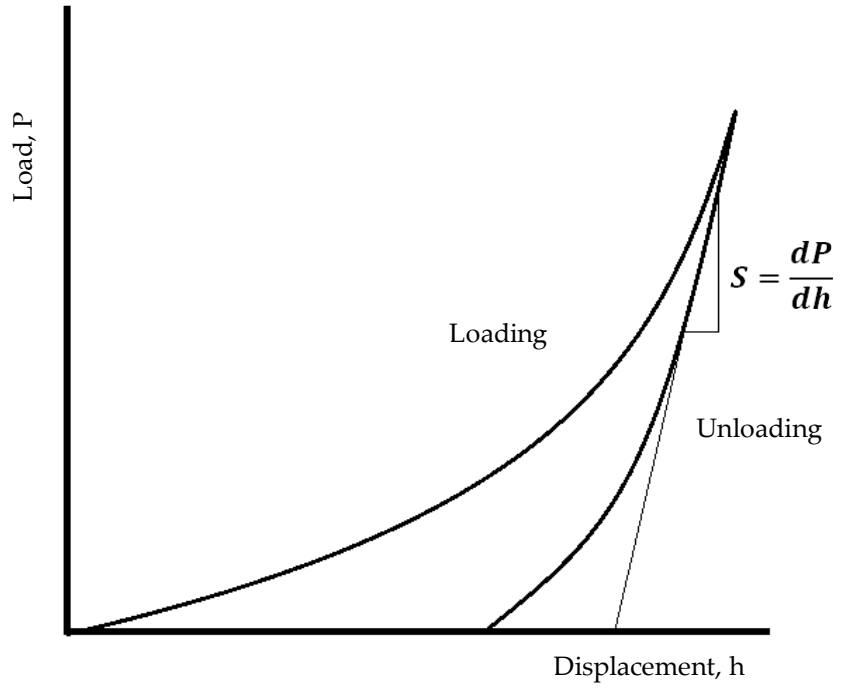

Figure 4: Schematic illustration of a load (P) versus displacement (h) indentation showing important measured parameters, which allow the calculation of the material stiffness (S) during the unloading process.

The parameter *P* designates the load and *h* the displacement relative to the initial non-deformed surface. The material response of polymers to deformation is assumed to be elastic and plastic in nature during indentation, while during unloading of the indenter only the elastic displacements are recovered. Therefore, the unloading curve facilitates the analysis [17]. In conventional tensile tests, the stiffness or elastic modulus is defined as the initial slope of the stress-strain diagram. The stiffness of the material *S* during indentation is defined as the slope of the upper portion of the unloading curve [17]. As said earlier, Figure 4 shows the response of a conical diamond-shaped or Berkovich indenter which has been used often in this particular application. Results obtained with such device need to be used with caution, as undesired effects can occur, such as material pile-up along the indenter walls which increases the contact area between the probe and the material. Hence other indenter tips have been used for nanoindentation [18]. For instance, the flat punch probe can be useful as the surface of indentation remains constant, but it is sensitive to misalignment and therefore not very useful while scanning a large library with numerous height differences. Using a spherical indenter should prevent most of misalignment problems and has been used in the high throughput context as well [42].

X-ray photoelectron spectroscopy (XPS)

XPS, or Electron Spectroscopy for Chemical Analysis (ESCA), determines the atomic composition of the surface of a solid to a depth of several nanometers. Upon exposure to X-ray photons, a surface ejects photoelectrons, these binding energies can be compared to reference values to identify the element and its oxidation state. The resulting spectrum is a plot of intensity versus binding energy. The intensity of the ejected photoelectrons relates directly to the atomic distribution of the material surface and can therefore be used to quantify percent atomic composition and stoichiometric ratios [25]. Since XPS is a rapid technique, it is suitable for high throughput analysis. For instance, a library of 576 different novel surface chemistries was analyzed with XPS offering a fast method of producing a library of chemical data [43-45]. Studies performed in the group of Voelcker also resulted in the successful application of XPS. They generated

multifunctional surface chemistries using poly(ethylene glycol)-methacrylates as a non-cell-adhering background and glycidyl methacrylate linkers to couple a variety of biologically active molecules [46].

Time-of-flight secondary ion mass spectrometry (ToF-SIMS)

Time-of-flight secondary ion mass spectrometry (ToF-SIMS) is a mass spectroscopy technique that is commonly used as a complementary technique with XPS, since ToF-SIMS does not provide quantitative results. ToF-SIMS is more sensitive than XPS, it makes use of primary ions which are sputtered on the sample surface causing secondary ions to eject from the surface. The mass of these secondary ions is determined by measuring the time that is needed for the secondary ions to move from the surface of the material to the detector. Hence, detailed information about the type and quantity of ionizable chemical groups of a surface to a depth of a few nanometers can be obtained [25]. The resulting spectrum depicts signal intensity versus mass to charge ratio and can be used to determine relative intensities of chemical species. For high throughput analysis, ToF-SIMS spectra of all samples of the library are acquired. Ion distribution images of the entire library then allow the rapid screening of the presence of certain ions [43-45].

Water contact angle (WCA)

WCA allows the assessment of surface hydrophilicity by measuring how much a droplet of water spreads on a surface. The lower the contact angle, the more hydrophilic the surface is [25]. However, the method is generally limited to macroscopic measurements because the base diameter of the droplet is usually greater than 1 mm. To allow water contact angle measurements in high throughput, piezo-electric dispensers producing picoliter sized droplets with micrometer precision were developed and applied [43, 47]. A piezo-dosing unit, similar to those used in inkjet printers, dispenses picoliter volumes of water onto the material yielding drops with a base of approximately 70 μm [47]. For high throughput purposes, sample positioning and data acquisition can be automated

using dual camera systems (one camera records a side profile of the drop, the other provides an overhead view) to ensure deposition on the center of each sample [43].

Atomic Force Microscopy (AFM)

In AFM, a cantilever with a tip moves over the surface. As the tip interacts with the surface it screens the surface of the polymer. The change in surface height is then measured by the location of a reflected laser beam in a photodetector and the surface topography is mapped from which the surface roughness can be determined. In tapping mode AFM, any friction between the tip and the surface that could distort the obtained image is avoided. AFM has been used very often in high throughput analyses of surfaces, because it generates topography maps with nanometer resolution very fast. Polymer bulk crystallinity results in topographical changes at the surface of materials as was discovered using AFM in the case of phase separation during cooling of two polymers [36] and different annealing temperatures for semi-crystalline polymers [9]. The AFM apparatus is very useful in both cases to correlate surface roughness with bulk crystallinity, morphology and biological interactions. As described in a paper by Yang et al., surface smoothness was essential to eliminate any influence of the topography on cellular response. AFM analysis revealed that the majority of the samples had a very low surface roughness (below 5 nm). The surface roughness was not found to correlate with cell adhesion, so a better correlation between surface chemical functionality and cell-material interaction could be made [44]. Furthermore, although it has not often been applied in high throughput mechanical testing, AFM has been shown to be very useful in the nanomechanical screening of ultrathin films (1-100 nm) [48].

Cited for almost 4000 times (Web of Knowledge, September 2015), the study performed by Engler et al. is highly influential in the biomaterials research field [49]. The research reinforced the fundaments of the correlations between physical properties of substrate materials and stem cell commitment. This paper shows that mesenchymal stem cells can differentiate into specific cell lineages by only sensing the stiffness of the substrate. Substrates with various elastic modulus values were obtained by the preparation of poly(acrylamide) gels in which the concentration of bis-acrylamide determined the crosslink density, hence the rigidity upon swelling

in water. The *E*-modulus was determined by AFM and varied from 0.1 kPa to 40 kPa. Characterizing the cells by observing cell shape, measuring RNA expression and staining specific proteins, showed that mesenchymal stem cells react to the stiffness of the substrate by differentiating into different cell lineages. The stiffness of the tissue to which the cells differentiated corresponded to the stiffness of the substrate onto which the cells were cultured.

High throughput synthesis – Preparation of material libraries

Combinatorial polymer microarrays

In order to allow the rapid screening of numerous materials, microarrays are very effective. Here, the materials are deposited at defined locations on a (glass) surface so that the specific material combination is traceable. A first demonstration of a biomaterial related microarray was performed by Xiang et al. where minerals were deposited on a surface using a mask which was sequentially placed in different positions so that samples as small as 200 by 200 microns were generated [50]. The first polymer-related microarrays were reported later that year [51]. It was in 2004 that the group of Anderson at MIT demonstrated contact printing of combinatorial microarrays using robot guided pins which deposited premixed combinations of 24 acrylate monomers onto poly(hydroxylethyl methacrylate) (pHEMA) treated glass slides [52]. The 1728 polymer spots were crosslinked by UV light and screened for their interaction with human embryonic stem cells, see Figure 5.

A high throughput material characterization of the library using techniques as XPS, ToF-SIMS and WCA was later assessed in 2007 [43]. This microarray contact printing was also used for a library of biodegradable polyesters (PLA, PCL and PGA) in a paper presented in 2005 [20] and later for the deposition of polyurethanes [53]. In 2009, Anderson's group prepared a library of 22 acrylates [54]. In a first study, the library was screened for chemical composition, protein adhesion and the formation of embryonic bodies of human embryonic stem cells [54]. Later, more comprehensive correlations between the physical properties and

human embryonic clonal bodies was made using AFM, ToF-SIMS, nanoindentation, Raman and XPS [44, 55]. In 2012, the same material library was also found to contain candidate materials with resistance against bacterial adhesion [56, 57].

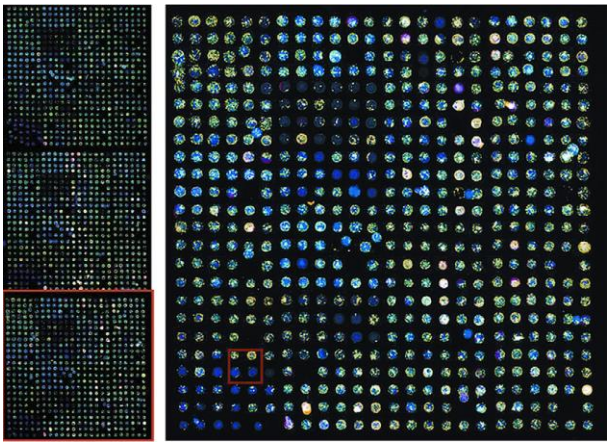

Figure 5 An example of a polymer microarray onto which hES cells are grown and stained. Taken from [52].

Ink-jet fabrication of combinatorial microarrays was first demonstrated by Bradley and coworkers in 2008 with water soluble acrylamides [58]. To provide an anchor for the hydrogels during polymerization, the glass slides were pretreated with 3-trimethoxysilyl)methacrylate. The paper discusses two principles of printing; the printing of premixed monomers and the mixing of monomers and subsequent polymerization on site. The printing processwas later optimized by deposition of the solutions onto agarose-coated slides covered with a thin layer of paraffin oil [59].

Gradient films

Combinatorial polymer gradient studies are predominantly developed at the National Institute of Standards and Technology (NIST) Polymers Division by

Meredith, Simon and coworkers [33]. These gradient libraries involve the gradual change in physical parameters like phase separation [60] and/or crystallinity [9] affecting surface topography. Furthermore, several studies demonstrate gradients in biologically active ligands like fibronectin [61], laminin and peptides [62]. The benefit of gradients is that in principle all possible ratios between two polymers are being produced. The first combinatorial polymer gradient was developed by Meredith and coworkers. This study involved the preparation of blends with a compositional gradient of PCL and PDLLA. Osteoblasts were cultured on the material surface and revealed an exceptional combination of 50/50 PCL/PDLLA annealed at 105 °C that was found to significantly enhance their differentiation [60].

Gradient scaffolds

As a more comparable model to physiological conditions, three dimensional (3D) scaffolds are being developed. Simon *et al.* has developed production methods for scaffold gradients and libraries [63] where the approach involves two syringe pumps and two different polymer solutions that come together in a static mixer as is schematically shown in Figure 6. The pumps are programmed such that one ramped down in velocity while the other ramped up creating a graded change in composition from A to B. The polymer solutions in solvents that can be freeze-dried or that contain leachable porogens are deposited into either a trough for a continuous gradient or into a 96-well plate for a scaffold library array. After deposition of polymer solutions, the gradients or arrays are freeze-dried to remove solvent and leached in water to remove NaCl so that polymer scaffold gradients or arrays with varying composition and properties were obtained.

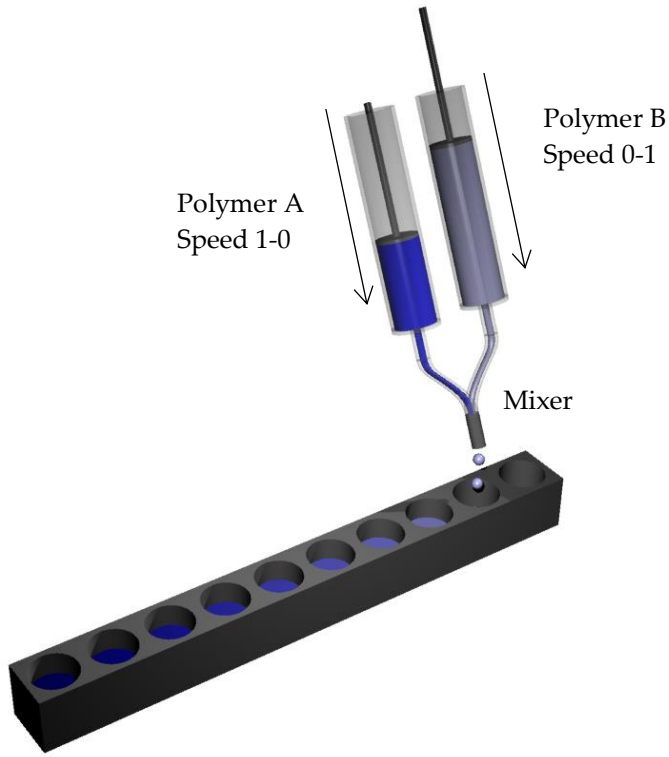

Figure 6. A schematic presentation of the setup developed by Simon et al. for the production of gradient scaffolds.

The setup was successfully used for gradient scaffolds produced by mixing two different polymers poly(desaminotyrosyl-tyrosine ethyl ester carbonate) (pDTEc) and poly(desaminotyrosyl-tyrosine octyl ester carbonate) (pDTOc). Both polymers have widely different physical properties and potentially different cell behaviors [64].

This mixing approach was also used to fabricate a gradient in stiffness of PEG hydrogels (10-300 kPa). Osteoblasts cultured within the gradient gels reacted by inducing mineralization in the harder regions of the gels, but not in the soft regions [65, 66].

Mano and colleagues have worked on another method to produce scaffolds using combinations of polymers. Depositing chitosan-alginate solutions in water on hydrophobically modified, anti-adherent and anti-proliferative polystyrene plates and subsequent freeze-drying was found to be an original method of combinatorial scaffold production [67].

Other

Polymer grafting or -imprinting by photoinduced polymerization is an innovation in high throughput material synthesis. In developing low fouling membranes, this approach was used by the Belfort group to graft glycidyl methacrylate- and amine compounds on poly(ether sulfone) (PES) surfaces in high throughput [68]. Next to the non-adhesiveness to proteins, glycidyl methacrylate comprises an epoxy moiety which can react with other functional groups by ring opening and polycondensation. The PES material readily produces radicals upon ultraviolet irradiation, which can subsequently initiate the radical polymerization of the glycidyl methacrylate. Using this chemistry, the group was able to produce numerous different membranes by coupling of the glycidyl polymer to 25 different amine monomers.

Belfort developed this technique together with Anderson, they described the modification of PES surfaces with 66 monomers [69]. The fact that the photo-induced graft polymerization was performed in a 96-well format allowed the evaluation of many monomers at the same time, hence a high throughput platform was produced to develop new membranes.

Conclusions

Materials with a vast variety of chemical and physical properties can be obtained through the combinatorial synthesis and mixing of synthetic polymers. In the last 20 years, this approach has become a powerful method to find new biomaterials for tissue engineering. A considerable amount of work has been done in producing large microarray material libraries obtained by the combinatorial mixing and

crosslinking of small molecules with diverging chemistries. Research on photo-crosslinked networks obtained from the combinatorial mixing of macromonomers (macromers) is very limited. Synthesis of networks based on combinatorial mixtures of macromers with diverging physical properties may lead to the identification of new polymer biomaterials with unexpected properties and could be of great interest for regenerative medicine applications.

References

1. Uhrich KE, Cannizzaro SM, Langer RS, and Shakesheff KM, Polymeric systems for controlled drug release. Chemical Reviews, 1999. 99(11): p. 3181-3198.
2. Van Krevelen DW and Te Nijenhuis K, Properties of polymers (fourth edition). 2009, Amsterdam: Elsevier.
3. Flory PJ, Principles of polymer chemistry. 1953: Cornell University Press.
4. Lanza R, Langer R, and Vacanti J, Principles of tissue engineering (third edition). 2007: Elsevier.
5. Buschow KHJ, Cahn RW, Flemings MC, Ilschner B, Kramer EJ, Mahajan S, and Veyssière P, Encyclopedia of materials: science and technology. 2001: Elsevier Ltd.
6. Kim B-S, Park I-K, Hoshiba T, Jiang H-L, Choi Y-J, Akaike T, and Cho C-S, Design of artificial extracellular matrices for tissue engineering. Progress in Polymer Science, 2011. 36(2): p. 238-268.
7. Pego AP, Grijpma DW, and Feijen J, Enhanced mechanical properties of 1,3-trimethylene carbonate polymers and networks. Polymer, 2003. 44(21): p. 6495-6504.
8. Pego AP, Poot AA, Grijpma DW, and Feijen J, Copolymers of trimethylene carbonate and epsilon-caprolactone for porous nerve guides: Synthesis and properties. Journal of Biomaterials Science-Polymer Edition, 2001. 12(1): p. 35-53.
9. Washburn NR, Yamada KM, Simon Jr CG, Kennedy SB, and Amis EJ, High-throughput investigation of osteoblast response to polymer crystallinity: Influence of nanometer-scale roughness on proliferation. Biomaterials, 2004. 25(7-8): p. 1215-1224.
10. Meijer HEH and Govaert LE, Mechanical performance of polymer systems: The relation between structure and properties. Progress in Polymer Science (Oxford), 2005. 30(8-9): p. 915-938.

11. Meijer HEH and Govaert LE, Multi-scale analysis of mechanical properties of amorphous polymer systems. Macromolecular Chemistry and Physics, 2003. 204(2): p. 274-288.
12. Reiner M, The Deborah Number. Phys. Today, 1964. 17(1): p. 62.
13. Eisele U, Introduction to polymer physics. First ed. 1990: Springer-Verlag.
14. Tweedie CA, Anderson DG, Langer R, and Van Vliet KJ, Combinatorial material mechanics: High-throughput polymer synthesis and nanomechanical screening. Advanced Materials, 2005. 17(21): p. 2599-2604.
15. Sundararajan G and Roy M, Hardness testing, in Encyclopedia of Materials: Science and Technology. 2001, Elsevier: Oxford. p. 3728-3736.
16. Oliver WC and Pharr GM, An improved technique for determining hardness and elastic modulus using load and displacement sensing indentation experiments. Journal of Materials Research, 1992. 7(6): p. 1564-1583.
17. Oliver WC and Pharr GM, Measurement of hardness and elastic modulus by instrumented indentation: Advances in understanding and refinements to methodology. Journal of Materials Resarch, 2004. 19(1): p. 3-20.
18. Kranenburg JM, Tweedie CA, van Vliet KJ, and Schubert US, Challenges and progress in high-throughput screening of polymer mechanical properties by indentation. Advanced Materials, 2009. 21(35): p. 3551-3561.
19. Folkman J and Moscona A, Role of cell-shape in growth-control. Nature, 1978. 273(5661): p. 345-349.
20. Anderson DG, Putnam D, Lavik EB, Mahmood TA, and Langer R, Biomaterial microarrays: Rapid, microscale screening of polymer-cell interaction. Biomaterials, 2005. 26(23): p. 4892-4897.
21. Brocchini S, James K, Tangpasuthadol V, and Kohn J, Structure-property correlations in a combinatorial library of degradable biomaterials. Journal of Biomedical Materials Research, 1998. 42(1): p. 66-75.
22. Hansen A, McMillan L, Morrison A, Petrik J, and Bradley M, Polymers for the rapid and effective activation and aggregation of platelets. Biomaterials, 2011. 32(29): p. 7034-7041.
23. Khan F, Tare RS, Kanczler JM, Oreffo ROC, and Bradley M, Strategies for cell manipulation and skeletal tissue engineering using high-throughput polymer blend formulation and microarray techniques. Biomaterials, 2010. 31(8): p. 2216-2228.
24. Thissen H, Johnson G, McFarland G, Verbiest BCH, Gengenbach T, and Voelcker NH. Microarrays for the evaluation of cell-biomaterial surface interactions. 2007. Adelaide.

25. Goddard JM and Hotchkiss JH, Polymer surface modification for the attachment of bioactive compounds. Progress in Polymer Science, 2007. 32(7): p. 698-725.
26. Bhat RR, Chaney BN, Rowley J, Liebmann-Vinson A, and Genzer J, Tailoring cell adhesion using surface-grafted polymer gradient assemblies. Advanced Materials, 2005. 17(23): p. 2802-2807.
27. Rezaei SM and Ishak ZAM, The biocompatibility and hydrophilicity evaluation of collagen grafted poly(dimethylsiloxane) and poly (2-hydroxyethylmethacrylate) blends. Polymer Testing, 2011. 30(1): p. 69-75.
28. Zainuddin, Barnard Z, Keen I, Hill DJT, Chirila TV, and Harkin DG, PHEMA hydrogels modified through the grafting of phosphate groups by ATRP support the attachment and growth of human corneal epithelial cells. Journal of Biomaterials Applications, 2008. 23(2): p. 147-168.
29. Chen H, Yuan L, Song W, Wu ZK, and Li D, Biocompatible polymer materials: role of protein-surface interactions. Progress in Polymer Science, 2008. 33(11): p. 1059-1087.
30. Saltzman WM and Kyriakides TR, Chapter 20 - Cell interactions with polymers, in Principles of Tissue Engineering (Third Edition). 2007, Elsevier Academic Press. p. 279-296.
31. Matsumoto T and Mooney D, Cell instructive polymers tissue engineering I, in. 2006, Springer Berlin / Heidelberg. p. 113-137.
32. Hook AL, Anderson DG, Langer R, Williams P, Davies MC, and Alexander MR, High throughput methods applied in biomaterial development and discovery. Biomaterials, 2010. 31(2): p. 187-198.
33. Simon Jr CG and Sheng LG, Combinatorial and high-throughput screening of biomaterials. Advanced Materials, 2011. 23(3): p. 369-387.
34. Kingshott P, Andersson G, McArthur SL, and Griesser HJ, Surface modification and chemical surface analysis of biomaterials. Curr Opin Chem Biol, 2011. 15(5): p. 667-76.
35. Dalby MJ, Gadegaard N, Tare R, Andar A, Riehle MO, Herzyk P, Wilkinson CDW, and Oreffo ROC, The control of human mesenchymal cell differentiation using nanoscale symmetry and disorder. Nature Materials, 2007. 6(12): p. 997-1003.
36. Lin NJ and Lin-Gibson S, Osteoblast response to dimethacrylate composites varying in composition, conversion and roughness using a combinatorial approach. Biomaterials, 2009. 30(27): p. 4480-4487.
37. Webster DC, Combinatorial and high-throughput methods in macromolecular materials research and development. Macromolecular Chemistry and Physics, 2008. 209(3): p. 237-246.

38. Menger FM, Eliseev AV, and Migulin VA, Phosphatase catalysis developed via combinatorial organic chemistry. The Journal of Organic Chemistry, 1995. 60(21): p. 6666-6667.
39. Brocchini S, James K, Tangpasuthadol V, and Kohn J, A combinatorial approach for polymer design. Journal of the American Chemical Society, 1997. 119(19): p. 4553-4554.
40. Lin NJ, Drzal PL, and Lin-Gibson S, Two-dimensional gradient platforms for rapid assessment of dental polymers: A chemical, mechanical and biological evaluation. Dental Materials, 2007. 23(10): p. 1211-1220.
41. Thorstenson JB, Petersen LK, and Narasimhan B, Combinatorial/high throughput methods for the determination of polyanhydride phase behavior. Journal of Combinatorial Chemistry, 2009. 11(5): p. 820-828.
42. Anderson DG, Tweedie CA, Hossain N, Navarro SM, Brey DM, Van Vliet KJ, Langer R, and Burdick JA, A combinatorial library of photocrosslinkable and degradable materials. Advanced Materials, 2006. 18(19): p. 2614-2618.
43. Urquhart AJ, Anderson DG, Taylor M, Alexander MR, Langer R, and Davies MC, High throughput surface characterisation of a combinatorial material library. Advanced Materials, 2007. 19(18): p. 2486-2491.
44. Yang J, Mei Y, Hook AL, Taylor M, Urquhart AJ, Bogatyrev SR, Langer R, Anderson DG, Davies MC, and Alexander MR, Polymer surface functionalities that control human embryoid body cell adhesion revealed by high throughput surface characterization of combinatorial material microarrays. Biomaterials, 2010. 31(34): p. 8827-8838.
45. Urquhart AJ, Taylor M, Anderson DG, Langer R, Davies MC, and Alexander MR, TOF-SIMS analysis of a 576 micropatterned copolymer array to reveal surface moieties that control wettability. Analytical Chemistry, 2008. 80(1): p. 135-142.
46. Kurkuri MD, Driever C, Johnson G, McFarland G, Thissen H, and Voelcker NH, Multifunctional polymer coatings for cell microarray applications. Biomacromolecules, 2009. 10(5): p. 1163-1172.
47. Alexander MR, Taylor M, Urquhart AJ, Zelzer M, and Davies MC, Picoliter water contact angle measurement on polymers. Langmuir, 2007. 23(13): p. 6875-6878.
48. Kovalev A, Shulha H, Lemieux M, Myshkin N, and Tsukruk VV, Nanomechanical probing of layered nanoscale polymer films with atomic force microscopy. Journal of Materials Research, 2004. 19(3): p. 716-728.
49. Engler AJ, Sen S, Sweeney HL, and Discher DE, Matrix elasticity directs stem cell lineage specification. Cell, 2006. 126(4): p. 677-689.

50. Xiang XD, Sun XD, Briceno G, Lou YL, Wang KA, Chang HY, Wallacefreedman WG, Chen SW, and Schultz PG, A combinatorial approach to materials discovery. Science, 1995. 268(5218): p. 1738-1740.
51. Healey BG and Walt DR, Fast temporal response fiber-optic chemical sensors based on the photodeposition of micrometer-scale polymer arrays. Analytical Chemistry, 1997. 69(11): p. 2213-2216.
52. Anderson DG, Levenberg S, and Langer R, Nanoliter-scale synthesis of arrayed biomaterials and application to human embryonic stem cells. Nature Biotechnology, 2004. 22(7): p. 863-866.
53. Tourniaire G, Collins J, Campbell S, Mizomoto H, Ogawa S, Thaburet JF, and Bradley M, Polymer microarrays for cellular adhesion. Chemical Communications, 2006(20): p. 2118-2120.
54. Mei Y, Gerecht S, Taylor M, Urquhart AJ, Bogatyrev SR, Cho S-W, Davies MC, Alexander MR, Langer RS, and Anderson DG, Mapping the interactions among biomaterials, adsorbed proteins, and human embryonic stem cells. Advanced Materials, 2009. 21(27): p. 2781-2786.
55. Mei Y, Saha K, Bogatyrev SR, Yang J, Hook AL, Kalcioglu ZI, Cho SW, Mitalipova M, Pyzocha N, Rojas F, Van Vliet KJ, Davies MC, Alexander MR, Langer R, Jaenisch R, and Anderson DG, Combinatorial development of biomaterials for clonal growth of human pluripotent stem cells. Nature Materials, 2010. 9(9): p. 768-778.
56. Hook AL, Chang CY, Yang J, Luckett J, Cockayne A, Atkinson S, Mei Y, Bayston R, Irvine DJ, Langer R, Anderson DG, Williams P, Davies MC, and Alexander MR, Combinatorial discovery of polymers resistant to bacterial attachment. Nat Biotechnol, 2012. 30(9): p. 868-75.
57. Sanni O, Chang CY, Anderson DG, Langer R, Davies MC, Williams PM, Williams P, Alexander MR, and Hook AL, Bacterial attachment to polymeric materials correlates with molecular flexibility and hydrophilicity. Advanced Healthcare Materials, 2015. 4(5): p. 695-701.
58. Zhang R, Liberski A, Khan F, Diaz-Mochon JJ, and Bradley M, Inkjet fabrication of hydrogel microarrays using in situ nanolitre-scale polymerisation. Chemical Communications, 2008(11): p. 1317-1319.
59. Liberski AR, Zhang R, and Bradley M, In situ nanoliter-scale polymer fabrication for flexible cell patterning. JALA - Journal of the Association for Laboratory Automation, 2009. 14(5): p. 285-293.
60. Meredith JC, Sormana JL, Keselowsky BG, Garcia AJ, Tona A, Karim A, and Amis EJ, Combinatorial characterization of cell interactions with polymer surfaces. Journal of Biomedical Materials Research Part A, 2003. 66A(3): p. 483-490.

61. Mei Y, Wu T, Xu C, Langenbach KJ, Elliott JT, Vogt BD, Beers KL, Amis EJ, and Washburn NR, Tuning cell adhesion on gradient poly(2-hydroxyethyl methacrylate)-grafted surfaces. Langmuir, 2005. 21(26): p. 12309-12314.
62. Kipper MJ, Kleinman HK, and Wang FW, Covalent surface chemistry gradients for presenting bioactive peptides. Analytical Biochemistry, 2007. 363(2): p. 175-184.
63. Simon CG, Stephens JS, Dorsey SM, and Becker ML, Fabrication of combinatorial polymer scaffold libraries. Review of Scientific Instruments, 2007. 78(7): p. -.
64. Yang Y, Bolikal D, Becker ML, Kohn J, Zeiger DN, and Simon CG, Combinatorial polymer scaffold libraries for screening cell-biomaterial interactions in 3D. Advanced Materials, 2008. 20(11): p. 2037-2043.
65. Chatterjee K, Young MF, and Simon CG, Fabricating gradient hydrogel scaffolds for 3D cell culture. Combinatorial Chemistry & High Throughput Screening, 2011. 14(4): p. 227-236.
66. Chatterjee K, Lin-Gibson S, Wallace WE, Parekh SH, Lee YJ, Cicerone MT, Young MF, and Simon Jr CG, The effect of 3D hydrogel scaffold modulus on osteoblast differentiation and mineralization revealed by combinatorial screening. Biomaterials, 2010. 31(19): p. 5051-5062.
67. Oliveira MB, Salgado CL, Song WL, and Mano JF, Combinatorial on-chip study of miniaturized 3D porous scaffolds using a patterned superhydrophobic platform. Small, 2013. 9(5): p. 768-778.
68. Yune PS, Kilduff JE, and Belfort G, Searching for novel membrane chemistries: Producing a large library from a single graft monomer at high throughput. Journal of Membrane Science, 2012. 390: p. 1-11.
69. Zhou MY, Liu HW, Kilduff JE, Langer R, Anderson DG, and Belfort G, High-throughput membrane surface modification to control NOM fouling. Environmental Science & Technology, 2009. 43(10): p. 3865-3871.

Chapter 3 - Combinatorial synthesis of photo-crosslinked biodegradable networks

Erwin Zant, Mirjam J. Bosman, Dirk W. Grijpma

Journal of Applied Biomaterials & Functional Materials, 2012. 10(3): p. 197-202.

Abstract

Photo-crosslinking is a technique that can accelerate the development of novel polymeric biomaterials. Here we show the development of a combinatorial platform to synthesize numerous synthetic biodegradable and biocompatible networks by photo-crosslinking mixtures of macromers. Combinations of dimethacrylate-terminated macromers based on hydrophobic D,L-lactide (DLLA), trimethylene carbonate (TMC), ε-caprolactone (CL) and hydrophilic polyethylene glycol (PEG) were crosslinked into polymer networks with widely differing properties. The interaction of cells with the network surfaces was evaluated by an *in vitro* cell seeding experiment in which the cell proliferation was assessed using a DNA proliferation assay. In this way, a hydrophilic material was identified that unexpectedly supported the proliferation of cells very well.

Introduction

Combinatorial and high throughput approaches are widely applied to material experimentations in to explore a large compositional space within a short time [1, 2]. In this way, researchers can rapidly develop structure-function relationships or find unexpected new biomaterials with a specific desired response. Producing vast combinatorial material libraries on a small scale that allows high throughput analyses can be of particular interest when there is no theoretical basis for predicting the performance of the materials. This is often the situation when considering synthetic polymeric biomaterials because there is still very limited knowledge regarding the factors that determine the interaction of cells with the surfaces of these materials. One of the important topics in tissue engineering, for example, is the development of materials with which to prepare scaffolds that provide a proper environment for the reconstruction of functional tissue. These materials primarily concern synthetic biodegradable polymers, as this class of materials offers advantages like control over composition and physical properties and induce a minimal chronic foreign body reaction when implanted *in vivo*. Furthermore, they are easy to produce. These materials can lead to better recovery of the tissue and are therefore often applied in tissue repair and -remodeling [3]. While many such materials have been considered, combinatorial and high throughput methods can be very effective in the development of novel synthetic biomaterials for tissue engineering.

Parallel polymer synthesis has gained much interest over the years, and researchers have evaluated different polymerization strategies to allow high throughput syntheses. The simultaneous high throughput preparation of a large number of different synthetic polymers was already published in 1997 by Kohn and coworkers [4]. These researchers were able to create 112 different materials using multiple polycondensations in parallel. This yielded an array of many chemically and physically distinct materials. Later, Anderson and coworkers reported on the use of photo-crosslinking low molecular weight diacrylate-functionalized oligomers [5]. These macromonomers (macromers) were synthesized from combinations of a variety of amines and diacrylates via Michael addition reactions. They showed that mixing such non-biodegradable low molecular weight molecules followed by radical crosslinking was a

straightforward way to synthesize many materials in a single step. Using biodegradable macromers and subsequent photo-crosslinking them can have huge benefits in developing new synthetic biomaterials for tissue engineering in high throughput.

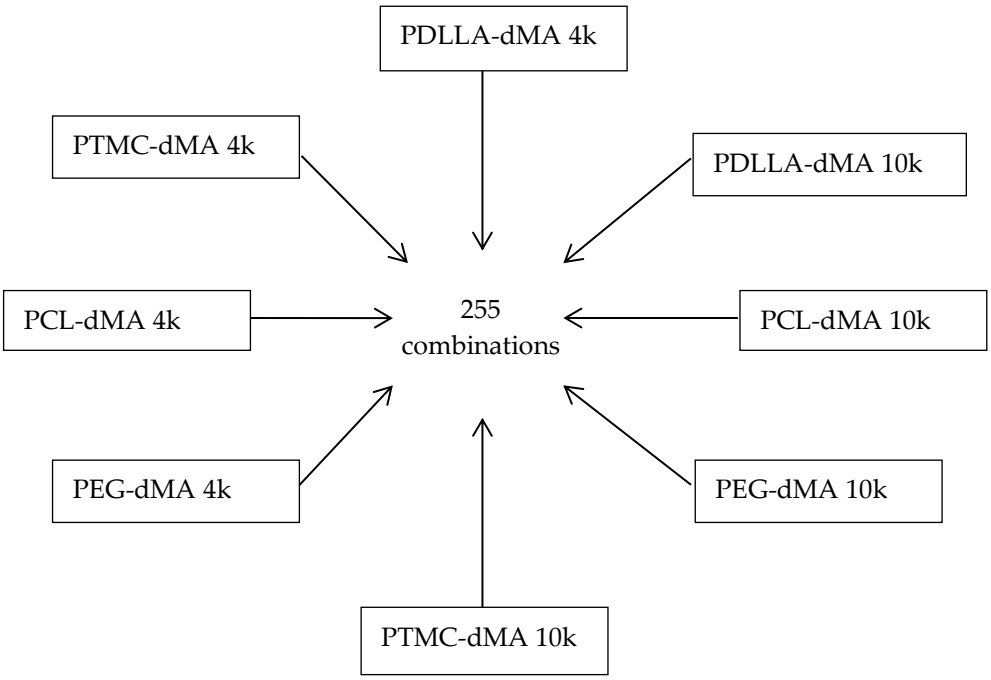

Figure 1. The eight starting materials which upon combinatorial mixing (the different macromers are either present in the mixture or not) and subsequent photo-crosslinking yield 255 different networks.

Figure 1 shows that the mixing of only 8 different dimethacrylate-terminated macromers based on hydrophobic D,L-lactide (DLLA), ε-caprolactone (CL), trimethylene carbonate (TMC) and hydrophilic polyethylene glycol (PEG) macromers can already lead to the simultaneous preparation of 255 (2^8-1) different polymer networks upon crosslinking.

This paper describes the development of a combinatorial platform to simultaneously synthesize large numbers of synthetic biodegradable and biocompatible polymer networks by photo-crosslinking mixtures of macromers. In

this manner we aim to find specific network compositions that show unexpected biological behavior.

Materials and methods

Materials

Trimethylene carbonate (1,3-dioxan-2-one, TMC) was obtained from Boehringer Ingelheim, Germany. D,L-lactide (DLLA) was obtained from Purac Biochem, The Netherlands. Stannous octoate ($Sn(Oct)_2$), ε-caprolactone (CL), 1,6-hexanediol, methacrylic anhydride, trimethylamine (TEA), calcium chloride, deuterated chloroform and polyethylene glycol (PEG) were purchased from Sigma-Aldrich, USA. Dichloromethane (DCM) was obtained from Biosolve, The Netherlands. Calcium hydride (CaH_2) was purchased from Merck, Germany. Ethanol and acetone were purchased from Assink Chemie, The Netherlands. Diethyl ether was obtained from Fisher Scientific, Germany. Irgacure 2959 was obtained from Ciba, Switzerland. DNA CyQUANT® cell proliferation kit, Phosphate Buffered Saline (PBS) and Dulbecco's Modified Eagles Medium (DMEM; containing glucose, L-glutamine, phenol red, fetal bovine serum (10%) and penicillin/streptomycin (1%)) were purchased from Invitrogen, USA.

Synthesis and characterization of dimethacrylate functionalized PTMC, PDLLA, PCL and PEG oligomers

Bifunctional oligomers with hydroxyl endgroups and molecular weights of 4,000 g/mol and 10,000 g/mol were prepared by ring-opening polymerization of TMC, DLLA or CL monomers. The polymerization was performed in an inert argon atmosphere in the presence of hexanediol as initiator and $Sn(Oct)_2$ as catalyst at 130°C for 2 days. The oligomers were dried at 120°C under vacuum for 2 h, and cooled to room temperature under argon. Dry DCM (dried over CaH_2) (3 mL/g oligomer) was added, then TEA (4 mol/mol oligomer, 100% excess) and methacrylic anhydride (4 mol/mol oligomer, 100% excess) was added. The contents

were thoroughly mixed. The functionalization reaction proceeded for 5 d at room temperature, the structure of the obtained macromers is presented in Figure 2. The macromers were purified by precipitation and subsequent drying. PTMC-dMA, PDLLA-dMA, and PCL-dMA were precipitated in ethanol while PEG-dMA) was precipitated in diethylether. Proton nuclear magnetic resonance (^{1}H-NMR) spectra were recorded on a Varian Inova 300 MHz NMR spectrometer, deuterated chloroform was used as a solvent. The oligomer and macromer number average molecular weights (Mn), and the degrees of functionalization (f) of the macromers were determined from the spectra.

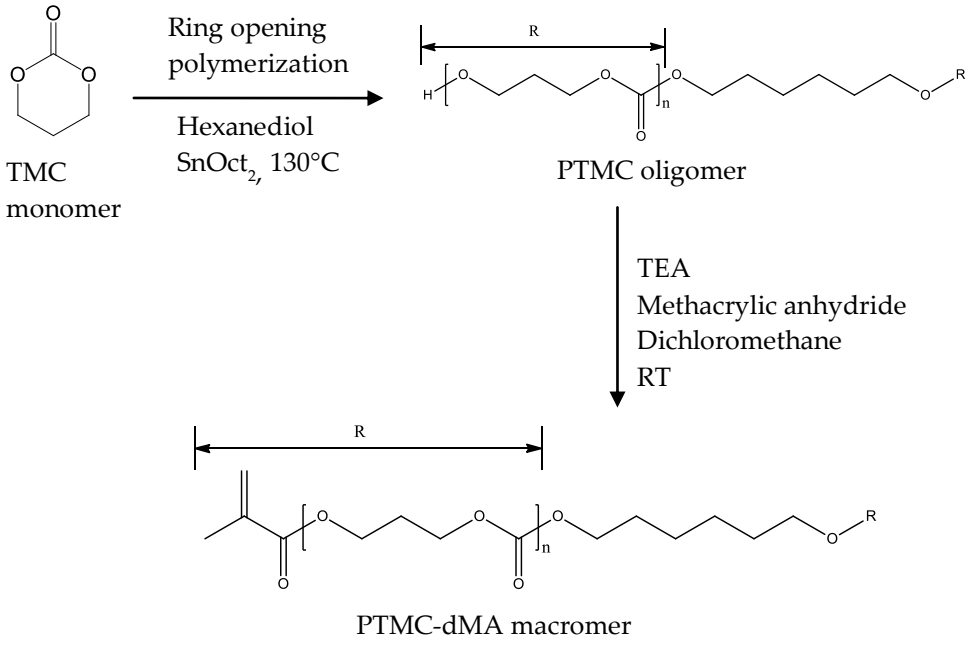

Figure 2: Synthesis of dimethacrylate functionalized linear PTMC macromers (PTMC-dMA). PDLLA-dMA and PCL-dMA macromers were prepared in an analogous way. PEG-dMA was prepared by reaction of commercially available PEG with methacrylic anhydride.

Preparation and characterization of networks

Networks were prepared from the PTMC-dMA, PDLLA-dMA, PCL-dMA and PEG-dMA macromers. The macromers were first dissolved in DCM (0.2 g/ml). Subsequently, 1 wt% (with respect to the macromer) of Irgacure 2959 photoinitiator was added. After mixing, the macromer solutions were poured into a Teflon mold, and photocrosslinked in an Ultralum (USA) crosslinking cabinet (365 nm, 3-5 mW/cm2, 20 min) under nitrogen atmosphere to prevent oxygen inhibition. Disk-shaped samples with a diameter of approximately 10 mm and thickness of approximately 0.5 mm were obtained. To determine the gel contents after crosslinking, the obtained network specimens (n=3) were vacuum-dried overnight and weighed (m_0), then extracted with acetone/water (50/50 volume mixture) for 3 days and vacuum dried until constant weight. The mass of the dry networks (m_1) was then determined. The gel content is defined as:

$$\text{gel content} = \frac{m_1}{m_0} \times 100\%$$

To determine the water uptake, network specimens (extracted, n=3) were incubated in distilled water for 1 day. Then the samples were removed from the water, blotted dry and weighed (m_s). The water uptake was calculated using:

$$\text{water uptake} = \frac{m_s - m_1}{m_1} \times 100\%$$

Mechanical tests were performed on crosslinked, dried and extracted strips (n=3) with final dimensions of 100x6x0.4mm^3. Elastic moduli (E_{mod}), strains at break (ε_b) and ultimate tensile strengths (σ_s) were determined using a Zwick Z020 tensile tester equipped with a 500 N load cell at 10mm/min at room temperature with a grip-to-grip separation of 50 mm.

Differential Scanning Calorimetry (DSC) was used to determine the glass transition temperature (T_g) and the melting temperature (T_m) of the synthesized networks. DSC measurements were done using a liquid nitrogen cooled Pyris 1 DSC (Perkin Elmer, USA). Dry samples weighing 5-10 mg were heated to 100°C at a rate of 10°C/min, kept for 1 min at 100°C and then cooled to -100°C at a rate of 200°C/min. After 5 min at this temperature, a second scan was recorded from -100°C to 100°C at 10°C/min. T_m and T_g of the specimens were determined in the second scan. Wet

samples equilibrated in water at room temperature weighing 5-10 mg were heated to 70°C at a rate of 10°C/min and then cooled to 5°C at a rate of 200°C/min. After 5 min at this temperature, a second scan was recorded from 5°C to 70°C at 10°C/min and T_m and T_g were determined.

In vitro cell culturing of C2C12 myoblasts

Sample preparation: 255 different macromer mixtures were prepared in a polypropylene 96 wells plate. UV crosslinking was performed for 30 min under nitrogen atmosphere. After drying the networks in a vacuum oven for 3 days, the plates were sprayed with 70% ethanol and subsequently dried in a laminar flow cabinet in order to disinfect the plates and specimens. Then the networks were incubated in 200 μL DMEM medium for 24h.

Cell culturing: C2C12 mouse myoblasts were cultured in humidified atmosphere of 5% CO_2 at 37°C in culture flasks containing DMEM medium. Cell seeding was performed onto the networks at a density of 5000 cells/cm^2. Culturing proceeded for 4 days. Cells were also seeded and cultured on tissue culture polystyrene (TCPS) (n=3) as a reference.

DNA proliferation assay: After the medium was discarded, the samples were washed twice with warm PBS (37°C) and subsequently lysed in lysing buffer (DNA proliferation kit, Invitrogen, diluted 20x in distilled water). Then, the samples were frozen at -80°C overnight and subsequently thawed to room temperature. After centrifugation at 3000 rpm for 3 min 50 μL of the supernatant was transferred to 96-well plates and mixed with 50 μL lysing agent. After 1 hour, 100 μL CyQUANT® GR dye (DNA proliferation kit, Invitrogen) (1:400 dilution with lysing agent) was added to the wells and the samples were incubated in the dark for 30 minutes. Subsequently fluorescence was measured.

Results and Discussion

Synthesis and characterization of dimethacrylate functionalized PTMC, PDLLA, PCL and PEG oligomers

With hexanediol as a bifunctional initiator, TMC, DLLA and CL were polymerized by ring opening polymerization to yield linear oligomers with targeted molecular weights of 4,000 g/mol and 10,000 g/mol. PEG with molecular weights 4,000 g/mol and 10,000 g/mol was used as received. Methacrylic anhydride was reacted with the oligomers to obtain crosslinkable macromers. The successful coupling was confirmed by the disappearance of the resonance peak from the $–CH_2-OH$ of the oligomer at δ 4.35 ppm and the appearance of a resonance peak from the $–CH_2=CH_2$ of the macromer at δ 6.14 ppm and δ 5.59 ppm in the ^{1}H-NMR spectra of the reaction products. The degrees of functionalization (f) and the obtained molecular weights are listed in Table 1.

Table 1: Obtained molecular weights and degrees of conversion of the synthesized macromers as determined by ^{1}H-NMR

Macromer	**Mn** kg/mol	**f** %
PTMC-dMA 4k	4.1	88
PDLLA-dMA 4k	4.5	84
PCL-dMA 4k	4.8	95
PEG-dMA 4k	5.1	97
PTMC-dMA 10k	9.3	90
PDLLA-dMA 10k	10.6	77
PCL-dMA 10k	9.6	100
PEG-dMA 10k	11.2	95

Synthesis and characterization of PTMC, PDLLA, PCL, and PEG networks

The macromers easily dissolved in DCM at a concentration of 0.2 g/ml. After crosslinking, extraction and drying, the gel contents of the obtained networks ranged between 75-99%. This confirmed a good conversion of the macromers to a network.

Table 2: Thermal properties of the different networks obtained after photo-crosslinking the homopolymeric macromers

Network component	**T_g dry** °C	**T_m dry** °C	**ΔH_m dry** J/g	**T_g wet** °C	**T_m wet** °C	**ΔH_m wet** J/g
PTMC-dMA 4k	-15.6	-	-	-	-	-
PDLLA-dMA 4k	50.9	-	-	-	-	-
PCL-dMA 4k	-63.2	51.1	52.9	-	51.2	52.3
PEG-dMA 4k		45.7	75.9	-	-	-
PTMC-dMA 10k	-14.4			-	-	-
PDLLA-dMA 10k	50.7			40	-	-
PCL-dMA 10k	-66.6	53.9	59.6	-	51.5	55.0
PEG-dMA 10k		55.1	99.8	-	-	-

The thermal analyses of the networks listed in Table 2, shows that T_g values of the obtained different networks widely varied. The table also shows that networks prepared from CL and PEG macromers were semi-crystalline. In the wet state, networks prepared from hydrophilic PEG-dMA macromers took up significant amounts of water. Consequently the crystallinity of these PEG domains disappeared, as can be observed by the absence of melting peaks the hydrated PEG-dMA 4k and PEG-dMA 10k networks. The glass transition temperature and the water uptake of the networks had a large effect on their mechanical properties. These values are presented in Table 3.

Table 3: Water uptake and tensile properties of the different networks obtained after photo-crosslinking the homopolymeric macromers

Network component	**Gel content**	**Water uptake**	**Emod dry**	**ε_b dry**	**σ_s dry**	**Emod wet**	**ε_b wet**	**σ_s wet**
	%	%	MPa	%	MPa	MPa	%	MPa
PTMC-dMA 4k	87	1	4	108	2	4	110	2
PDLLA-dMA 4k	80	10	1150	1	-	869	1	6
PCL-dMA 4k	96	2	238	-	11	269	6	9
PEG-dMA 4k	90	641	232	7	9	0.3	-	-
PTMC-dMA 10k	87	9	6	243	3	1	160	1
PDLLA-dMA 10k	94	23	1867	1	20	978	1	10
PCL-dMA 10k	99	2	394	10	17	172	6	6
PEG-dMA 10k	75	1706	295	9	14	0.03	9	-

In vitro cell culturing of C2C12 myoblasts on the different photo-crosslinked networks

Knowing that the mechanical-, thermal properties and water uptake of networks prepared from the homopolymeric macromer starting materials widely differ, the interaction of cells with the surfaces of the networks can also be highly diverse. However, while the thermal and mechanical properties of networks prepared from combinations of the abovementioned macromers are as could be expected, their biological performance remains completely unpredictable.

Single screening experiment. In order to facilitate the rapid discovery of networks that show good cell support, 255 different networks were simultaneously prepared from macromer mixtures in the wells of polypropylene 96 wells plates. A 4 day cell culture experiment showed that the surfaces of some of the prepared networks allowed good cell adhesion and proliferation. With the use of data binning, as shown in Figure 3, networks which supported high cell growth and adhesion could be identified.

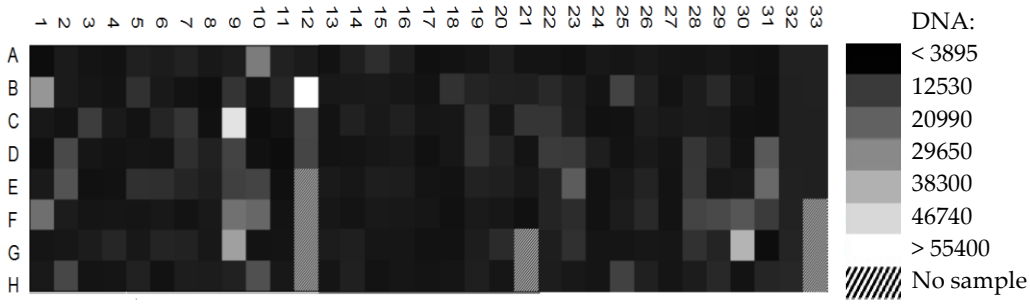

Figure 3: Results of DNA Cyquant assay analyses of cells cultured on the surfaces of different photo-crosslinked networks prepared from mixtures of PTMC-dMA, PDLLA-dMA, PCL-dMA and PEG-dMA macromers. High DNA contents (high numbers of adhering cells) are shown in white or light grey, low DNA contents in black.

Repeated cell culturing experiments. It is known from literature that cells respond to the hydrophilicity or wettability of material surfaces [6]. Both highly hydrophilic and highly hydrophobic surfaces allow limited cell attachment and growth. The *in vitro* cell seeding and culturing experiments were repeated for several of the very hydrophilic networks. Water uptake can be considered as a measure for the hydrophilicity of polymer networks [7]. The hydrophilic networks with their corresponding water uptakes are listed in Table 4.

Table 4: Network compositions and water uptake of hydrophilic networks used in the repeated cell culturing experiments. The values indicate the weight percentages of the respective macromers in the photo-crosslinked mixtures.

Network number	PTMC-dMA 4k	PDLLA-dMA 4k	PCL-dMA 4k	PEG-dMA 4k	PTMC-dMA 10k	PDLLA-dMA 10k	PCL-dMA 10k	PEG-dMA 10k	Water uptake %
1		33	33	33					104
2		33				33		33	174
3			33	33			33		59
4				33	33		33		43
5					33	33		33	260
6	17	17			17	17	17	17	88

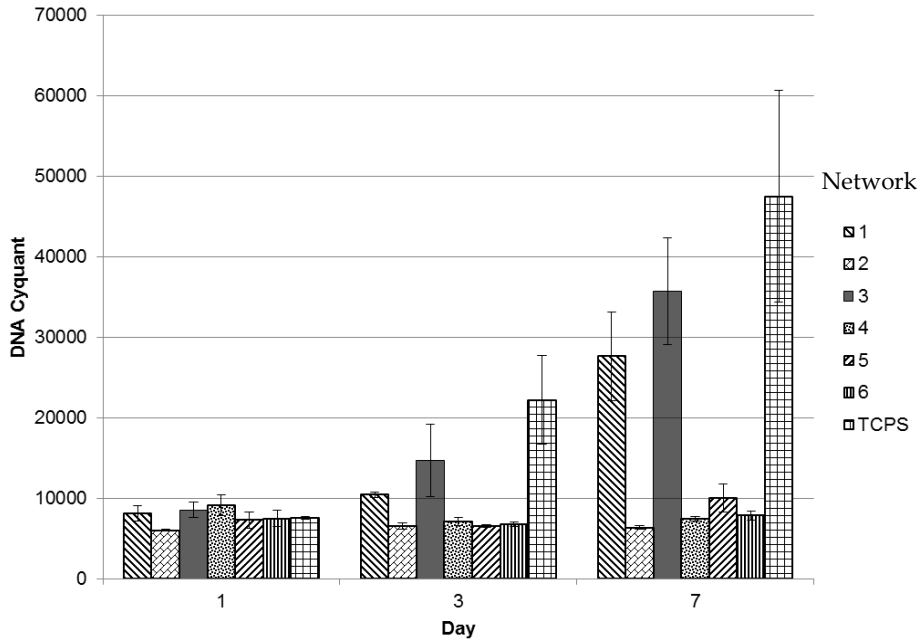

Figure 4: DNA Cyquant® proliferation assay results in which the amount of DNA of adherent cells at day 1, 3 and 7 on the surface of the networks presented in Table 4 was determined. On day 7 networks 1 and 3 had statistically equal amounts of adhering cells on their surface as TCPS. Other specimens performed significantly worse than networks 1, 3 and TCPS. The means were compared using an independent samples T-test (95% confidence interval).

The performance of these materials with regard to allowing the adhesion and proliferation of cells were evaluated again in a repeated more extensive *in vitro* cell culturing experiment. The cells were seeded on 5 replicate specimens and at time-points of 1, 3 and 7 days. The DNA from the adherent cells was extracted and quantified, resulting in the data presented in Figure 4. The figure shows that cell growth was quite pronounced on networks 1 and 3. It is quite unexpected that network 1 shows such good cell attachment and proliferation, as this network also takes up very high amounts of water. Other network specimens with high water uptake (networks 2, 5 and 6) do not show good support for cell adhesion. From this data, no correlation could be found between water uptake and cell adhesion numbers.

Conclusions

A fast method to synthesize a large number of different materials in a single step was developed. Combinatorial mixing of eight different macromers at different concentrations and subsequent photo-crosslinking yielded networks with highly differing physical and biological characteristics. Especially interesting is that specific combinations yielded hydrophilic compounds which at the same time showed very good interaction with cells. The results presented in this paper revealed that a combination of 33 wt.% of PDLLA-dMA 4k, 33 wt.% PCL-dMA 4k and 33 wt.% PEG-dMA 4k, while having a fairly high water uptake of 104%, performed surprisingly good in supporting C2C12 cell proliferation. Networks prepared from this combination of macromers can therefore be of particular interest for tissue engineering applications.

It should be noted that in this work dichloromethane was used to dissolve and to photo-crosslink the macromers in. Premature evaporation of this volatile solvent in many cases resulted in macroscopically phase separated networks with relatively poor mechanical properties. In later work we made use of a non-volatile solvent (propylene carbonate) and photo-crosslinked networks with much better mechanical properties were obtained. This is described in Chapters 4 and 5 of this thesis.

Acknowledgements

We would like to acknowledge the Netherlands Institute for Regenerative Medicine (NIRM) (Grant No. FES0908).for financial support.

References

1. Simon Jr CG and Sheng LG, Combinatorial and high-throughput screening of biomaterials. Advanced Materials, 2011. 23(3): p. 369-387.
2. Webster DC, Combinatorial and high-throughput methods in macromolecular materials research and development. Macromolecular Chemistry and Physics, 2008. 209(3): p. 237-246.

3. Lanza R, Langer R, and Vacanti J, Principles of tissue engineering (third edition). 2007: Elsevier.
4. Brocchini S, James K, Tangpasuthadol V, and Kohn J, A combinatorial approach for polymer design. Journal of the American Chemical Society, 1997. 119(19): p. 4553-4554.
5. Anderson DG, Tweedie CA, Hossain N, Navarro SM, Brey DM, Van Vliet KJ, Langer R, and Burdick JA, A combinatorial library of photocrosslinkable and degradable materials. Advanced Materials, 2006. 18(19): p. 2614-2618.
6. Folkman J and Moscona A, Role of cell-shape in growth-control. Nature, 1978. 273(5661): p. 345-349.
7. Hoffman AS, Hydrogels for biomedical applications. Advanced Drug Delivery Reviews, 2002. 54(1): p. 3-12.

Chapter 4 - Tough biodegradable mixed-macromer networks and hydrogels by photo-crosslinking in solution

Erwin Zant, Dirk W. Grijpma

Acta Biomaterialia, resubmitted after revision

Abstract

The preparation of polymeric networks that are both tough and biodegradable remains a challenge. Here we show a very straightforward method to produce tough biodegradable networks from low molecular weight macromers for applications such as tissue engineering. Photo-crosslinking combinatorial mixtures of methacrylate-functionalized poly(1,3-trimethylene carbonate) (PTMC), poly(D,L-lactide) (PDLLA), poly(ε-caprolactone) (PCL) and poly(ethylene glycol) (PEG) oligomers in propylene carbonate (PC) allowed the preparation of network films with excellent tensile characteristics and resistance to tearing. This method enabled the production of both very tough mixed-macromer elastomers as well as mixed-macromer hydrogels. A mixed-macromer hydrogel prepared from 33 wt.% PTMC, 33 wt.% PCL and 33 wt.% PEG had a very high tearing energy of 0.81 kJ/m^2, which is comparable to tearing energies determined for articular cartilage.

Introduction

Tough biodegradable polymer networks have great potential to be used as load bearing implants, for example in tissue engineering applications. Specifically elastomeric polymer networks are of interest. They can be designed to have mechanical properties that match those of load bearing tissues like cartilage and withstand dynamic loading [1]. Much attention has been paid to improve the toughness of biodegradable elastomers, but simultaneously achieving biodegradability and toughness remains a challenge.

To obtain high toughness and tear strength in polymer networks, the growth of micro-cracks should be hindered [2]. This has been studied extensively for natural and synthetic elastomers. Micro-crack growth has been slowed down by the addition of filler particles, the introduction of crystallizable domains in the polymer network, crosslinking chains with bimodal chain length distributions, and crosslinking in a diluted state [3-8]. Much of the fundamental research on toughening has been conducted using non-biodegradable elastomers like polyisoprene and poly(dimethyl siloxane) (PDMS). However, the development of tough and tear-resistant biodegradable elastomers is very limited.

We have prepared flexible, elastic and tough networks that are biocompatible and biodegradable by γ-irradiation of high molecular weight poly(1,3-trimethylene carbonate) (PTMC) [9-11] and by photo-crosslinking methacrylate-functionalized PTMC oligomers (PTMC macromers) [12, 13]. In the latter case, toughness was found to improve with increasing molecular weight of macromers. As such, PTMC networks were found to show even higher toughness than high molecular weight linear PTMC. Furthermore, the tear propagation strength was found to increase from 1.9 N/mm to 9.3 N/mm when high molecular weight PTMC compounded with pentaerythritol triacrylate (PETA) was γ-irradiated [14]. Amsden and co-workers photo-crosslinked an acrylated poly(ε-caprolactone-*co*-D,L-lactide) P(CL-*co*-DLLA) oligomer dissolved at different concentrations in dichloromethane. The obtained networks became less rigid and strong, and more extendable with decreasing macromer concentrations during the crosslinking [15]. Photo-crosslinking fumarate-functionalized copolymers with different contents of TMC, DLLA and CL yielded elastomers with a wide range of mechanical properties [16].

Hydrogels (hydrophilic polymer networks) are another class of networks that are of great interest for use in tissue engineering. In aqueous environments these networks have high water contents and low rigidity, and as a rule are fragile and very weak [17]. Toughening of polyvinylalcohol (PVA), polyacrylamide (PAA), poly(hydroxyethylmethacrylate) (PHEMA) or polyethylene glycol (PEG) hydrogels has been done by preparing interpenetrating networks, ionic networks or composite networks [18]. Although the tensile strengths and tearing energies of the hydrogels are much improved compared to the unmodified hydrogels, these hydrogels are still less tough than load bearing tissues. They are also non-biodegradable. Extremely high toughness in PAA hydrogels has been achieved by Gong and co-workers. Interpenetrating double networks comprising a loosely crosslinked PAA network and a densely crosslinked poly(2-acrylamido-2-methylpropanesulfonic acid) (PAMPS) network were prepared, yielding hydrogels with exceptionally high strengths and toughnesses [19]. PAA is, however, non-biodegradable and residues of the acrylamide monomer are potentially toxic. Recently, we prepared tough biodegradable hydrogels based on PEG by crosslinking methacrylate-functionalized PTMC-PEG-PTMC [20] and PDLLA-PEG-PDLLA [21] triblock copolymers. Although the hydrogels were shown to be quite resilient, their mechanical properties were not extensively studied.

It is clear that considerable work has been done to prepare (co)polymer networks with optimized mechanical properties for specific applications. However, the design and the syntheses of the networks is time-consuming and the number of network compositions that can be prepared is limited. The discovery of new materials may be more efficient if a combinatorial chemistry approach is taken. Combinatorial chemistry has been successfully used to discover new drugs and polymeric biomaterials [22, 23]. However, the preparation of tough combinatorial networks based on combinations of macromers (mixed-macromer networks) has not yet been reported.

In this paper we describe the preparation of mixed-macromer networks and hydrogels by photo-crosslinking combinatorial mixtures of methacrylate-functionalized PTMC-, PDLLA-, PCL- and PEG- macromers in solution using an inert solvent with low vapor pressure and a high boiling. We anticipated that the crosslinking of mixed-macromer networks would yield networks with high

toughness since multiphase networks can possibly contribute to an increase of the tearing strength. Furthermore, crosslinking in solution was also expected to improve the toughness of the networks significantly.

Materials and methods

Materials

Polyethylene glycol (PEG) (Mn=10 kg/mol), stannous octoate ($Sn(Oct)_2$), ε-caprolactone (CL), 1,6-hexanediol, methacrylic anhydride, triethylamine (TEA), deuterated chloroform, trifluoroacetic anhydride (TFAA) were purchased from Sigma-Aldrich (The Netherlands). Trimethylene carbonate (1,3-dioxan-2-one, TMC) was obtained from Huizhou Foryou Medical Devices Co (China). D,L-lactide (DLLA) was obtained from Purac Biochem (The Netherlands). Dichloromethane (DCM) was obtained from Biosolve (The Netherlands). Calcium hydride (CaH_2) and propylene carbonate (PC, boiling point 242 °C) were purchased from Merck (Germany). Ethanol was obtained from Assink Chemie (The Netherlands). Diethyl ether was obtained from Fisher Scientific. Irgacure 2959 (2-hydroxy-4-(2-hydroxyethoxy)-2-methylpropiophenone) was obtained from Ciba (Switzerland).

Synthesis of dimethacrylate-functionalized PTMC, PDLLA, PCL and PEG oligomers

Linear oligomers were prepared by ring-opening polymerization of TMC-, DLLA- or CL monomers. Polymerization was performed in an inert argon atmosphere in the presence of 1,6-hexanediol as initiator (0.25 mmol/g monomer to obtain an oligomer with Mn=4 kg/mol, and 0.1 mmol/g monomer to obtain an oligomer with Mn=10 kg/mol) at 130 °C for two days. Sn(Oct2) was used as catalyst (0.02 mmol/g monomer). The oligomers were dried at 120 °C under vacuum for 2 h, and cooled to room temperature under argon. Dry DCM (dried over CaH_2 and distilled, 3 mL/g oligomer) was added, then TEA (4 mol/mol oligomer) and methacrylic anhydride (4 mol/mol oligomer) were added. The functionalization reaction

proceeded for five days at room temperature. The dimethacrylate (dMA)-functionalized macromers were purified by precipitation. PTMC-dMA, PDLLA-dMA, and PCL-dMA were precipitated in cold ethanol (-25°C) and PEG-dMA was precipitated in cold diethylether (-25°C). The macromers were subsequently dried under vacuum at 40-50 °C for 3 days.

Preparation of photo-crosslinked networks

PTMC-dMA, PDLLA-dMA, PCL-dMA and PEG-dMA single-macromer networks were prepared by crosslinking the individual macromers in propylene carbonate solutions containing 1 wt.% Irgacure 2959 photo initiator. To assess the effect of the macromer concentration during crosslinking, PTMC-dMA was photo-crosslinked in solutions containing 20, 33 and 50 wt.% macromer first. The solutions were cast on a glass plate at a thickness of 0.5 mm and crosslinked by irradiation at 365 nm for 20 minutes at 10 mW/cm^2 in a nitrogen atmosphere at 50°C. The crosslinked films were extracted with a mixture of acetone and ethanol (50/50 vol./vol.), the solvent was refreshed every 24h during three days. The extracted films were washed with ethanol and dried under reduced pressure at 50 °C until a constant weight was reached. To crosslink in bulk, a PTMC-dMA solution in DCM that contained 33 wt.% macromer was prepared and cast on glass, then the DCM was allowed to evaporate. Crosslinking, extraction, washing, and drying was performed as described above.

Eleven different mixed-macromer networks were then prepared by crosslinking mixtures of PTMC-dMA, PDLLA-dMA, PCL-dMA and PEG-dMA macromers dissolved in PC. In these mixtures the macromers were present in equal weight percentages and the concentration of macromers was 33 wt.%. The mixed-macromer solutions were cast, crosslinked, dried and extracted as described above. See Table 4 for an overview. Although PCL-dMA 10k is soluble in PC at 50°C, the solubility of this macromer was much lower in the presence of other macromers. As it was found that in solution mixtures with PCL-dMA 4k were clear, only this macromer was used to prepare mixed-macromer networks.

Characterization of macromers and photo-crosslinked networks

The macromer number average molecular weights (Mn) and the degrees of functionalization (f) were determined using a Varian Inova 400 MHz ^{1}H-NMR spectrometer in deuterated chloroform.

Differential Scanning Calorimetry (DSC) was used to determine the glass transition temperature (T_g), the melting temperature (T_m) and melting enthalpy (ΔH_m) of the macromers and networks. DSC measurements were performed using a liquid nitrogen-cooled Pyris 1 DSC (Perkin Elmer, USA). Samples weighing 5-10 mg were heated to 100 °C at a rate of 10 °C/min, kept for one minute at 100 °C and then cooled to -100 °C at a rate of 200 °C/min. After five minutes at -100 °C, a second scan was recorded from -100 °C to 100 °C at 10 °C/min. The thermal transitions of the specimens, T_g (midpoint), T_m (peak) and ΔH_m were determined in the second heating scan.

The mechanical properties of the dry and the hydrated networks were assessed using a Zwick Z020 tensile tester (Germany), equipped with a 500 N load cell at room temperature (20°C). The elongation of the samples was derived from the grip-to-grip separation, which was initially 35 mm. Experiments were conducted in triplicate, unless otherwise mentioned. Tensile modulus (E), ultimate strength (σ_{max}) and elongation at break (ε_{max}) were determined according to ASTM D882 using dumbbell-shaped specimens (50 x 9 mm) at a test speed of 10 mm/min. The toughness ($W_{tensile}$, expressed in N/mm^2) of the tensile specimens was defined as the area under the stress-strain curve. The average- (TPS_{ave}) and maximum (TPS_{max}) tear propagation strengths were determined according to ASTM D1938 using trouser shaped specimens (37.5 x 12.5 mm with a 25 mm slit) at a test speed of 250 mm/min. The tearing energy (G, expressed in kJ/m^2) was calculated according to [3]:

$$G = \frac{2F}{t}$$

Here, F is the average force during tearing (N) and t is the thickness of the sample (mm).

The fracture surface of tear specimens torn in the dry state was visualized by scanning electron microscopy (SEM, Philips XL 30 ESEM-FEG). Cross-sections of the specimens were gold-sputtered. The more hydrophilic networks containing PEG were immersed in distilled water for 48h yielding swollen mixed-macromer hydrogels. Water uptake was calculated using:

$$\text{water uptake} = \frac{m_s - m_0}{m_0} \times 100\%$$

Where m_s is the weight of a swollen network (g) and m_0 the weight of an extracted and dried network (g).

Results and discussion

Synthesis and characterization of macromers

Linear dimethacrylate end-capped macromers were synthesized as described. The molecular weights (M_n) and conversions determined by ^{1}H-NMR of all macromers are listed in Table 1 (the ^{1}H-NMR spectra are shown in Figure SI1). Successful reaction of the oligomers with methacrylic anhydride was confirmed by the appearance of –C=CH$_2$ and the –CH$_3$ peaks of methacrylate endgroups at δ=6.11, δ=5.57 and δ=1.94 ppm. The degree of functionalization of PTMC macromers was determined by comparing the integral values of the –CH$_2$– peak of hexanediol at δ 1.68 and the –C=CH$_2$ peaks at δ=6.11 and δ=5.57 ppm. For PDLLA macromers, the integral value of the –O–CH$_2$– peak of hexanediol at δ 4.12 ppm was used. For PCL macromers, the integral value of the HO–CH$_2$– peak of any residual oligomer at δ 3.64 ppm was used. The degree of functionalization of PEG macromers was determined after addition of TFAA: residual, unreacted OH-groups of the oligomer will react with this highly electronegative anhydride yielding a peak at δ=4.50 ppm. The integral values of this peak and the –CH$_2$–O– peak of the macromer at δ 4.31 ppm was used to determine the degree of functionalization. For all macromers conversions of at least 85% were observed, suggesting suggesting high conversion. Glass transitions and melting points of the macromers, determined by DSC, are also listed in Table 1.

Table 1: Characteristics of the different synthesized dimethacrylate-functionalized macromers. Number average molar masses (M_n) and degrees of functionalization (f) were determined by ^{1}H-NMR. Glass transition temperature (T_g), melting temperature (T_m) and melt enthalpy (ΔH_m) were determined by DSC.

Macromer	**Mn** kg/mol	**f** %	**Tg** °C	**Tm** °C	**ΔHm** J/g
PTMC-dMA 10k	9.5	90	-21.0	-	-
PDLLA-dMA 10k	10.0	85	36.1	-	-
PCL-dMA 4k	4.2	100	-55.8	53.9	74.6
PCL-dMA 10k	10.6	95	-62.3	56.9	61.7
PEG-dMA 10k	11.5	100	-48.1	57.1	137.3

Photo-crosslinking in solution

Photo-crosslinking mixtures of macromers dissolved in a common inert solvent is an approach to prepare macroscopically homogenous mixed-macromer networks. However, the concentration of the components in the solution during crosslinking will have an effect on the process of network formation and on the characteristics of the network formed. Decreasing the concentration of precursor network chains during crosslinking by dilution has a pronounced effect on the elongation at break of the networks upon extraction (de-swelling) [4, 5, 8]. And thus on their toughness. In elastomers, the maximum extensibility is mainly determined by the length of the polymeric chains between crosslinks and the number of trapped entanglements. When crosslinking in solution, the maximal elongation relates to the initial concentration of the macromer (φ) as follows [7]:

$$\lambda_{max} = {N_{e,melt}}^{1/2} \phi^{-5/6}$$

Here, $N_{e,\ melt}$ is the number of monomeric units between crosslinks or trapped entanglements when crosslinked in the absence of solvent (*i.e.* crosslinked in the melt). The maximum extensibility of a network λ_{max} will increase with decreasing concentration of the macromer during crosslinking φ.

The PTMC macromers with a molar mass of approximately 10 kg/mol were dissolved in propylene carbonate at different concentrations, cast and photo-crosslinked to give swollen networks. These were then extracted and dried. Photo-crosslinked PTMC films were also prepared in the absence of a diluent. Table 2 gives an overview of the thermal- and tensile properties of the obtained network films. As can be seen, all networks are amorphous and have low glass transition temperatures. The glass transition temperature of the networks was somewhat higher than that of the PTMC-dMA macromer. The table also shows that with increasing PC diluent concentration during crosslinking, the elongation at break and the maximum tensile strength of the networks significantly increase.

Table 2: Thermal- and tensile properties of PTMC networks obtained by photo-crosslinking PTMC-dMA 10k in PC solutions. Tensile data is presented as a mean value of triplicate measurements with the standard deviation in parentheses.

Macromer concentration in PC	**T_g**	**E**	**σ_{max}**	**ε_{max}**	**$W_{tensile}$**	**TPS_{ave}**	**TPS_{max}**	**G**
wt.%	°C	MPa	MPa	%	N/mm^2	N/mm	N/mm	kJ/m^2
20 [a]	-	-	-	-	-	-	-	-
33	-17.1	6 (2)	6.4 (1.6)	1,003 (85) [b]	3,239 (832) [b]	7.8 (0.6) [c]	9.1 (0.8) [c]	16 (1) [c]
50	-18.5	4 (1)	6.2 (2.9)	657 (89)	1,731 (661)	3.8 (0.3)	4.4 (0.6)	8 (1)
Bulk	-17.8	6 (1)	3.5 (1.2)	243 (92)	533 (301)	0.5 (0.3)	1.2 (0.3)	1 (1)
100 [d]	-16.3	5 (0)	3.7 (0.4)	244 (9)	426 (38)	-	-	-

[a] crosslinking unsuccessful, no network was obtained; [b] specimen slipped from the clamps during tensile testing; [c] n=2; [d] Network prepared by photo-crosslinking 10.3 kg/mol PTMC macromers in bulk, data from Schuller-Ravoo et al. [13]

When crosslinking in the absence of solvent (in bulk) the maximum tensile strength and elongation at break of the PTMC networks are respectively 3.5 MPa and 243 %, while crosslinking the macromer at a concentration of 33 wt.% gives networks with a maximum tensile strength of 6.4 MPa and an elongation at break of 1,003 % after extraction and drying. The E modulus is not significantly affected by crosslinking in solution. The effect of crosslinking in solution is more clearly illustrated in Figure 1a. Attempts to prepare networks at a lower concentration of 20 wt. % were not successful. No networks were obtained, likely due to too low concentrations of reactive end-groups and radicals which resulted in incomplete crosslinking and high sol contents.

With an increase in the elongation to break, the toughness of the networks also increases. The area under the tensile stress strain curve is a measure of the toughness ($W_{tensile}$) of a specimen. The toughness of PTMC networks increases very significantly from 533 N/mm^2 when prepared by photo-crosslinking PTMC-dMA 10k in the absence of diluent to 3,239 N/mm^2 when crosslinked at 33 wt.%. Schuller et al. showed that the toughness of PTMC networks can also be improved by increasing the molecular weight of the macromer [13]. Crosslinking a network from PTMC with a molar mass of 10.3 kg/mol in bulk was found to yield a yield a network with a $W_{tensile}$ of 426 N/mm^2, while the value for a network prepared from a macromer with a molar mass of 41.0 kg/mol was 5,504 N/mm^2.

The toughness was also assessed in tear propagation experiments. The resulting tearing stress-strain diagrams are shown in Figure 1b. It can be seen that the increase in toughness of PTMC networks obtained by crosslinking solution is reflected by increased tear propagation strengths. The results presented in Table 2 show that the average TPS as well as the maximum TPS increase with decreasing concentrations of PTMC-dMA 10k during crosslinking. The networks prepared from a 33 wt.% solution yielded a TPS_{ave} of 7.8 N/mm, a TPS_{max} of 9.1 N/mm and a G of 16 kJ/m^2. This latter value was even higher than that of carbon filled natural rubber (11 kJ/m^2)[3].

PDLLA-, PCL- and PEG single-macromer networks were also prepared by photo-crosslinking the respective dimethacrylate-functionalized oligomers in solution. After dissolving the macromers in PC at a macromer concentration of 33 wt.%,

films were cast, photo-crosslinked, extracted and dried as described. Table 3 gives an overview of the thermal- and tensile properties of the prepared networks. It is clear from the Table, and from Figures 1c and 1d, that these homo-macromer networks have very distinct physical characteristics. The PTMC networks are amorphous, rubber-like materials with a low glass transition of approximately -17 ^{o}C. The PDLLA networks show the typical properties of a brittle, glassy amorphous network: a high value of the elasticity modulus (3,083 MPa) and maximum tensile strength (31.0 MPa), but a low value of the elongation at break (2 %). The PCL- and PEG networks are much more ductile materials as they have a low glass transition temperature and are semi-crystalline materials at room temperature. The PEG networks have maximum tensile strengths of approximately 12.6 MPa and elongations at break of 335 %, the PCL networks have tensile strengths of approximately 18 MPa and elongations at break of 185 %. In the latter case, it does not seem that the PCL-dMA macromer has a significant effect on the tensile properties of the network. The toughness of these semi-crystalline networks is very much higher than that of the PDLLA networks.

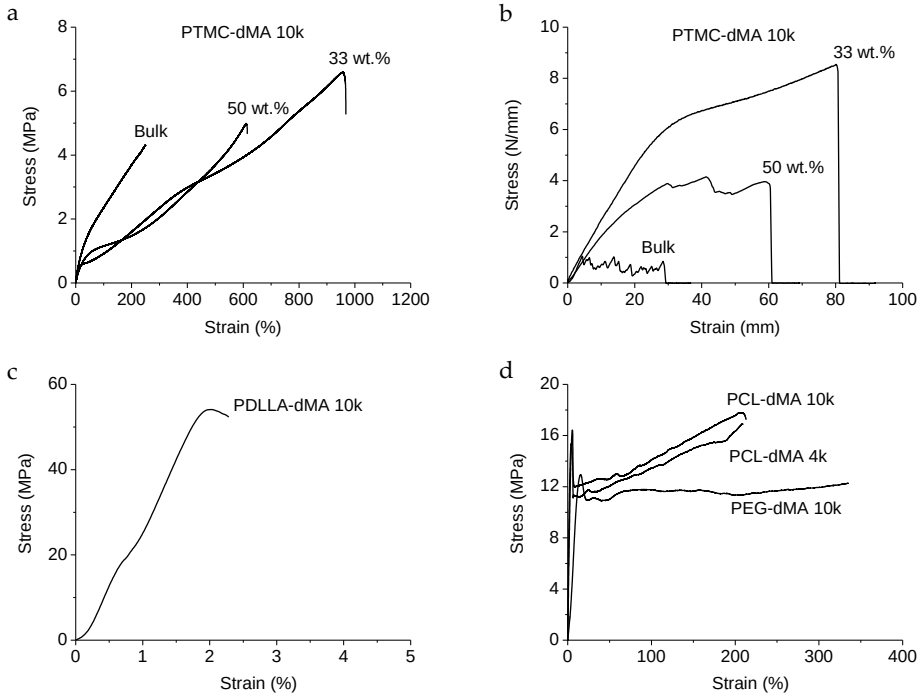

Figure 1: Stress-strain curves (a) and tearing stress-strain curves (b) for PTMC networks obtained by photo-crosslinking PTMC-dMA 10k macromers in bulk and at concentrations of 33 and 50 wt.% in PC. Stress-strain curves for a photo-crosslinked PDLLA-dMA network (c) and for photo-crosslinked PCL-dMA and PEG-dMA networks (d) obtained by photo-crosslinking at a concentration of 33 wt.% in PC.

Table 3: Thermal- and tensile properties of single-macromer networks prepared by photo-crosslinking PTMC-dMA 10k, PDLLA-dMA 10k, PCL-dMA 4k, PCL-dMA 10k and PEG-dMA 10k at a concentration of 33 wt.% in PC. Tensile data is presented as a mean value of triplicate measurements with the standard deviation in parentheses.

Single-macromer network	**T_g**	**T_m**	**ΔH**	**E**	**σ_{max}**	**ε_{max}**	**$W_{tensile}$**	**TPS_{ave}**	**TPS_{max}**	**G**
	°C	°C	J/g	MPa	MPa	%	N/mm^2	N/mm	N/mm	kJ/m^2
PTMC-dMA 10k [a]	-17.8	-	-	6 (2)	6.4 (1.6)	1,003 (85)	3,239 (832)	7.8 (0.6)	9.1 (0.8)	16 (1)
PDLLA-dMA 10k	38.3	-	-	3,083 (451)	31.0 (20.1)	2 (1)	30 (34)	- [b]	- [b]	- [b]
PCL-dMA 4k	-58.1	45.1	48.1	498 (31)	16.8 (0.1)	179 (81)	2,300 (1,065)	10.1 (1.3)	10.9 (1.2)	20 (3)
PCL-dMA 10k	-61.2	55.2	40.1	825 (79)	20.5 (1.7)	189 (122)	3,048 (2,033)	15.6 (5.0)	22.6 (9.1)	31 (10)
PEG-dMA 10k	-56.3	54.1	86.6	129 (3)	12.6 (0.5)	335 (247)	2,563 (3,032)	6.8 (2.6)	9.0 (3.5)	14 (5)

[a] data from Table 2; [b] could not be determined, network too brittle to measured

Properties of photo-crosslinked mixed-macromer networks

Mixed-macromer network films were prepared by photo-crosslinking combinatorial mixtures of PTMC-dMA, PDLLA-dMA, PCL-dMA and PEG-dMA macromers in propylene carbonate solutions, followed by extraction and drying. The macromer concentration was 33 wt.% in PC. It was not possible to prepare macroscopically homogeneous photo-crosslinked films in the absence of the solvent, see Supporting Information Figure SI2.

The thermal- and mechanical properties of the resulting homogeneous mixed-macromer network films photo-crosslinked in solution were assessed by differential scanning calorimetry, and in tensile tests and tear propagation experiments in the dry state. An overview of the data is given in Table 4.

The thermal characteristics of the networks presented in the Table indicate that all networks are microphase separated. The amorphous PTMC/PDLLA networks show two distinct glass transitions corresponding to the different macromers. In compositions prepared from PTMC and PCL and/or PEG, a glass transition corresponding to the PTMC phase as well as a melting temperature of the crystalline phase of the other components can be observed. In other networks a mixed amorphous phase and a crystalline phase can be recognized.

The tensile properties of the prepared mixed-macromer networks are also given in Table 4. The stress-strain graphs in Figure 2 show that all networks are ductile materials with clear yield points and relatively high elongations at break. The networks that have relatively high modulus values, high (yield) strengths and high elongations at break are the materials are the ones that are the toughest having the largest area under the tensile stress-strain curve. This is the case for well-microphase separated networks with an amorphous rubber phase and a rigid amorphous or crystalline component. Networks 1 (PTMC and PDLLA), network 3 (PTMC and PEG) and network 8 (PTMC, PDLLA and PEG) were the toughest with toughness values of respectively 3,585, 2,879 and 3,522 N/mm^2.

Tough networks also had high tearing strengths, as Table 4 shows. Tearing stress-strain diagrams are shown in Figure SI3 of the Supporting Information. The Table shows that the average tear propagation strength TPS_{ave} varies between 1 and 24 N/mm, the maximum value of the tear propagation strength TPS_{max} varies between 6 and 32 N/mm. In these experiments, network 4 (PDLLA and PEG) had the lowest maximal tear strength. Network 8 (PTMC, PDLLA and PEG) was found to be the toughest and had the highest maximal tear strength.

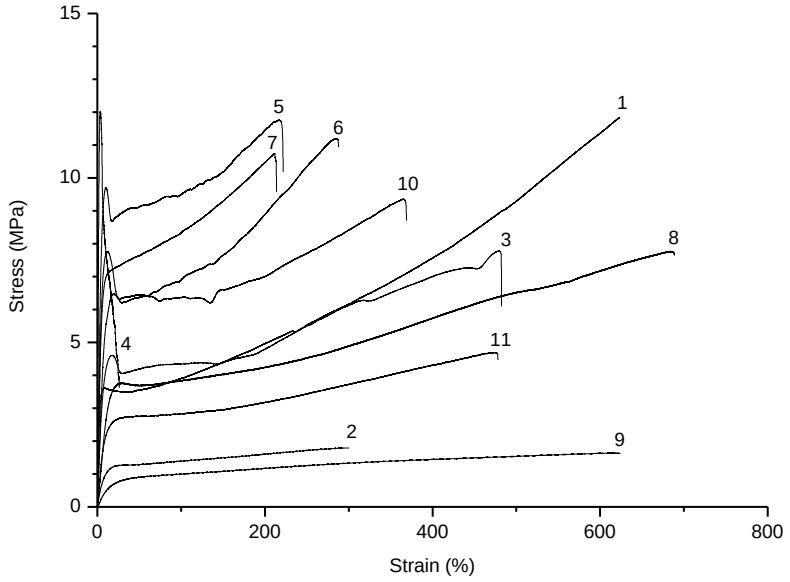

Figure 2: Tensile stress-strain diagrams of photo-crosslinked mixed-macromer networks. The numbers in the figure correspond to networks of which the composition is given in Table 4.

With its low glass transition temperature, amorphous PTMC contributes much to the phase-separated amorphous rubbery component of mixed-macromer networks. When comparing network number 7 (TPS_{ave}: 19 N/mm, TPS_{max}: 23 N/mm) with network number 6 (TPS_{ave}: 8 N/mm, TPS_{max}: 13 N/mm), a much higher resistance to tearing is observed. PDLLA is also amorphous but has a much higher

glass transition temperature. A phase-separated amorphous rigid phase can lead to enhanced tear resistance as shown by the amorphous mixed-macromer network composed of PTMC-dMA 10k and PDLLA-dMA 10k (network number 1). The TPS_{ave} of this network is 19 N/mm, more than twice as high as that of a PTMC single-macromer network crosslinked at a concentration of 33 wt.% and also much higher than that of a photo-crosslinked PTMC network prepared in bulk from high molar mass macromers (Mn=41.0 kg/mol) (7.1 N/mm) [13].

PCL and PEG are semi-crystalline polymers, and when present in mixed-macromer networks will result in the presence of crystalline domains in the networks. These crystalline domains will obstruct the propagation of growing tears, leading to the formation of networks with high resistance to tearing. Mixed-macromer networks containing PCL and PEG components show very high tear propagation strengths, network 8 was found to have the highest tear propagation strength (TPS_{ave}= 24 N/mm, TPS_{max}= 32 N/mm).

From the average tearing force, the tearing energy G can be calculated. It follows from the Table that the tearing energies of the mixed macromer networks we prepared ranged from 2 to 47 kJ/m^2. These values are much higher than those reported for well-known elastomers such as PDMS (0.08 kJ/m^2 [24]), ethylene propylene diene monomer (EPDM) rubber (4-16 kJ/m^2 [25]), styrene-butadiene rubber (SBR) (2-3.5 kJ/m^2 [25]) or even natural rubber (3-12 kJ/m^2 [26]). Especially this last comparison is remarkable, as natural rubber is considered the superior elastomer in terms of tearing resistance.

Figure 3 gives an overview of SEM micrographs of tears in the different mixed-macromer networks after the tearing experiments. Rough tear fracture surfaces indicate that much energy has been dissipated during propagation of the tear, this implies a high tear propagation strength. When the surface of the tear fracture is smooth, tear propagation is unhindered and the material has low resistance to tearing. The Figure shows that networks 3, 7, 8, 10 and 11 have relatively rough undulating tear fracture surfaces, and from the data in Table 4 it can be seen that these networks are quite tough and have high tear strengths. By contrast, the fracture surface of network 4 was very smooth indicating brittle failure. Indeed, this network had the lowest tear propagation strength.

Table 4: Thermal- and mechanical properties of photo-crosslinked networks prepared from combinatorial mixtures of PTMC-dMA 10k, PDLLA-dMA 10k, PCL-dMA 4k and PEG-dMA 10k. The macromers in the different networks (colored grey) are present in equal weight percentages. Tensile data is presented as a mean value of triplicate measurements with the standard deviation in parentheses.

Sample number	Network component				T_g	T_m	ΔH	E	σ_{max}	ε_{max}	$W_{tensile}$	TPS_{ave}	TPS_{max}	G
	PTMC-dMA 10k	PDLLA-dMA 10k	PCL-dMA 4k	PEG-dMA 10k	°C	°C	J/g	MPa	MPa	%	N/mm^2	N/mm	N/mm	kJ/m^2
1					-11.7/ 41.4	-	-	162 (28)	10.5 (1.2)	577 (67)	3,585 (523)	19 (0)	27 (0)	39 (1)
2					-15.0	53.3	17.7	16 (3)	1.7 (0.4)	223 (86)	323 (164)	11 (4)	14 (4)	23 (8)
3					-15.5	54.0	53.9	71 (7)	8.1 (2.7)	457 (265)	2,879 (1,651)	23 (5)	28 (1)	46 (10)
4					-25.4	48.1	32.1	668 (63)	11.6 (0.5)	25 (22)	169 (147)	1 (1)	6 (5)	2 (1)
5					-5.0	53.7	29.8	280 (17)	12.0 (0.8)	223 (15)	2,252 (233)	7 (3)	8 (3)	14 (6)
6					-65.1	54.7	76.5	89 (21) [a]	10.7 (0.7) [a]	285 (7) [a]	2,128 (209)	8 (1) [a]	13 (1) [a]	16 (1) [a]
7					-16.0	53.1	46.9	151 (11)	10.5 (0.4)	213 (6)	1,754 (112)	19 (0)	23 (1)	38 (0)
8					-13.2	46.4	8.8	33 (8)	8.1 (0.4)	680 (46)	3,522 (489)	24 (1)	32 (2)	47 (2)
9					-12.4	52.0	19.2	6 (1)	1.6 (0.1)	605 (21)	752 (67)	10 (2)	11 (2)	20 (3)
10					-15.0	50.8	42.0	173 (13) [a]	9.2 (0.8) [a]	337 (76) [a]	2,461 (615)	18 (3) [a]	23 (1) [a]	35 (5) [a]
11					-12.1	52.6	27.3	31 (3)	4.9 (0.4)	473 (60)	1,756 (351)	16 (4)	20 (2)	32 (8)

[a] *n=2*

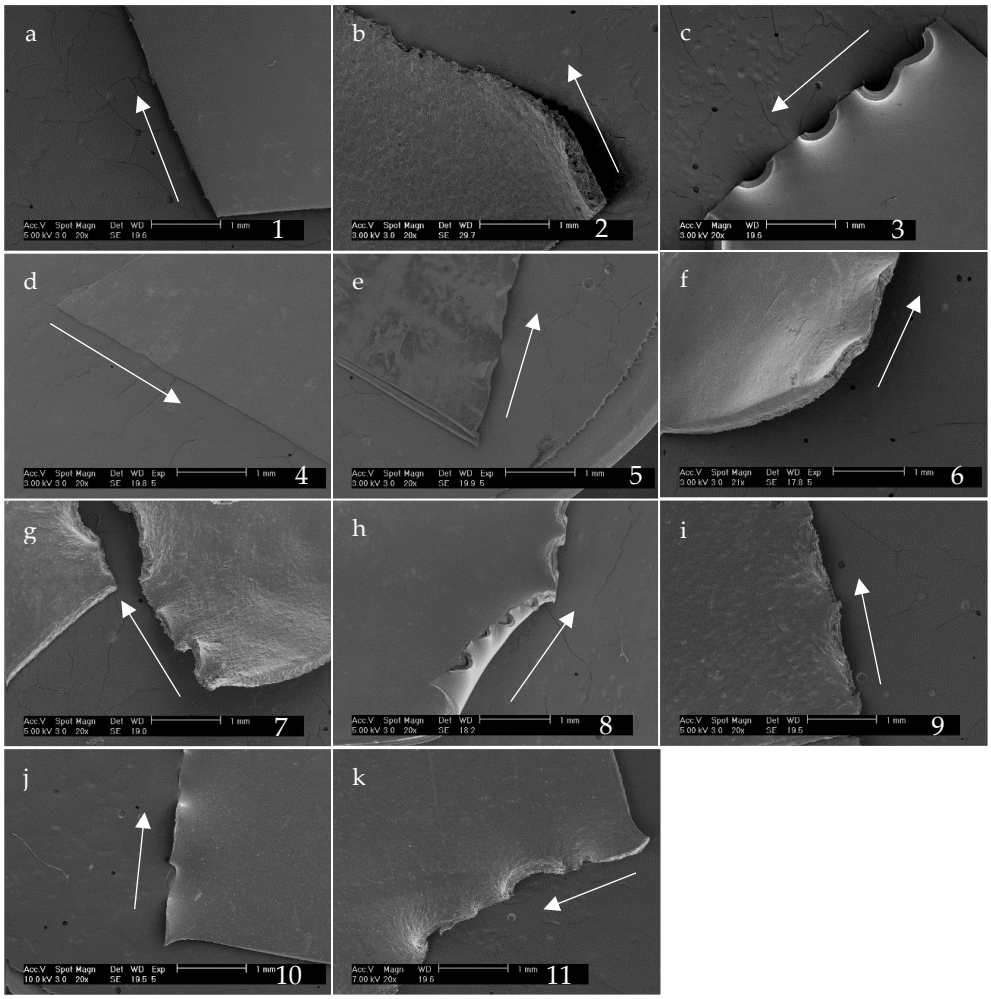

Figure 3: SEM micrographs of the tear surface of mixed-macromer networks after tear propagation experiments. The direction of tearing is indicated by the white arrow. The scale bar = 1 mm.

Properties of hydrated mixed-macromer networks (hydrogels) photo-crosslinked in solution

The mixed-macromer networks that did not contain a PEG component (network numbers 1, 2, 5 and 9 in Table 4) did not take up much water when immersed in distilled water. For these networks water uptake was between 3 and 10 wt.%. In contrast, the mixed-macromer networks that did contain a PEG component (networks numbers 3, 4, 6, 7, 8, 10 and 11 in Table 4) absorbed significant amounts of water (74 wt.% or more as shown in Table 5) when hydrated. These mixed-macromer networks can thus be termed hydrogels.

Besides the water uptake of the mixed-macromer networks, which ranges from 74 to 303 wt.%, the tensile properties of the water-swollen networks and their tearing characteristics are also given in Table 5. (Network 4 prepared from PDLLA- and PEG macromers was too weak and brittle to evaluate by tensile testing in the hydrated state.) The tensile modulus of these networks varied between 0.32 and 2.11 MPa. The values of the maximum tensile strengths (varying between 0.62 and 1.08 MPa) and the elongations at break (varying between 60 and 813 %) were exceptionally high for hydrogel networks containing such large amounts of water. Such high values of modulus, maximum tensile strength and elongation at break lead to high values of toughness of the networks. This is illustrated in the tensile stress-strain diagrams shown in Figure 4. Especially network number 8 composed of PTMC-, PDLLA- and PEG components is very resilient in the hydrated state, it has a tensile toughness of 243 N/mm^2.

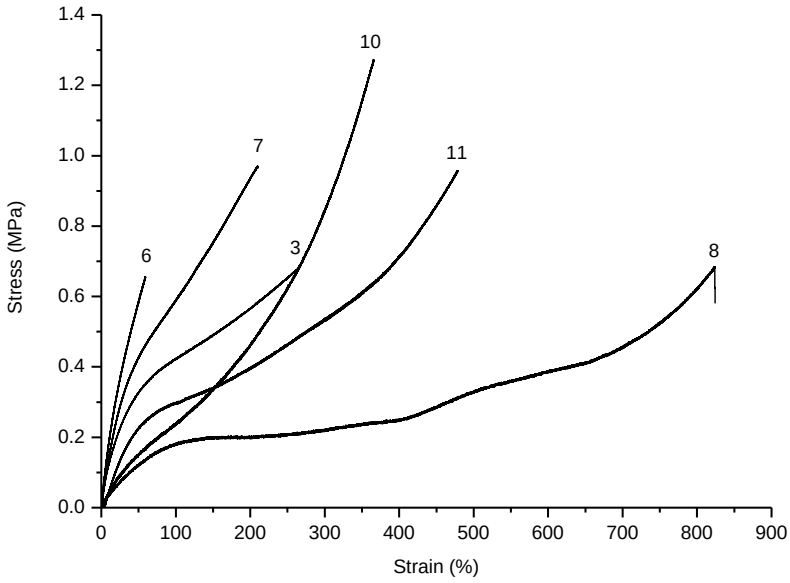

Figure 4: Tensile stress-strain diagrams of photo-crosslinked mixed-macromer networks in the water-swollen state. The numbers in the figure correspond to networks of which the characteristics are given in Table 5. Network 4 could not be evaluated by tensile testing in the hydrated state.

Table 5: Water uptake and tensile properties in the hydrated state of photo-crosslinked networks (hydrogels) prepared from combinatorial mixtures of PTMC-dMA 10k, PDLLA-dMA 10k, PCL-dMA 4k and PEG-dMA 10k. The macromers in the different networks (colored grey) are present in equal weight percentages, see also Table 4. Tensile data is presented as a mean value of triplicate measurements with the standard deviation in parentheses.

Sample number	Network component				Water uptake	E	σ_{max}	ε_{max}	$W_{tensile}$	TPS_{ave}	TPS_{max}	G
	PTMC-dMA 10k	PDLLA-dMA 10k	PCL-dMA 4k	PEG-dMA 10k	wt. %	MPa	MPa	%	N/mm^2	N/mm	N/mm	kJ/m^2
3	■			■	303 (27)	1.10 (0.10)	0.72 (0.22)	235 (90)	116 (63)	0.09 (0.00)	0.16 (0.01)	0.18 (2)
4		■		■	223 (62)	- [a]	- [a]	- [a]	- [a]	- [a]	- [a]	- [a]
6			■	■	109 (13)	2.11 (0.16)	0.70 (0.04)	60 (10)	25 (5)	0.25 (0.09)	0.74 (0.31)	0.50 (0.18)
7	■		■	■	87 (42)	1.50 (0.04) [b]	0.94 (0.05) [b]	200 (14) [b]	113 (15)	0.41 (0.02)	0.64 (0.07)	0.81 (0.47)
8	■	■		■	171 (67)	0.32 (0.04)	0.62 (0.11)	813 (90)	243 (55)	0.02 (0.02)	0.05 (0.01)	0.03 (0.04)
10		■	■	■	132 (59)	0.43 (0.04)	1.08 (0.47)	320 (78)	146 (71)	0.04 (0.02)	0.07 (0.02)	0.09 (0.04)
11	■	■	■	■	74 (35)	0.74 (0.040	0.97 (0.12)	473 (31)	225 (27)	0.29 (0.02)	0.61 (0.08)	0.58 (0.05)
PEG [c]					1900 [d]	0.02	- [g]	300	- [g]	- [g]	- [g]	0.01
PEG-PDMS [c]					450 [d]	0.03	- [g]	170	- [g]	- [g]	- [g]	0.08
PAA [e]					900 [d]	0.03	- [g]	50	- [g]	- [g]	- [g]	0.01-0.1
PAMPS [e]					- [g]	- [g]	- [g]	- [g]	- [g]	- [g]	- [g]	0.001-0.01
PAA-PAMPS (DN) [f]					900 [d]	0.10	0.3	1000	- [g]	- [g]	- [g]	0.3
Cartilage [f]					400 [d]	2.50	1.5	100	- [g]	- [g]	- [g]	1

[a] too fragile to be measured; [b] n=2; [c] data from Cui et al. on networks based on PEG and PDMS precursors [27]; [d] recalculated from the original data; [e] data from Tanaka et al. on poly(acryl amide) (PAA) and PAA-poly(2-acrylamido-2-methylpropanesulfonic acid) (PAMPS) [28]; [f] data from Li et al. on canine patella cartilage [29, 30]; [g] data not reported.

In the table also tear strength data of the hydrated mixed-macromer hydrogel networks is presented. The tear stress-strain curves of the tear propagation experiments are shown in Figure SI4.

Hydrated network specimens number 3, 8 and 10 show relatively low values of the tear propagation strength, and the tearing stress-strain diagrams in Figure SI4 show that these tearing forces are relatively constant. Still, the tearing energies were comparable to those of a mixed-macromer network based PEG and polydimethyl siloxane (PDMS) and much higher than those of PEG, poly(acryl amide) (PAA) and poly(2-acrylamido-2-methylpropanesulfonic acid) (PAMPS) hydrogels [27, 28].

Most interestingly, Table 5 shows that mixed-macromer networks 6, 7 and 11 show very high resistance against tearing in the wet state. In these cases the tear propagation strengths are high and the tearing stress-strain curves (Figure SI4) show characteristic stick-slip tearing behavior [31]. This behavior can most probably be attributed to the presence of crystalline PCL domains homogenously distributed throughout the hydrated matrix of the networks.

Mixed-macromer hydrogel network number 7, prepared from PTMC-, PCL and PEG-macromers, was found to be extremely tough with an average tear propagation strength of 0.41 N/mm and an extremely high tearing energy (G) of 0.81 kJ/m^2. The tearing energy of this hydrogel was found to be much higher than that of any other synthetic hydrogel described in the scientific literature [17, 27, 28]. Double-network hydrogels prepared from PAA, for example, were shown to have tearing energies of approximately 0.3 kJ/m^2 [28]. The tearing energy of this hydrogel is comparable to the tearing energy of articular cartilage (1 kJ/m^2) [29].

Conclusions

While networks prepared by photo-crosslinking PTMC-dMA macromers with a relatively low molar mass of 10 kg/mol in bulk are brittle, we could obtain resilient networks by photo-crosslinking the same macromers in propylene carbonate at concentrations of 33 wt.%. These amorphous rubber-like PTMC networks were

strong (σ_{max}=6.4 MPa), highly extensible (ε_{max}=1,003%) and very tough (G=16 kJ/m^2) after extraction and drying.

Crosslinking in solution also allowed the preparation of macroscopically homogeneous networks from mixtures of macromers. Networks prepared from mixtures of PTMC-dMA, PDLLA-dMA, PCL-dMA and PEG-dMA macromers in this manner showed a microphase-separated structure. Tensile testing and tear propagation experiments showed that these mixed-macromer networks had even better mechanical properties than those of single-macromer networks. The toughest network had a high maximum tensile strength of 8.1 MPa), a maximum elongation at break of 680 %) and a very high tearing energy of 47 kJ/m^2 after extraction and drying. Mixed-macromer networks prepared using PEG-dMA showed could take up 74 to 303 wt.% water. It was found that in the hydrated state, most of these mixed-macromer hydrogel networks were also extremely tough. The toughest mixed-macromer hydrogel was prepared from PTMC-dMA, PCL-dMA and PEG-dMA macromers and had a maximum tensile strength of 0.94 MPa), a maximum elongation at break of 200 %) and a very high tearing energy of 0.81 kJ/m^2. These values are significantly higher than for any other synthetic hydrogel and comparable to the tearing energy of articular cartilage (1 kJ/m^2).

As these tough networks and hydrogels are prepared from biocompatible and biodegradable components, they are promising materials for application in biomedical engineering such as cartilage tissue engineering.

Acknowledgements

This work was supported by a grant from the Dutch government to the Netherlands Institute for Regenerative Medicine (NIRM, grant No. FES0908).

References

1. Amsden B, Curable, biodegradable elastomers: emerging biomaterials for drug delivery and tissue engineering. Soft Matter, 2007. 3(11): p. 1335-1348.
2. Smith TL, Strength of elastomers - perspective. Polymer Engineering and Science, 1977. 17(3): p. 129-143.

3. Fatt MSH, Chen L, and Al-Quraishi AA, Fracture parameters for natural rubber under dynamic loading. Strain, 2011. 47: p. E505-E518.
4. Premachandra JK and Mark JE, Effects of dilution during crosslinking on strain-induced crystallization in cis-1,4-polyisoprene networks. I. Experimental results. Journal of Macromolecular Science-Pure and Applied Chemistry, 2002. 39(4): p. 287-300.
5. Johnson RM and Mark JE, Properties of poly(dimethylsiloxane) networks prepared in solution, and their use in evaluating the theories of rubberlike elasticity. Macromolecules, 1972. 5(1): p. 41-45.
6. Mark JE, Improved elastomers through control of network chain-length distributions. Rubber Chemistry and Technology, 1999. 72(3): p. 465-483.
7. Urayama K, Network topology-mechanical properties relationships of model elastomers. Polymer Journal, 2008. 40(8): p. 669-678.
8. Vasiliev VG, Rogovina LZ, and Slonimsky GL, Dependence of properties of swollen and dry polymer networks on the conditions of their formation in solution. Polymer, 1985. 26(11): p. 1667-1676.
9. Pego AP, Grijpma DW, and Feijen J, Enhanced mechanical properties of 1,3-trimethylene carbonate polymers and networks. Polymer, 2003. 44(21): p. 6495-6504.
10. Bat E, Plantinga JA, Harmsen MC, van Luyn MJA, Zhang Z, Grijpma DW, and Feijen J, Trimethylene carbonate and epsilon-caprolactone based (co)polymer networks: mechanical properties and enzymatic degradation. Biomacromolecules, 2008. 9(11): p. 3208-3215.
11. Song Y, Kamphuis MMJ, Zhang Z, Sterk LMT, Vermes I, Poot AA, Feijen J, and Grijpma DW, Flexible and elastic porous poly(trimethylene carbonate) structures for use in vascular tissue engineering. Acta Biomaterialia, 2010. 6(4): p. 1269-1277.
12. Hou Q, Grijpma DW, and Feijen J, Creep-resistant elastomeric networks prepared by photocrosslinking fumaric acid monoethyl ester-functionalized poly(trimethylene carbonate) oligomers. Acta Biomaterialia, 2009. 5(5): p. 1543-1551.
13. Schuller-Ravoo S, Feijen J, and Grijpma DW, Flexible, elastic and tear-resistant networks prepared by photo-crosslinking poly(trimethylene carbonate) macromers. Acta Biomaterialia, 2012. 8(10): p. 3576-3585.
14. Bat E, Kothman BHM, Higuera GA, van Blitterswijk CA, Feijen J, and Grijpma DW, Ultraviolet light crosslinking of poly(trimethylene carbonate) for elastomeric tissue engineering scaffolds. Biomaterials, 2010. 31(33): p. 8696-8705.

15. Amsden BG, Misra G, Gu F, and Younes HM, Synthesis and characterization of a photo-cross-linked biodegradable elastomer. Biomacromolecules, 2004. 5(6): p. 2479-2486.
16. Grijpma DW, Hou Q, and Feijen J, Preparation of biodegradable networks by photo-crosslinking lactide, [epsilon]-caprolactone and trimethylene carbonate-based oligomers functionalized with fumaric acid monoethyl ester. Biomaterials, 2005. 26(16): p. 2795-2802.
17. Calvert P, Hydrogels for soft machines. Advanced Materials, 2009. 21(7): p. 743-756.
18. Peak CW, Wilker JJ, and Schmidt G, A review on tough and sticky hydrogels. Colloid and Polymer Science, 2013. 291(9): p. 2031-2047.
19. Gong JP, Katsuyama Y, Kurokawa T, and Osada Y, Double-network hydrogels with extremely high mechanical strength. Advanced Materials, 2003. 15(14): p. 1155-1158.
20. Sharifi S, Blanquer SBG, van Kooten TG, and Grijpma DW, Biodegradable nanocomposite hydrogel structures with enhanced mechanical properties prepared by photo-crosslinking solutions of poly(trimethylene carbonate)-poly(ethylene glycol)-poly(trimethylene carbonate) macromonomers and nanoclay particles. Acta Biomaterialia, 2012. 8(12): p. 4233-4243.
21. Seck TM, Melchels FPW, Feijen J, and Grijpma DW, Designed biodegradable hydrogel structures prepared by stereolithography using poly(ethylene glycol)/poly(d,l-lactide)-based resins. Journal of Controlled Release, 2010. 148(1): p. 34-41.
22. Anderson DG, Levenberg S, and Langer R, Nanoliter-scale synthesis of arrayed biomaterials and application to human embryonic stem cells. Nature Biotechnology, 2004. 22(7): p. 863-866.
23. Brocchini S, James K, Tangpasuthadol V, and Kohn J, Structure-property correlations in a combinatorial library of degradable biomaterials. Journal of Biomedical Materials Research, 1998. 42(1): p. 66-75.
24. Kumudinie C and Mark JE, Tearing energies for in-situ reinforced poly(dimethylsiloxane) networks. Materials Science & Engineering C-Biomimetic and Supramolecular Systems, 2000. 11(1): p. 61-66.
25. Kok CM and Yee VH, The effects of cross-link density and cross-link type on the tensile and tear strengths of NR, SBR and EPDM gum vulcanizates. European Polymer Journal, 1986. 22(4): p. 341-345.
26. Sakulkaew K, Thomas AG, and Busfield JJC, The effect of temperature on the tearing of rubber. Polymer Testing, 2013. 32(1): p. 86-93.
27. Cui J, Lackey MA, Tew GN, and Crosby AJ, Mechanical properties of end-linked PEG/PDMS hydrogels. Macromolecules, 2012. 45(15): p. 6104-6110.

28. Tanaka Y, Kuwabara R, Na YH, Kurokawa T, Gong JP, and Osada Y, Determination of fracture energy of high strength double network hydrogels. Journal of Physical Chemistry B, 2005. 109(23): p. 11559-11562.
29. Li JY, Illeperuma WBK, Suo ZG, and Vlassak JJ, Hybrid hydrogels with extremely high stiffness and toughness. Acs Macro Letters, 2014. 3(6): p. 520-523.
30. Chin-Purcell MV and Lewis JL, Fracture of articular cartilage. Journal of Biomechanical Engineering, 1996. 118(4): p. 545-556.
31. Liang SM, Flu J, Wu ZL, Kurokawa T, and Gong JP, Toughness enhancement and stick-slip tearing of double-network hydrogels in poly(ethylene glycol) solution. Macromolecules, 2012. 45(11): p. 4758-4763.

Supplementary Information

^{1}H-NMR spectra recorded for the macromers.

The molecular weights and conversions of the macromers were determined by ^{1}H-NMR. The spectra are shown in Figure SI1.

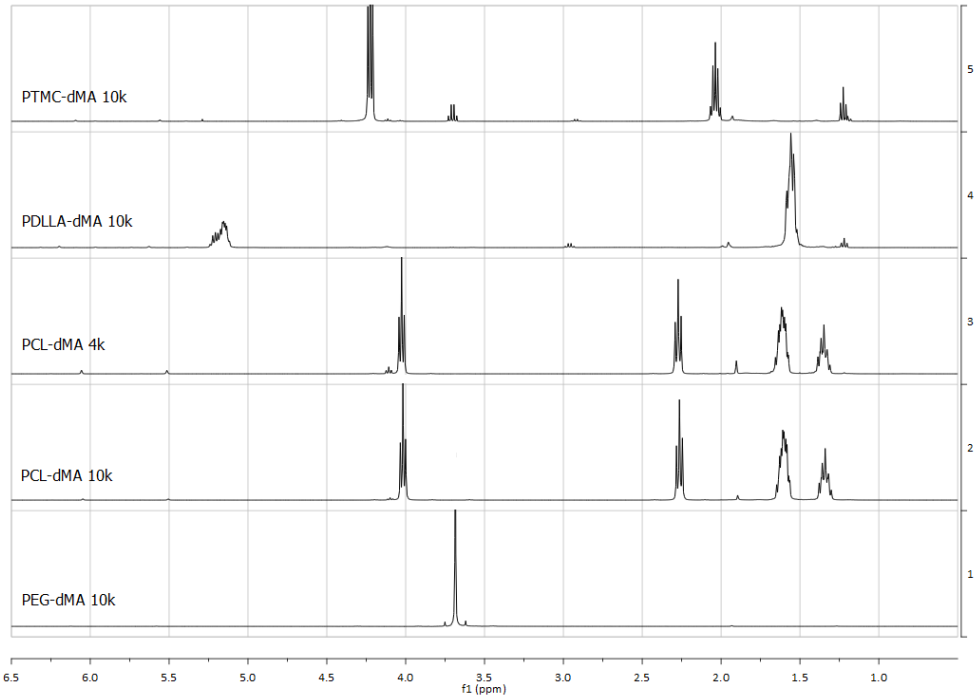

Figure SI1: ^{1}H-NMR spectra of all macromers. The molecular weights and conversions determined from the spectra are listed in Table 1.

Photo-crosslinking mixtures of macromers

Photo-crosslinking mixtures of macromers in the absence of a solvent did not lead to the formation of macroscopically homogeneous network films. For example, Figure SI2 shows two mixed-macromer network films obtained by photo-crosslinking a mixture of PDLLA-dMA 10k, PCL-dMA 4k and PEG-dMA 10k. Figure SI2a shows a photographic image of the network film obtained after casting the macromer mixture dissolved in dichloromethane, evaporation of the solvent and photo-crosslinking. The film is fragmented and heterogeneous, showing macroscopic phase separation in which the size of the domains is in the order of millimeters. These films have very poor mechanical properties and cannot be tested in tensile tests. In contrast, Figure SI2b shows the network film that is obtained after casting from a solution in propylene carbonate, subsequent photo-crosslinking, extraction and drying. This film prepared from the same mixture of PDLLA-dMA, PCL-dMA and PEG-dMA macromers is very homogeneous and has excellent handling characteristics and mechanical properties, See Table 4. The films are slightly opaque, indicating microphase separation.

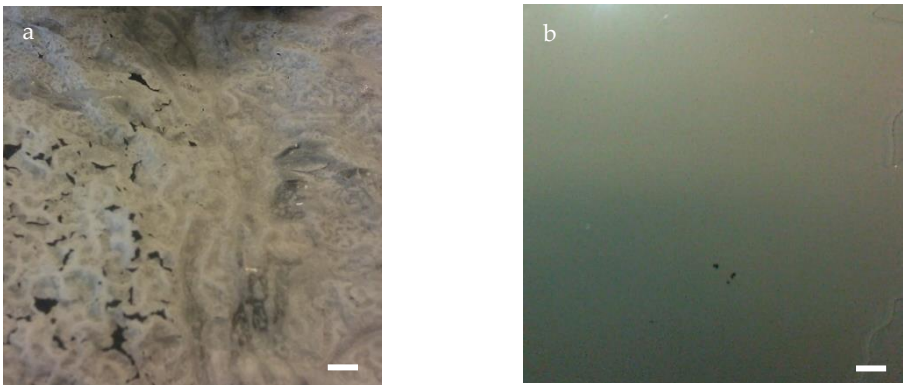

Figure SI2: Network films obtained after photo-crosslinking a mixture of PDLLA-dMA, PCL-dMA and PEG-dMA in the absence of a solvent (bulk, a) or in solution (33 wt.%, b). The scale bar = 1 cm.

Tearing stress-strain diagrams

Figure SI3 illustrates the tearing stress-strain diagrams of the different photo-crosslinked mixed-macromer networks in the dry state. These diagrams illustrate the wide range of tearing characteristics of the different networks that were prepared.

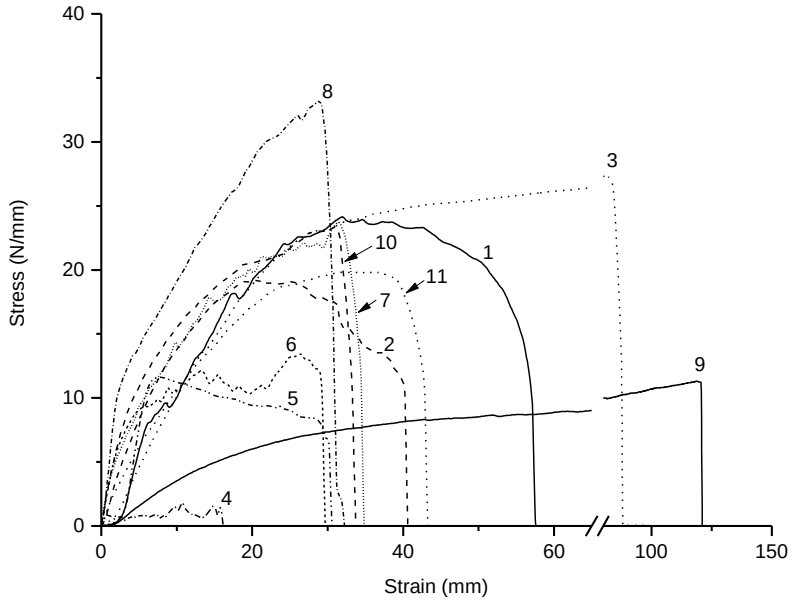

Figure SI3: Tear propagation strength determinations of mixed-macromer networks in the dry-state. In these graphs, the stress is normalized to the thickness of the specimen (N/mm). The numbers in the figure correspond to the networks described in Table 4.

Figure SI4 illustrates the tearing stress-strain behavior of different photo-crosslinked mixed-macromer networks in the hydrated state. These diagrams illustrate the wide range of tearing characteristics of the different hydrogel networks that were prepared. In some cases characteristic stick-slip tearing behavior can be observed. Networks that display this behavior show high tear propagation strength.

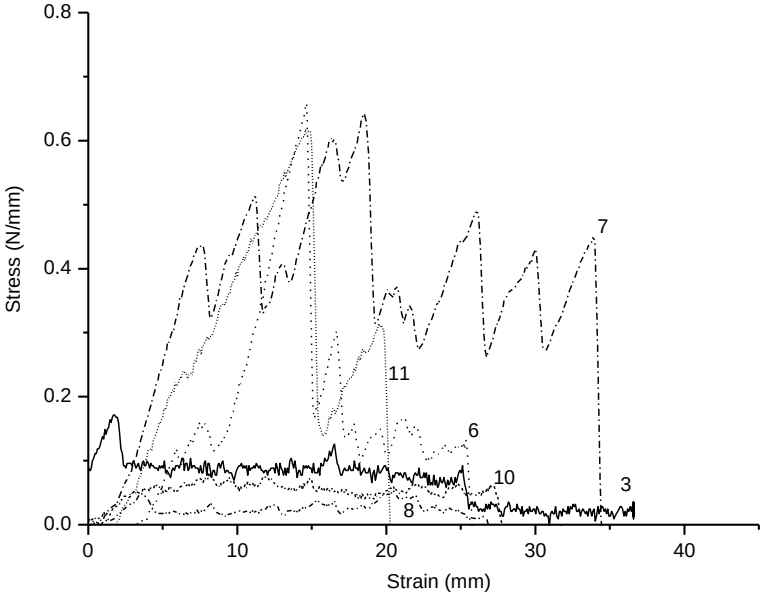

Figure SI4: Tear propagation strength determinations for hydrophilic mixed-macromer networks in the hydrated state. In these graphs, the stress is normalized to the thickness of the specimen (N/mm). The numbers in the figure correspond to the networks described in Table 5.

Chapter 5 - Synthetic biodegradable hydrogels with excellent mechanical properties and good cell adhesion characteristics obtained by the combinatorial synthesis of photo-crosslinked networks

Erwin Zant, Dirk W. Grijpma

Biomacromolecules, submitted

Abstract

Major drawbacks of synthetic hydrogels are their poor mechanical properties and their limited ability to allow cell attachment and proliferation. By photo-crosslinking mixtures of dimethacrylate-functionalized oligomers (macromers) in a combinatorial manner in solution, synthetic hydrogels with high water uptake and the remarkable ability to promote cell adhesion and proliferation were prepared.

A total of 255 different networks based on poly(trimethylene carbonate) (PTMC)-, poly(D,L-lactide) (PDLLA)-, poly(ε-caprolactone) (PCL)- and poly(ethylene glycol) (PEG) macromers were synthesized simultaneously and screened for their ability to allow the adhesion of human mesenchymal stem cells (hMSCs) in a high throughput manner. Of these networks, several hydrogels could be identified that were able to take up large amounts of water while at the same time allowed the adhesion of cells. By synthesizing these hydrogel networks anew and analyzing the cell adhesion and proliferation behavior of human mesenchymal stem cells to these synthetic hydrogels in more detail, it was confirmed that mixed-macromer hydrogel networks prepared from equal amounts of PTMC-dMA 4k, PDLLA-dMA 4k, PCL-dMA 4k, PEG-dMA 4k and PEG-dMA 10k and hydrogel networks prepared from PTMC-dMA 4k, PDLLA-dMA 4k, PEG-dMA 4k, PTMC-dMA 10k and PEG-dMA 10k were highly hydrophilic (water uptake was respectively 181 ± 2 and 197 ± 18 wt.% water) and allowed very good cell adhesion and proliferation. Furthermore, these networks were extremely resilient in the hydrated state, with tearing energies of respectively 0.64 ± 0.34 and 0.27 ± 0.04 kJ/m^2. This is much higher than other synthetic hydrogels described in literature and close to articular cartilage (1 kJ/m^2).

Introduction

Hydrogels prepared from biological materials are of great interest in tissue engineering research as natural materials often have the ability to bind cells. Despite their intrinsic bioactivity, the use of natural polymers has important limitations such as the need for difficult and complex purification steps, the potential of an immunogenic response and the possibility of disease transmission [1]. Moreover, natural polymers are difficult to process with large variabilities in their physical and chemical properties. Therefore, synthetic polymeric hydrogels have been much investigated for application in tissue engineering. The ease with which they are prepared and processed, and the ability to tailor their physico-chemical properties offer great advantages. Examples of such hydrogels are hydrogels based on poly(vinyl alcohol) (PVA), poly(acrylamide) (PAA), poly(2-hydroxyethyl methacrylate) (PHEMA) and poly(ethylene glycol) (PEG). A major drawback of synthetic hydrogels is their limited ability to adsorb proteins and allow cell attachment [2]. In addition, water-swollen synthetic hydrogels are often fragile materials. This limits their use as an implant or a replacement tissue [3].

To improve the attachment of cells to synthetic hydrogels, natural proteins such as fibronectin, collagen, vitronectin and laminin are frequently bound to these hydrogels [4]. This can be done by reaction of acrylate-functionalized synthetic polymers with the amine side groups of the proteins. Cell-binding peptide sequences, like RGD, have also been incorporated into synthetic hydrogels [5-8] allowing cells to interact with the hydrogels via their integrin cell surface receptors [9]. Although the attachment of cells to synthetic hydrogels can be significantly improved in these manners, the purification and possible immunogenic responses of the natural components still needs to be taken into account. Synthetic peptides are not readily available and can only be obtained through expensive and time-consuming synthesis routes.

To improve the compatibility of (biodegradable) synthetic hydrogels with proteins and cells, block copolymers consisting of a hydrophilic segment and a hydrophobic segment have been prepared. Examples are amphiphilic copolymers of PEG with poly(ε-caprolactone) (PCL) [10], poly(lactide-co-glycolide) (PLGA) [11] and poly(L-lactide) (PLLA) [12], which have been used in drug delivery applications [13] and

in tissue engineering [14-16]. By systematic variation of the polymer composition, hydrogels with useful characteristics can be obtained. However, materials with optimized properties for a specific application can only be found after careful variation of a large number of variables such as the nature of the monomers and cross-linkers used, their composition, the reaction conditions employed (catalysts, initiators, temperatures, concentrations, solvents, etc.) and other factors that may influence the system. Because of the large number of variations, this can indeed be a daunting task.

A combinatorial chemistry approach allows researchers to simultaneously prepare large numbers of different polymeric materials [17, 18]. By combining the synthesis of such material libraries with high throughput analyses new biomaterials that perform unexpectedly well can be found. This has been done by polymerizing many combinations of monomers that were printed in microarrays [19].

The simultaneous preparation of large numbers of different polymeric networks using combinatorial mixtures of macro-monomers (macromers) has not been investigated in detail. In this work we set out to prepare biodegradable [20] synthetic hydrogels with good cell adhesion characteristics. A large number of different combinations of methacrylate-functionalized macromers based on poly(trimethylene carbonate) (PTMC), poly(D,L-lactide) (PDLLA), PCL and PEG were prepared in solution and subsequently photo-crosslinked simultaneously to yield a library of (biodegradable hydrogel) networks with widely differing properties. Cell culturing experiments using human mesenchymal stem cells (hMSCs) were then conducted to evaluate their cell binding characteristics.

Materials and methods

Materials

Trimethylene carbonate (1,3-dioxan-2-one, TMC) was obtained from Huizhou Foryou Medical Devices Co. (China). D,L-lactide (DLLA) was obtained from Purac Biochem (The Netherlands). ε-Caprolactone (CL) (Sigma-Aldrich, U.S.A.) was dried over ground calcium hydride (CaH_2) (Merck, Germany) and purified by distillation under reduced argon atmosphere. Stannous octoate ($Sn(Oct)_2$), 1,6-hexanediol, methacrylic anhydride (MAAh), triethylamine (TEA), deuterated chloroform, trifluoroacetic anhydride (TFAA), 3-(trimethoxysilyl)propyl methacrylate (MEMO), gelatin from porcine skin (Type A, gel strength 90-110 g Bloom, molar mass approximately 20 kg/mol), polyethylene glycol with number average molecular weight M_n = 4 kg/mol (PEG 4k) and PEG with M_n = 10 kg/mol (PEG 10k) were purchased from Sigma-Aldrich (U.S.A.). Dichloromethane (DCM) was obtained from Biosolve (The Netherlands), dried over ground CaH_2 and distilled before use. Ethanol and isopropanol were obtained from Assink Chemie (The Netherlands). Diethyl ether was obtained from Fisher Scientific (The Netherlands). Irgacure 2959 (2-hydroxy-4-(2-hydroxyethoxy)-2-methylpropiophenone) was obtained from Ciba (Switzerland). Propylene carbonate (PC) was purchased from Merck, Germany.

Synthesis and characterization of dimethacrylate-functionalized PTMC-, PDLLA-, PCL- and PEG oligomers

Hydroxyl-group terminated linear oligomers with number average molecular weight, M_n , of 4 kg/mol and 10 kg/mol were prepared by ring-opening polymerization (ROP) of TMC, DLLA and CL monomers using hexanediol as initiator and $Sn(Oct)_2$ as catalyst. The polymerizations were conducted in an inert argon atmosphere at 130 °C for two days. The synthesized oligomers, PEG 4k and PEG 10k were dried at 120 °C under vacuum for 2 h, then cooled to room temperature under argon. The oligomers were functionalized in DCM (3 mL/g oligomer) by reaction with MAAh (4 mol/mol oligomer) in the presence of TEA (4

mol/mol oligomer). The functionalization reaction was let to proceed at room temperature for five days. The dimethacrylate (dMA)-functionalized oligomers (macromers) were then purified by precipitation. PTMC-dMA, PDLLA-dMA and PCL-dMA were precipitated in cold ethanol (-25 °C), while PEG-dMA was precipitated in cold diethylether (-25 °C). The macromers were subsequently dried under reduced pressure at 40-50 °C for 3 days. The number average molecular weights (M_n) and the degrees of functionalization (f) of the macromers were determined using a Varian Inova 400 MHz NMR spectrometer and deuterated chloroform as solvent. Differential Scanning Calorimetry (DSC) was used to determine the midpoint glass transition temperature (T_g) and the peak melting temperature (T_m) of the macromers. DSC measurements were performed using a Pyris 1 DSC (Perkin Elmer, USA). Samples weighing 5-10 mg were heated to 100 °C at a rate of 10 °C/min, kept for one min at 100 °C and then cooled to -100 °C at a rate of 200 °C/min. After five minutes at -100 °C, a second scan was recorded from -100 °C to 100 °C at 10 °C/min. T_m and T_g of the specimens were determined in the second heating scan.

Combinatorial synthesis of 255 photo-crosslinked single- and mixed-macromer networks

PTMC-dMA 4k, PDLLA-dMA 4k, PCL-dMA 4k, PEG-dMA 4k, PTMC-dMA 10k, PDLLA-dMA 10k, PCL-dMA 10k and PEG-dMA 10k macromers were dissolved at 50 °C at a concentration of 33 wt.% in PC containing Irgacure 2959 photo-initiator (1 wt.% with respect to the macromer) and hydroquinone inhibitor (0.1 wt.% with respect to the macromer). The solutions were mixed in a combinatorial manner in the wells of a 96 wells non-treated polystyrene cell culturing plate to yield 255 different macromer mixtures (see Table 1 for an overview). The volume of the macromer solutions was 250 μl and the total macromer concentration was 33 wt.%.

Amounts of 20 μl of each single- or mixed solution were transferred into wells of other 96 wells plates (n=3) and photo-crosslinked by UV irradiation (365nm, 10mW/cm^2, 20 min, 50 °C, nitrogen atmosphere). The networks were carefully extracted using first a 50/50 vol./vol. mixture of PC and ethanol for 3 days (the extraction medium was refreshed daily), then for 1 day using a 25/75 vol./vol.

mixture of PC and ethanol and finally for another day using ethanol only. After drying under atmospheric conditions for 1 day, the specimens were dried for another 3 days under reduced pressure at 45 °C. The mass of the dried network specimens (m_0) and that of the hydrated network specimens after immersion in distilled water for 48 hours and dry blotting of the surfaces (m_s) was then determined.

The water uptake (WU) of the networks was then calculated using:

$$\mathrm{WU} = \frac{m_s - m_0}{m_0} \times 100\%$$

Table 1: Composition of the mixtures of PTMC-, PDLLA-, PCL- and PEG macromers (in total 33 wt.%.) in PC which were used to prepare 255 combinatorial networks by photo-crosslinking. The macromers present in the different mixtures (colored grey) are present in equal amounts by weight.

Number	PTMC-dMA 4k	PDLLA-dMA 4k	PCL-dMA 4k	PEG-dMA 4k	PTMC-dMA 10k	PDLLA-dMA 10k	PCL-dMA 10k	PEG-dMA 10k
1	■							
2		■						
3			■					
4				■				
5					■			
6						■		
7							■	
8								■
9	■	■						
10	■		■					
11	■			■				
12	■				■			
13	■					■		
14	■						■	
15	■							■
16		■	■					
17		■		■				
18		■			■			
19		■				■		
20		■					■	
21		■						■
22			■	■				
23			■		■			
24			■			■		
25			■				■	
26			■					■
27				■	■			
28				■		■		
29				■			■	
30				■				■
31					■	■		
32					■		■	
33					■			■

Number	PTMC-dMA 4k	PDLLA-dMA 4k	PCL-dMA 4k	PEG-dMA 4k	PTMC-dMA 10k	PDLLA-dMA 10k	PCL-dMA 10k	PEG-dMA 10k
26						■	■	
27						■		■
28							■	■
29	■	■	■					
30	■	■		■				
31	■	■			■			
32	■	■				■		
33	■	■					■	
42	■	■						■
43	■		■	■				
44	■		■		■			
45	■		■			■		
46	■		■				■	
47	■		■					■
48	■			■	■			
49	■			■		■		
50	■			■			■	
51	■			■				■
52	■				■	■		
53	■				■		■	
54	■				■			■
55	■					■	■	
56	■					■		■
57	■						■	■
58		■	■	■				
59		■	■		■			
60		■	■			■		
61		■	■				■	
62		■	■					■
63		■		■	■			
64		■		■		■		
65		■		■			■	
66		■		■				■

Table 1: (continued)

Number	PTMC-dMA 4k	PDLLA-dMA 4k	PCL-dMA 4k	PEG-dMA 4k	PTMC-dMA 10k	PDLLA-dMA 10k	PCL-dMA 10k	PEG-dMA 10k
67		■			■	■		
68		■			■		■	
69		■			■			■
70		■				■	■	
71		■				■		■
72		■					■	■
73			■	■	■			
74			■	■		■		
75			■	■			■	
76			■	■				■
77			■		■	■		
78			■		■		■	
79			■		■			■
80			■			■	■	
81			■			■		■
82			■				■	■
83				■	■	■		
84				■	■		■	
85				■	■			■
86				■		■	■	
87				■		■		■
88				■			■	■
89					■	■	■	
90					■	■		■
91					■		■	■
92						■	■	■
93	■	■	■	■				
94	■	■	■		■			
95	■	■	■			■		
96	■	■	■				■	
97	■	■	■					■
98	■	■		■	■			
99	■	■		■		■		
100	■	■		■			■	
101	■	■		■				■
102	■	■			■	■		
103	■	■			■		■	

Number	PTMC-dMA 4k	PDLLA-dMA 4k	PCL-dMA 4k	PEG-dMA 4k	PTMC-dMA 10k	PDLLA-dMA 10k	PCL-dMA 10k	PEG-dMA 10k
104	■	■			■			■
105	■	■				■	■	
106	■	■				■		■
107	■	■					■	■
108	■		■	■	■			
109	■		■	■		■		
110	■		■	■			■	
111	■		■	■				■
112	■		■		■	■		
113	■		■		■		■	
114	■		■		■			■
115	■		■			■	■	
116	■		■			■		■
117	■		■				■	■
118	■			■	■	■		
119	■			■	■		■	
120	■			■	■			■
121	■			■		■	■	
122	■			■		■		■
123	■			■			■	■
124	■				■	■	■	
125	■				■	■		■
126	■				■		■	■
127	■					■	■	■
128		■	■	■	■			
129		■	■	■		■		
130		■	■	■			■	
131		■	■	■				■
132		■	■		■	■		
133		■	■		■		■	
134		■	■		■			■
135		■	■			■	■	
136		■	■			■		■
137		■	■				■	■
138		■		■	■	■		
139		■		■	■		■	
140		■		■	■			■

Table 1: (continued)

Number	PTMC-dMA 4k	PDLLA-dMA 4k	PCL-dMA 4k	PEG-dMA 4k	PTMC-dMA 10k	PDLLA-dMA 10k	PCL-dMA 10k	PEG-dMA 10k
141		■		■		■	■	
142		■		■		■		■
143		■		■			■	■
144		■			■	■	■	
145		■			■	■		■
146		■			■		■	■
147		■				■	■	■
148			■	■	■	■		
149			■	■	■		■	
150			■	■	■			■
151			■	■		■	■	
152			■	■		■		■
153			■	■			■	■
154			■		■	■	■	
155			■		■	■		■
156			■		■		■	■
157			■			■	■	■
158				■	■	■	■	
159				■	■	■		■
160				■	■		■	■
161				■		■	■	■
162					■	■	■	■
163	■	■	■	■	■			
164	■	■	■	■		■		
165	■	■	■	■			■	
166	■	■	■	■				■
167	■	■	■		■	■		
168	■	■	■		■		■	
169	■	■	■		■			■
170	■	■	■			■	■	
171	■	■	■			■		■
172	■	■	■				■	■
173	■	■		■	■	■		
174	■	■		■	■		■	
175	■	■		■	■			■
176	■	■		■		■	■	
177	■	■		■		■		■

Number	PTMC-dMA 4k	PDLLA-dMA 4k	PCL-dMA 4k	PEG-dMA 4k	PTMC-dMA 10k	PDLLA-dMA 10k	PCL-dMA 10k	PEG-dMA 10k
178	■	■		■			■	■
179	■	■			■	■	■	
180	■	■			■	■		■
181	■	■			■		■	■
182	■	■				■	■	■
183	■		■	■	■	■		
184	■		■	■	■		■	
185	■		■	■	■			■
186	■		■	■		■	■	
187	■		■	■		■		■
188	■		■	■			■	■
189	■		■		■	■	■	
190	■		■		■	■		■
191	■		■		■		■	■
192	■		■			■	■	■
193	■			■	■	■	■	
194	■			■	■	■		■
195	■			■	■		■	■
196	■			■		■	■	■
197	■				■	■	■	■
198		■	■	■	■	■		
199		■	■	■	■		■	
200		■	■	■	■			■
201		■	■	■		■	■	
202		■	■	■		■		■
203		■	■	■			■	■
204		■	■		■	■	■	
205		■	■		■	■		■
206		■	■		■		■	■
207		■	■			■	■	■
208		■		■	■	■	■	
209		■		■	■	■		■
210		■		■	■		■	■
211		■		■		■	■	■
212		■			■	■	■	■
213			■	■	■	■	■	
214			■	■	■	■		■

Table 1: (continued)

Number	PTMC-dMA 4k	PDLLA-dMA 4k	PCL-dMA 4k	PEG-dMA 4k	PTMC-dMA 10k	PDLLA-dMA 10k	PCL-dMA 10k	PEG-dMA 10k
215			■	■	■		■	■
216			■	■		■	■	■
217			■		■	■	■	■
218				■	■	■	■	■
219	■	■	■	■	■	■		
220	■	■	■	■	■		■	
221	■	■	■	■	■			■
222	■	■	■	■		■	■	
223	■	■	■	■		■		■
224	■	■	■	■			■	■
225	■	■	■		■	■	■	
226	■	■	■		■	■		■
227	■	■	■		■		■	■
228	■	■	■			■	■	■
229	■	■		■	■	■	■	
230	■	■		■	■	■		■
231	■	■		■	■		■	■
232	■	■		■		■	■	■
233	■	■			■	■	■	■
234	■		■	■	■	■	■	
235	■		■	■	■	■		■
236	■		■	■	■		■	■
237	■		■	■		■	■	■
238	■		■		■	■	■	■
239	■			■	■	■	■	■
240		■	■	■	■	■	■	
241		■	■	■	■	■		■
242		■	■	■	■		■	■
243		■	■	■		■	■	■
244		■	■		■	■	■	■
245		■		■	■	■	■	■
246			■	■	■	■	■	■
247	■	■	■	■	■	■	■	
248	■	■	■	■	■	■		■
249	■	■	■	■	■		■	■
250	■	■	■	■		■	■	■
251	■	■	■		■	■	■	■

Number	PTMC-dMA 4k	PDLLA-dMA 4k	PCL-dMA 4k	PEG-dMA 4k	PTMC-dMA 10k	PDLLA-dMA 10k	PCL-dMA 10k	PEG-dMA 10k
252	■	■		■	■	■	■	■
253	■		■	■	■	■	■	■
254		■	■	■	■	■	■	■
255	■	■	■	■	■	■	■	■

As a control material, a hydrogel based on gelatin was prepared. Gelatin is obtained by hydrolysis of collagen and has excellent cell binding characteristics [21]. Gelatin was functionalized by reaction of the amine groups with MAAh. After dissolution in PBS (0.0125g/ml) at 40 °C and subsequent cooling to room temperature, TEA (0.18g/g gelatin) and MAAh (0.28g/g gelatin) were added and the functionalization reaction was let to proceed for 2h. The reaction mixture was dialyzed at 40°C against distilled water for 48h using dialysis bags (Spectre/Por® 3 Dialysis Membrane, MWCO 3.5 kg/mol) and freeze-dried. The degree of functionalization of the prepared gelatin-methacrylamide was assessed using NHS-fluorescein (FITC, Life Technologies). Gelatin hydrogels were prepared by photo-crosslinking as previously described. In this case the solvent was water, the gelatin-methacrylamide concentration was 33 wt.%.

Cell culturing experiments on 255 photo-crosslinked single-and mixed-macromer networks

Of each single- or mixed macromer solution, 50 µl was transferred into wells of non-treated polystyrene 48 wells plates (n=3). The network specimens were photo-crosslinked, extracted and dried as described before. To ensure that the networks remain submerged in the medium during cell culturing, each well contained a MEMO-functionalized glass disk (Ø 10 mm) to which the networks covalently bind during the crosslinking. Functionalization of the glass disks with MEMO was done by immersing the glass disks for 5 min in a solution of 2 wt% MEMO in a 95/5 mixture of ethanol and water which was adjusted to pH 4.5-5.5 with acetic acid. The disks were then rinsed with isopropanol and placed in an oven at 120 °C for 30 minutes to allow reaction of MEMO with the glass.

Human mesenchymal stem cells (hMSCs, p=5) were cultured at 37 °C in humidified air (5 % CO_2) in 175 cm^2 culture flasks (Greiner) containing αMEM (Glutamax, penicillin/streptavidin, FBS). The medium was refreshed three times a week until the cells reached confluency. Upon confluence, the cells were trypsinized and counted.

The dry single- and mixed-macromer network specimens were disinfected with ethanol (75 % in water) for 3 hours and allowed to dry overnight under

atmospheric conditions. To extract any remains of ethanol, the specimens were washed once with PBS and kept in αMEM (Glutamax, penicillin/streptavidin, FBS) overnight at 37°C. The hMSCs cells were seeded on the network specimens at a density of 10,000 cells/cm^2 and cultured at 37°C in humidified air (5 % CO_2) for a period of 10 days. The medium was refreshed three times every week.

On day 10, the network specimens were washed in warm PBS (37°C) to remove excess medium and non-adhering cells. The adhering cells were lyzed using CyQuant lysis buffer (Life Sciences) for 30 minutes at room temperature and stored at -80°C. The DNA content of the adhering cells was then quantified using CyQuant GR dye (Life Sciences) by measuring the fluorescence at an excitation wavelength of 480 nm and an emission wavelength of 520 nm using a Tecan Saphire fluorometer.

Detailed cell culturing experiments on selected newly-synthesized photo-crosslinked hydrogel networks

Following the high throughput screening cell culturing experiments, more elaborate cell culturing experiments (n=6) using hMSCs were conducted on the mixed macromer hydrogel network specimens that had high water uptake (more than 200 %) as well as large numbers of adhering cells. Several networks with comparable water uptake values but with low numbers of adhering cells were evaluated as well. Gelatin-methacrylamide and PEG-dMA networks were used as positive and negative controls. The materials for these studies were prepared *de novo* according to the methods described earlier. The network specimens were photo-crosslinked, extracted and dried in the wells of 48 wells polystyrene cell culture plates as described before.

The hMSCs cells were seeded on the network specimens at a density of 10,000 cells/cm^2 and cultured at 37°C in humidified air (5 % CO_2) for periods of up to 10 days. The medium was refreshed three times every week. At 1, 6 and 10 days, the network specimens were washed in warm PBS (37°C) to remove excess medium and non-adhering cells. The DNA content of the adhering cells was quantified as previously described.

Mechanical properties of selected photo-crosslinked hydrogel networks

The mechanical properties of mixed-macromer hydrogel network specimens that had high water uptake (more than 200 %) as well as large numbers of adhering cells were determined by compression- and tensile testing. Their properties in the hydrated state were compared to those of photo-crosslinked gelatin-methacrylamide and PEG-dMA networks. Cylindrical network specimens measuring 5 mm in height and 5 mm in diameter for compression testing were prepared using Teflon® molds. The mold cavities were filled with the (mixed) macromer solutions and photo-crosslinked as previously described. The specimens were extracted and dried as described before, then equilibrated in distilled water for 48 hours. The compressive properties of the water-swollen networks were determined in triplicate according to ASTM 695 at a compression rate of 30% per min. The compressive modulus, E_c, was determined at 17.5 % compressive strain.

For the preparation of specimens for tensile testing and tearing experiments, network films (approximately 11 cm x 11 cm x 0.5 mm) were prepared by casting the (mixed) macromer solutions on glass plates, followed by photo-crosslinking, extracting and drying as described previously. Tensile modulus (E_t), ultimate strength (σ_{max}) and elongation at break (ε_{max}) were determined according to ASTM D882. Dumbbell specimens (with a length of 50 mm and a thickness of 0.4 mm) were punched out from the network films and tested in triplicate at a rate 10 mm/min. The grip-to-grip separation was 35 mm. Tearing experiments in which the average- (TPS_{ave}) and maximum (TPS_{max}) tear propagation strengths were determined in triplicate, were conducted according to ASTM 1938 at a rate of 250 mm/min using trouser tear specimens (37.5 mm x 12.5 mm, with a 25 mm slit) that were punched out from the network films. The tearing energy (G, expressed in kJ/m^2) was calculated according to [22]:

$$G = \frac{2F}{t}$$

Here, F is the average force during tearing (N) and t is the thickness of the sample (mm).

Results and discussion

Synthesis and characterization of macromers

A series of different macromers with molar masses of approximately 4 kg/mol and 10 kg/mol were prepared by ring opening polymerization of TMC, DLLA and CL, which yields hydroxyl group-terminated oligomers, and subsequent functionalization with methacrylic anhydride. Also PEG was functionalized by reaction with methacrylic anhydride. The molecular weights (M_n) and the degrees of functionalization of the synthesized macromers as determined by ^{1}H-NMR are listed in Table 2.

M_n of the PTMC macromers was determined using the peak integrals at δ=1.68 ppm (hexanediol, 4H) and δ=2.05 ppm (PTMC, –CH_2–). M_n of the PDLLA macromers was determined using the peak integrals at δ=4.12 ppm (hexanediol, 4H) and δ=5.16 ppm (PDLLA, >CH–). M_n of the PCL macromers was determined using the peak integrals at δ=1.68 ppm (hexanediol, 4H) and δ=4.06 ppm (PCL, –CH_2–). M_n of the PEG macromers was determined using the peak integrals at δ=4.31 ppm (methacrylate, 4H) and δ=3.7 ppm (PEG, –C_2H_4–).

Table 2: Characteristics of the synthesized macromers and single-macromer networks. The molecular weight (M_n) and the degree of functionalization (f) were determined by ^{1}H-NMR, T_g and T_m were determined by DSC. Water uptake is given as a mean value of triplicate measurements with the standard deviation in parentheses.

Number	Macromer	Macromer properties				Network properties		
		M_n kg/mol	f %	T_g °C	T_m °C	T_g °C	T_m °C	Water uptake (wt.%) (sd)
1	PTMC-dMA 4k	4.2	89	-22.3	-	-19.9	-	0 (0)
2	PDLLA-dMA 4k	4.7	95	26.1	-	35.4	-	3 (1)
3	PCL-dMA 4k	4.2	100	-55.8	53.9	-63.2	51.1	0 (0)
4	PEG-dMA 4k	5.1	100	-54.0	51.9	-54.2	45.7	890 (40)
5	PTMC-dMA 10k	9.5	90	-21.0	-	-17.1	-	1 (0)
6	PDLLA-dMA 10k	10.0	85	36.1	-	38.3	-	4 (0)
7	PCL-dMA 10k	10.6	100	-62.3	56.9	-61.2	55.2	1 (0)
8	PEG-dMA 10k	11.5	100	-48.1	56.9	-56.3	54.1	1700 (62)

Successful reaction of the oligomers with methacrylic anhydride was confirmed by the appearance of –C=CH_2 and the –CH_3 peaks of methacrylate end-groups at δ=6.11, δ=5.57 and δ=1.94 ppm. The degree of functionalization of PTMC macromers was determined by comparing the integral values of the –CH_2– peak of hexanediol at δ 1.68 with the –C=CH_2 peaks at δ=6.11 and δ=5.57 ppm. For PDLLA macromers, the integral value of the –O–CH_2– peak of hexanediol at δ=4.12 ppm was used. For PCL macromers, the integral value of the HO–CH_2– peak of unreacted OH-groups of the oligomer at δ= 3.64 ppm was used. The degrees of functionalization of PEG macromers was determined after addition of TFAA: residual, unreacted OH-groups of the oligomer will react with this highly electronegative anhydride yielding a peak at δ=4.50 ppm. The integral value of this peak and that of the –CH_2–O– peak of the macromer at δ 4.31 ppm were used to determine the degree of functionalization. For all macromers the degrees of functionalization were in excess of 85%, suggesting that functionalization of the oligomers was essentially complete.

The macromers were first photo-crosslinked in solution separately to yield single-macromer networks. To a large extent, the characteristics of the macromers will determine the physical properties of the networks. Table 2 also includes thermal properties and water uptake data of the single-macromer networks prepared. It can be seen that, like the macromers, networks prepared from PTMC-dMA or PDLLA-dMA macromers are amorphous materials with corresponding glass transition temperatures. Therefore, the PTMC networks are flexible and rubber-like materials, while the PDLLA networks are rigid and glassy ones. PCL-dMA and PEG-dMA are semi-crystalline compounds with low glass transition temperatures, and networks prepared from these macromers are semi-crystalline as well.

PTMC, PDLLA and PCL are hydrophobic polymers, while PEG is water soluble. Therefore, networks prepared from PEG-dMA are hydrogels and capable of taking up large amounts of water. Due to the larger mesh size, networks prepared from the PEG macromer with the highest molecular weight have the highest uptake of water.

The degree of functionalization of gelatin-methacrylamide was 67 %. A gelatin network was formed by photo-crosslinking the methacrylamide-functionalized gelatin in water. The water uptake of this hydrogel was 671 wt.% water (sd = 4 wt.%).

When preparing mixed-macromer networks by photo-crosslinking mixtures of macromers, networks with micro-phase separated morphologies and a very broad range of physical properties can be obtained. In earlier work we showed that elastomeric networks and hydrogels with exceptional mechanical properties could be prepared in this manner [23]. As it was not possible to predict this *a priori*, tough synthetic hydrogels with good cell adhesive properties might also be prepared in this manner.

Combinatorial synthesis of 255 photo-crosslinked single- and mixed-macromer networks

The different mixtures of PTMC-dMA 4k, PDLLA-dMA 4k, PCL-dMA 4k, PEG-dMA 4k, PTMC-dMA 10k, PDLLA-dMA 10k, PCL-dMA 10k and PEG-dMA 10k macromers in propylene carbonate were simultaneously photo-crosslinked in the wells of tissue culture plates. The obtained 255 different single- and mixed-macromer networks, of which the composition is given in Table 1, were subsequently extracted and dried. As it is our aim to develop cell-adhering synthetic hydrogels, measuring the amounts of water taken up by the networks was found to be a convenient manner to first assess the physical characteristics of this large number of networks. See below for results.

Cell culturing experiments on 255 photo-crosslinked single-and mixed-macromer networks

The simultaneous preparation of large numbers of different photo-crosslinked single- and mixed-macromer networks in the wells of cell culturing plates also allows the assessment of their cell-binding properties in a very practical manner. As the physical properties of the macromers used in preparing the 255 mixed-macromer networks are very different, it can be expected that the interaction of the mixed-macromer networks with cells will be highly diverse and unpredictable. To assess cell adhesion and proliferation, screening cell culturing experiments on the different mixed-macromer networks using hMSCs were conducted for a time period of 10 days.

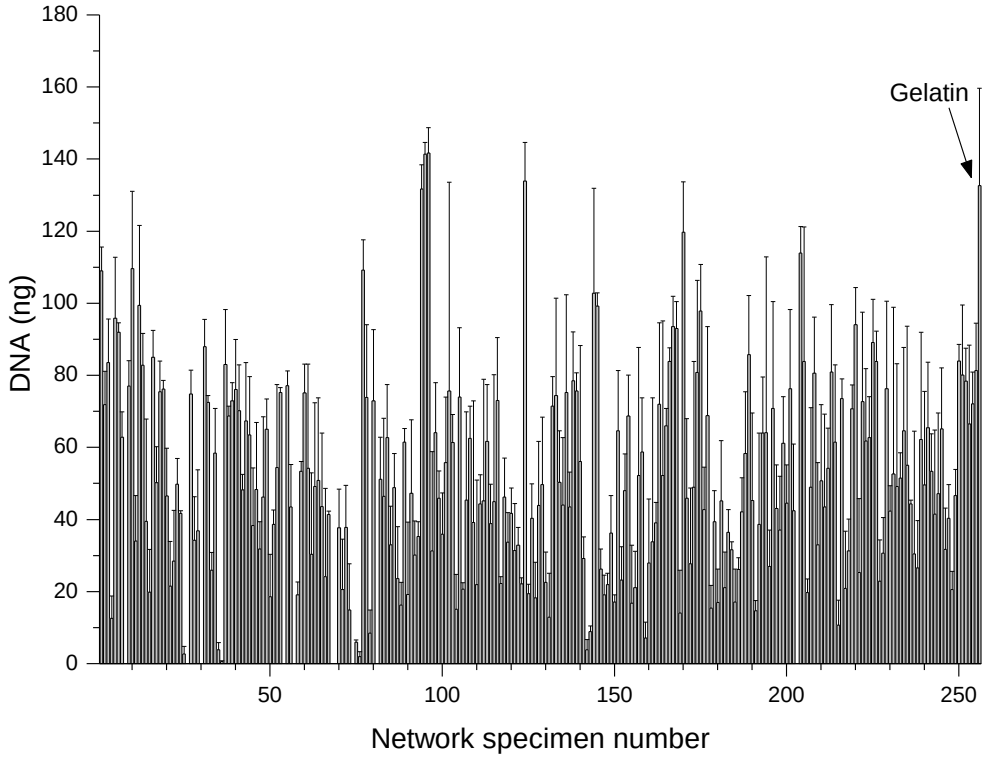

Figure 1: The DNA content of hMSC cells adhering to 255 different photo-crosslinked mixed-macromer networks after a cell culturing period of 10 days. The DNA content in ng is a measure of the number of cells adhering to the surface of the networks. The numbers of the network specimens correspond to those in Table 1, where their composition is given. The photo-crosslinked gelatin-methacrylamide network was used as a positive control. Data is presented as mean ± sd for n=3.

After washing, the amount of DNA of the cells adhering to the networks was determined by fluorescence. The amount of DNA is a measure of the number of cells present on the surface of the networks. The results of these experiments are presented in Figure 1. The figure shows that the amount of DNA of cells attaching to the different network specimens varies significantly for the different networks. While several networks show very limited attachment of hMSCs to their surface, other photo-crosslinked mixed-macromer networks show extensive cell attachment similar to that of the gelatin networks.

Although it might be expected that the affinity of cells towards synthetic polymeric biomaterials decreases with increasing hydrophilicity [24], the question remains if we have not synthesized mixed-macromer networks within our library that have good cell adhesion as well as high water uptake.

In Figure 2 the DNA content of cells adhering to the most hydrophilic photo-crosslinked mixed-macromer networks of the combinatorial library and the water uptake of those networks are presented at the same time. In the figure, the cell adhesion data is presented in order of decreasing water uptake of the networks. Although the amount of DNA, and thus the number of cells adhering to these synthetic hydrogels, is lower than that on the gelatin network specimens, there are several combinatorial mixed-macromer networks in our library that show high water uptake as well as very good cell attachment in these screening cell culturing experiments. Mixed-macromer networks nr. 27 (prepared from PEG-dMA 4k and PTMC-dMA 10k), nr. 166 (prepared from PTMC-dMA 4k, PDLLA-dMA 4k, PCL-dMA 4k, PEG-dMA 4k and PEG-dMA 10k) and nr. 175 (prepared from PTMC-dMA 4k, PDLLA-dMA 4k, PEG-dMA 4k, PTMC-dMA 10k and PEG-dMA 10k) show high numbers of adhering cells and take up large amounts of water. The values for these synthetic mixed-macromer hydrogels are respectively 75 ng DNA and 299% water uptake, 84 ng DNA and 215 % water uptake, 98 ng DNA and 243 % water uptake.

These results suggest that by combinatorial synthesis of mixed-macromer networks by photo-polymerization of PTMC-, PDLLA, PCL- and PEG macromers and high throughput screening cell culturing experiments we have been able to

prepare and identify biodegradable synthetic hydrogels with good cell adhesion characteristics.

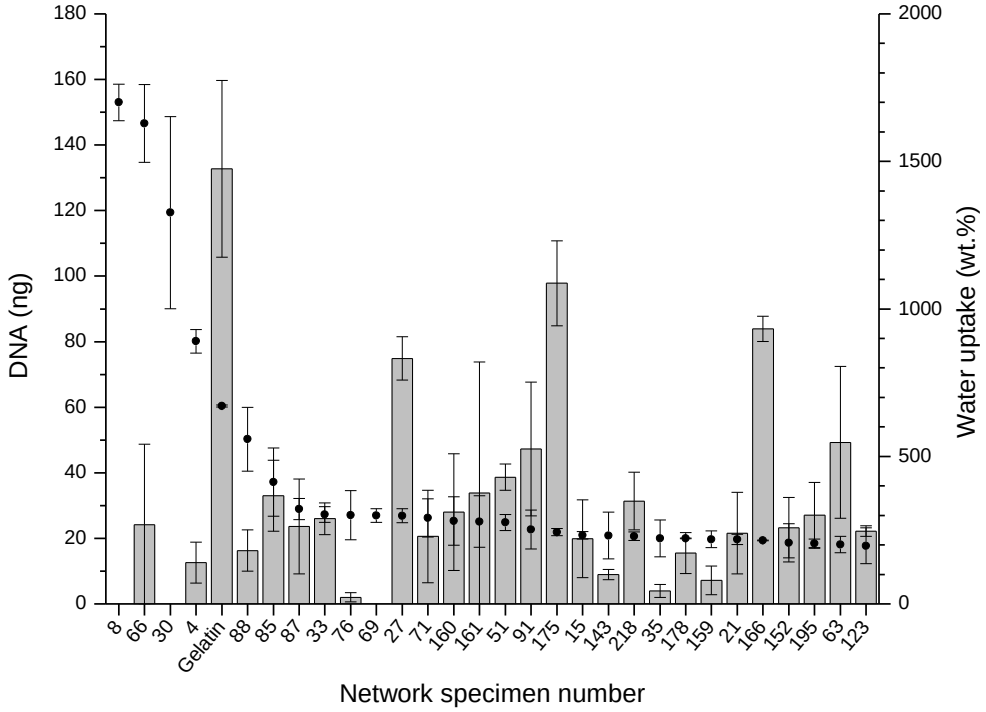

Figure 2: The DNA content of hMSC cells adhering to the most hydrophilic photo-crosslinked mixed-macromer networks after a cell culturing period of 10 days (bars) and the water uptake of those networks (●). The DNA content (ng) is a measure of the number of cells adhering to the surface of the networks. The numbers of the network specimens correspond to those in Table 1, where their composition is given. The photo-crosslinked gelatin-methacrylamide network was used as a positive control. Data is presented as mean ± sd for n=3 in the order of decreasing water uptake.

Detailed cell culturing experiments on selected newly synthesized photo-crosslinked hydrogel networks

To validate the findings of the high throughput screening cell culturing experiments which showed good hMSC cell attachment to several photo-crosslinked mixed-macromer hydrogel networks (network compositions nr. 27, nr. 166 and nr. 175 in Table 1), a second series of fully independent experiments was conducted. Elaborate cell culturing experiments were conducted on selected hydrogel networks that were prepared by photo-crosslinking mixed-macromers that were synthesized anew.

Table 3 shows characteristics of the different macromers and water uptakes of the corresponding mixed-macromer networks that were newly prepared. The table also shows the composition of the networks that were used in the hMSC cell culturing experiments. Networks with compositions corresponding to the mixed-macromer hydrogel networks that showed high water uptake and good cell attachment in the high throughput cell culturing experiment (networks nr. 27-2, nr. 166-2 and nr. 175-2) were again prepared. Also networks that had comparable values of water uptake but low DNA contents and limited cell adhesion (networks nr. 76-2, nr. 143-2 and nr. 159-2) were again prepared. A negative control prepared from PEG-dMA 4k and PEG-dMA 10k (network nr. 30-2), and a positive control (photo-crosslinked gelatin methacrylamide) was used. The table shows that the features of these newly synthesized macromers and networks are very similar to those prepared earlier (see Table 2 and Figure 2).

Table 3: Characteristics of the newly synthesized dimethacrylate-functionalized PTMC-, PDLLA-, PCL- and PEG macromers, and the composition and water uptake of the photo-crosslinked networks used in the detailed cell culturing experiments. Water uptake is given as a mean value of triplicate measurements with the standard deviation in parentheses. The molecular weights (M_n) and the degrees of functionalization (f) of the macromers were determined by ^{1}H-NMR. The macromers present in the different networks (colored grey) are present in equal amounts by weight.

Macromer	**PTMC-dMA 4k**	**PDLLA-dMA 4k**	**PCL-dMA 4k**	**PEG-dMA 4k**	**PTMC-dMA 10k**	**PDLLA-dMA 10k**	**PCL-dMA 10k**	**PEG-dMA 10k**	
M_n (kg/mol)	4.0	4.6	41	5.1	9.5	10.6	10.3	11.5	
f (%)	92	94	92	100	90	91	91	100	
Network	**Network composition**								**Water uptake** wt.%
27-2				■	■				232 (21)
166-2	■	■	■	■				■	181 (2)
175-2	■	■		■	■			■	197 (18)
76-2			■	■				■	257 (51)
143-2		■		■			■	■	197 (74)
159-2				■	■	■		■	235 (2)
30-2				■				■	1189 (315)
4-2				■					890 (40)

Detailed cell culturing experiments were done on the newly prepared networks presented in Table 3 and on a newly prepared gelatin-methacrylamide network. The hMSCs used were from the same donor and of the same passage as those used in the first screening experiment on 255 mixed-macromer networks. For each network six specimens were used, and the amount of DNA of the adherent hMSCs was determined after 1, 6 and 10 days. This allows assessment of the initial adhesion of the cells and of their rate of proliferation. The results are presented in Figure 3.

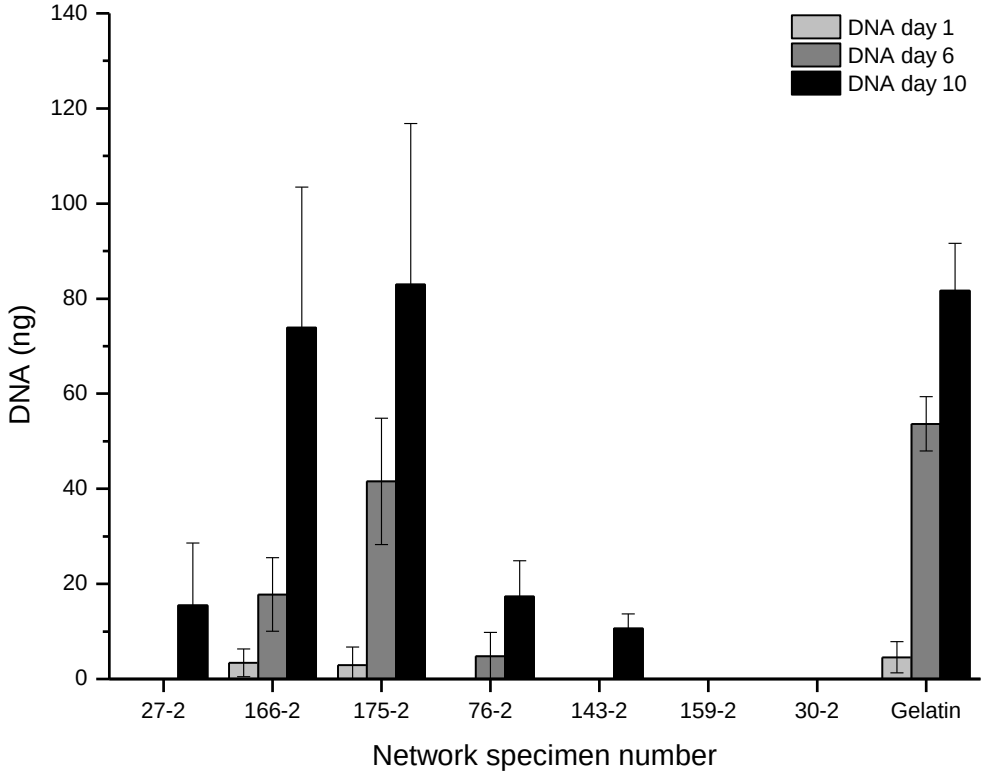

Figure 3: The DNA content of hMSC cells adhering to hydrophilic photo-crosslinked mixed-macromer networks after culturing for 1, 6 and 10 days. The DNA content in ng is a measure of the number of cells adhering to the surface of the networks. The numbers of the network specimens correspond to those in Table 3, where their composition is given. The photo-crosslinked PEG network nr. 30-2 is used as a negative control, the photo-crosslinked gelatin-methacrylamide network was used as a positive control. Data is presented as mean ± sd for n=6.

The figure shows that cell adhesion and proliferation on the control networks is as could be expected: no adhesion nor cell proliferation on the nr. 30-2 PEG networks and adequate initial cell adhesion and extensive cell proliferation on the gelatin networks. Similar to the results of the high throughput screening cell culturing experiments, combinatorial hydrogel network specimens nr. 76-2, nr. 143-2 and nr. 159-2 with high uptakes of water of respectively 257, 197 and 235 wt.% show very limited initial cell adhesion and proliferation.

In contrast, although the mixed-macromer networks nr. 166-2 and nr. 175-2 take up similar amounts of water, these networks do show good initial cell attachment and high rates of proliferation of the hMSCs similar to that found for the control gelatin network. These results confirm the earlier findings that these synthetic networks can not only take up large amounts of water, but at the same allow for good cell adhesion and proliferation.

Hydrogel network nr. 27-2 , which in the first screening experiment showed high numbers of attached cells after 10 days, now did not show initial cell adhesion. Although this result was not expected, it should be considered that in the screening of large numbers of specimens in high throughput it is possible to find false positive or false negative results.

Mechanical properties of mixed-macromer hydrogels showing good cell attachment

Besides their excellent properties regarding the adhesion and proliferation of hMSCs, it was noticed that networks nr. 166, nr. 166-2, nr. 175 and nr. 175-2 had excellent handling characteristics. In contrast to the PEG-dMA and the gelatin-methacrylate networks, these mixed-macromer networks were very strong and resilient. This is important when these materials are to be used as medical implants or in tissue engineering.

The mechanical properties of these mixed-macromer hydrogels were evaluated in the hydrated state by compression testing, tensile testing and by conducting tear tests. Their properties were compared to those of a hydrogel network prepared from gelatin-methacrylamide. The results are shown in Figure 4 and Table 4.

Figures 4a and 4b show that the water-swollen mixed-macromer hydrogel networks showed excellent compressive properties, especially when compared to the gelatin-methacrylamide network. While the latter network failed catastrophically and shattered at a compressive strain of 44 %, which is comparable to the behavior of synthetic single-macromer hydrogels [3], hydrogels nr. 166-2 and nr. 175-2 did not fail during the compression test. The compression modulus, E_c, of these swollen networks was 0.7 MPa, somewhat lower than measured for the gelatin-methacrylamide network (3.3 MPa). Interestingly, when the mixed-macromer hydrogel networks were again placed in water, the specimens returned to their original shapes and dimensions. This illustrates the remarkable elastic properties of these networks.

The hydrated photo-crosslinked gelatin-methacrylamide network was too brittle to allow testing in tension. In contrast, the tensile properties of the hydrated mixed-macromer networks were outstanding and could be evaluated without any difficulty. Characteristic tensile stress-strain diagrams of water-swollen mixed-macromer hydrogel networks nr. 166-2 and nr. 175-2 are shown in Figure 4c. It can be seen in Table 4 that the tensile modulus for these hydrogels is respectively 1.49 MPa for network nr. 166-2 and 1.27 MPa for network nr. 175-2. The values of the maximum tensile strengths (respectively 1.81 and 0.72 MPa) and the elongations at break (283 and 186 %) are extraordinarily high for hydrogel networks containing such large amounts of water. It was even possible to conduct tearing experiments with these hydrogels.

In Figure 4d the normalized tearing force (N/mm) during propagation of the tear is given. The force required to tear network nr. 166-2 is much higher than that required for network nr. 175-2, the behavior of the tearing force is also much more erratic. This behavior is characteristic of stick-slip tearing behavior [25], and can be due to the presence of crystallized PCL domains in the hydrated network. Interestingly, the high tearing energy of the hydrated hydrogel network nr. 166-2 (0.64 kJ/m^2) was found to be very much higher than that of any other synthetic hydrogel described in the literature. As far as we are aware of, the highest tearing energies described are those of a double network composed of poly(acryl amide) and PAA-poly(2-acrylamido-2-methylpropanesulfonic acid (0.30 kJ/m^2) [26] and a network composed of PEG and polydimethylsiloxane chains (0.08 kJ/m^2) [27].

Importantly, the tearing energy of hydrogel nr. 166-2 is comparable to the tearing energy of articular cartilage (1 kJ/m²) [28].

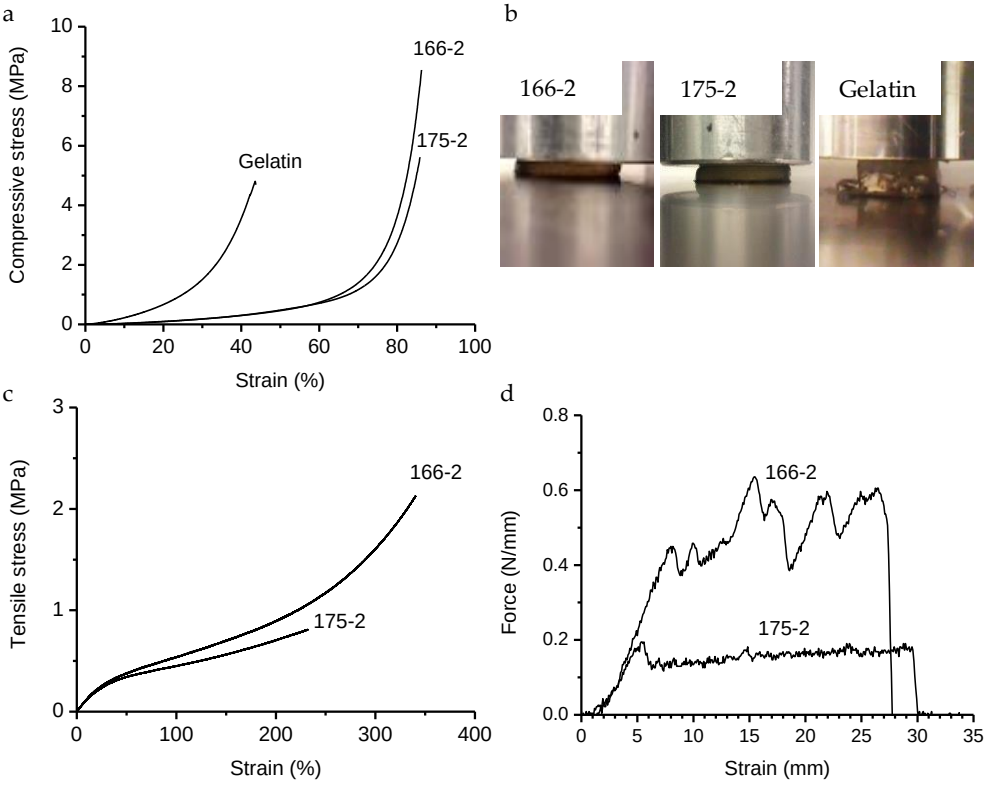

Figure 4: Mechanical properties of mixed-macromer hydrogel networks nr. 166-2 and nr. 175-2 in the hydrated state. The composition of the networks and their water uptake is given in Table 3. The compressive properties of a hydrated gelatin-methacrylamide network are given as well. a) Characteristic compressive stress-strain diagrams; b) images of the compressed network specimens at maximal compression; c) characteristic tensile stress-strain diagrams; d) characteristic tear propagation strength determinations, the tearing force is normalized to the thickness of the specimen (N/mm).

Table 4: Compressive- and tensile properties in the hydrated state of photo-crosslinked mixed-macromer hydrogel networks. The data is presented as a mean value of triplicate measurements with the standard deviation in parentheses. The photo-crosslinked gelatin-methacrylamide network was too brittle to allow testing in tension.

Network	E_c MPa	E_t MPa	σ_t MPa	ε_t %	TPS_{ave} N/mm	TPS_{max} N/mm	G kJ/m^2
166-2	0.7 (0.1)	1.49 (0.38)	1.81 (0.31)	283 (60)	0.32 (0.17)	0.49 (0.24)	0.64 (0.34)
175-2	0.7 (0.1)	1.24 (0.18)	0.72 (0.08)	186 (38)	0.13 (0.02)	0.20 (0.02)	0.27 (0.04)
Gelatin	3.3 (0.2)	-	-	-	-	-	-

Conclusions

Using a combinatorial approach, mixtures of eight different macromers based on poly(trimethylene carbonate), poly(D,L-lactide), poly(ε-caprolactone) and polyethylene glycol were simultaneously photo-crosslinked in solution yielding 255 different networks with widely differing properties. Water uptake and cell culturing experiments performed in a high throughput manner allowed the identification of several hydrogel networks that were able to take up large amounts of water and at the same time allowed good cell adhesion. This was confirmed by conducting more detailed cell culturing experiments on selected newly-synthesized mixed hydrogel networks. It was additionally found, that these networks had outstanding mechanical properties, with tearing energies close to those of articular cartilage.

Acknowledgements

This work was supported by a grant from the Dutch government to the Netherlands Institute for Regenerative Medicine (NIRM, grant No. FES0908).

References

1. Nair LS and Laurencin CT, Biodegradable polymers as biomaterials. Progress in Polymer Science, 2007. 32(8-9): p. 762-798.
2. Zhu JM, Bioactive modification of poly(ethylene glycol) hydrogels for tissue engineering. Biomaterials, 2010. 31(17): p. 4639-4656.
3. Calvert P, Hydrogels for soft machines. Advanced Materials, 2009. 21(7): p. 743-756.
4. Patel A and Mequanint K, Synthesis and characterization of polyurethane-block-poly(2-hydroxyethyl methacrylate) hydrogels and their surface modification to promote cell affinity. Journal of Bioactive and Compatible Polymers, 2011. 26(2): p. 114-129.
5. Burdick JA and Anseth KS, Photoencapsulation of osteoblasts in injectable RGD-modified PEG hydrogels for bone tissue engineering. Biomaterials, 2002. 23(22): p. 4315-4323.
6. Hern DL and Hubbell JA, Incorporation of adhesion peptides into nonadhesive hydrogels useful for tissue resurfacing. Journal of Biomedical Materials Research, 1998. 39(2): p. 266-276.
7. Salinas CN and Anseth KS, The influence of the RGD peptide motif and its contextual presentation in PEG gels on human mesenchymal stem cell viability. Journal of Tissue Engineering and Regenerative Medicine, 2008. 2(5): p. 296-304.
8. Zhang Z, Lai YX, Yu L, and Ding JD, Effects of immobilizing sites of RGD peptides in amphiphilic block copolymers on efficacy of cell adhesion. Biomaterials, 2010. 31(31): p. 7873-7882.
9. Hubbell JA, Biomaterials in tissue engineering. Bio-Technology, 1995. 13(6): p. 565-576.
10. Gong CY, Shi SA, Dong PW, Kan B, Gou ML, Wang XH, Li XY, Luo F, Zhao X, Wei YQ, and Qian ZY, Synthesis and characterization of PEG-PCL-PEG thermosensitive hydrogel. International Journal of Pharmaceutics, 2009. 365(1-2): p. 89-99.
11. Jeong B, Bae YH, and Kim SW, Drug release from biodegradable injectable thermosensitive hydrogel of PEG-PLGA-PEG triblock copolymers. Journal of Controlled Release, 2000. 63(1-2): p. 155-163.
12. Cohn D and Hotovely-Salomon A, Biodegradable multiblock PEO/PLA thermoplastic elastomers: molecular design and properties. Polymer, 2005. 46(7): p. 2068-2075.
13. He CL, Kim SW, and Lee DS, In situ gelling stimuli-sensitive block copolymer hydrogels for drug delivery. Journal of Controlled Release, 2008. 127(3): p. 189-207.

14. Huang MH, Li SM, Hutmacher DW, Schantz JT, Vacanti CA, Braud C, and Vert M, Degradation and cell culture studies on block copolymers prepared by ring opening polymerization of epsilon-caprolactone in the presence of poly(ethylene glycol). Journal of Biomedical Materials Research Part A, 2004. 69A(3): p. 417-427.
15. Wang SF, Lu LC, Gruetzmacher JA, Currier BL, and Yaszemski MJ, Synthesis and characterizations of biodegradable and crosslinkable poly(epsilon-caprolactone fumarate), poly(ethylene glycol fumarate), and their amphiphilic copolymer. Biomaterials, 2006. 27(6): p. 832-841.
16. Zhu AP, Chan-Park MB, and Gao JX, Foldable micropatterned hydrogel film made from biocompatible PCL-b-PEG-b-PCL diacrylate by UV embossing. Journal of Biomedical Materials Research Part B-Applied Biomaterials, 2006. 76B(1): p. 76-84.
17. Brocchini S, James K, Tangpasuthadol V, and Kohn J, Structure-property correlations in a combinatorial library of degradable biomaterials. Journal of Biomedical Materials Research, 1998. 42(1): p. 66-75.
18. Webster DC, Combinatorial and high-throughput methods in macromolecular materials research and development. Macromolecular Chemistry and Physics, 2008. 209(3): p. 237-246.
19. Anderson DG, Putnam D, Lavik EB, Mahmood TA, and Langer R, Biomaterial microarrays: Rapid, microscale screening of polymer-cell interaction. Biomaterials, 2005. 26(23): p. 4892-4897.
20. Amsden B, Misra G, Marshall M, and Turner N, Synthesis and characterization of biodegradable networks providing saturated-solution prolonged delivery. Journal of Pharmaceutical Sciences, 2008. 97(2): p. 860-874.
21. Van Vlierberghe S, Vanderleyden E, Dubruel P, De Vos F, and Schacht E, Affinity study of novel gelatin cell carriers for fibronectin. Macromolecular Bioscience, 2009. 9(11): p. 1105-1115.
22. Fatt MSH, Chen L, and Al-Quraishi AA, Fracture parameters for natural rubber under dynamic loading. Strain, 2011. 47: p. E505-E518.
23. Zant E and Grijpma DW, Tough biodegradable mixed-macromer networks and hydrogels by photo-crosslinking in solution. Acta Biomaterialia, resubmitted after revision. Chapter 4 of this thesis
24. Folkman J and Moscona A, Role of cell-shape in growth-control. Nature, 1978. 273(5661): p. 345-349.
25. Liang SM, Flu J, Wu ZL, Kurokawa T, and Gong JP, Toughness enhancement and stick-slip tearing of double-network hydrogels in Poly(ethylene glycol) solution. Macromolecules, 2012. 45(11): p. 4758-4763.

26. Tanaka Y, Kuwabara R, Na YH, Kurokawa T, Gong JP, and Osada Y, Determination of fracture energy of high strength double network hydrogels. Journal of Physical Chemistry B, 2005. 109(23): p. 11559-11562.
27. Cui J, Lackey MA, Tew GN, and Crosby AJ, Mechanical properties of end-linked PEG/PDMS hydrogels. Macromolecules, 2012. 45(15): p. 6104-6110.
28. Chin-Purcell MV and Lewis JL, Fracture of articular cartilage. Journal of Biomechanical Engineering, 1996. 118(4): p. 545-556.

Chapter 6 - A combinatorial photo-crosslinking method for the preparation of porous structures with widely differing properties

Erwin Zant, Maarten M. Blokzijl, Dirk W. Grijpma

Macromolecular Rapid Communications, 2015. 36 (21): p. 1902-1909
DOI:10.1002/MARC.201500229.

Abstract

A novel method for the simultaneous preparation of a large number of porous polymeric structures with highly differing physical properties has been developed. Low molecular weight methacrylate end-functionalized polymers (macromers) were dissolved in ethylene carbonate, cooled to below the melting temperature of the solvent and subsequently photo-crosslinked. The crystallized and phase separated ethylene carbonate was extracted with water, upon which a porous crosslinked polymer network was obtained. The method was applied to combinatorial mixtures of methacrylate end-functionalized polymers that are relevant in the biomedical field: poly(trimethylene) (PTMC-dMA) poly(D,L-lactide) (PDLLA-dMA) and polyethylene glycol (PEG-dMA) dissolved in ethylene carbonate at concentrations of approximately 25 wt. %. In this manner, we were able to simultaneously prepare 63 different porous polymeric structures with a very wide range of physical properties. In the hydrated state the compressive moduli of the prepared structures ranged from 0.01 to 60 MPa, as water uptake ranged between 3 and 1500 wt.%.

Introduction

As cells are surrounded by a three dimensional (3D) extracellular matrix, tissue engineering makes use of scaffolding structures to replace damaged or diseased tissue. Synthetic polymeric biomaterials have been widely used to prepare such structures. In the development of novel polymeric scaffolding structures, high throughput (HT) production of 3D porous structures has gained much interest. Simon and coworkers mixed solutions of polymers using automated syringe pumps [1, 2] to generate a concentration gradient of a specific component in an array of polymeric scaffolds. In this way poly(ε-caprolactone) (PCL) scaffolds with a gradient in calcium phosphate content [3] and poly(ethylene glycol) (PEG) scaffolds with a gradient in compressive stiffness [4] were produced. In 2009, Bradley and coworkers produced porous hydrogels from combinationa of chitosan and poly(ethylenimine) [5]. More recently, Mano and coworkers prepared porous scaffolds from 18 different combinations of alginate and chitosan on a single chip [6]. The random (but reproducible) preparation of large numbers of different polymeric scaffolds has not been investigated in detail.

Novel polymeric biomaterials have been developed using combinatorial chemistry [7-18]. Especially interesting is the combinatorial synthesis of biodegradable polymeric networks obtained by photo-crosslinking mixtures of solutions low molecular weight end-functionalized oligomers (macromers) [19]. To simultaneously prepare large numbers of very different porous structures for application in tissue engineering, thermally induced phase separation (TIPS) of polymer solutions can be combined with a combinatorial chemistry approach [20]. Solvents like 1,4-dioxane, dimethyl sulfoxide or water have been used to prepare porous structures in this way [6, 21-28].

In this paper, we show a unique and straightforward combinatorial method to produce porous structures with a wide range of physical properties. Ethylene carbonate (EC), a benign water soluble compound melting at 37 °C that has also been used in preparing poly(lactic-*co*-glycolic acid) [29] and poly(trimethylene carbonate) (PTMC) tissue engineering scaffolds [30] by TIPS, was used to dissolve mixtures of methacrylate end-functionalized oligomers (macromers). Poly(trimethylene carbonate-dimethacrylate) (PTMC-dMA), poly(D,L-lactide-

dimethacrylate) (PDLLA-dMA) and poly(ethylene glycol-dimethacrylate) (PEG-dMA) macromers were selected to prepare the porous structures, as these polymer biomaterials are well known in the field and differ significantly in their thermal characteristics, stiffnesses and hydrophilicities [19]. Photo-crosslinking and extraction with water after crystallization of the solvent, allowed us to simultaneously prepare polymer scaffolds with a very wide range of physical properties in high throughput. As poly(ε-caprolactone) (PCL) was found to be insoluble in ethylene carbonate, PCL microspheres could be incorporated into the porous structures. In this manner, tissue engineering scaffolds that include a drug- or growth factor delivery system can be prepared (Supporting Information).

Materials and methods

Materials

Trimethylene carbonate (1,3-dioxane-2-one, TMC) was obtained from Huizhou Foryou Medical Devices Co. (China). D,L-lactide (DLLA) was obtained from Purac Biochem (The Netherlands). ε-Caprolactone (CL) (Sigma-Aldrich, U.S.A.) was dried over ground calcium hydride (CaH_2) (Merck, Germany) and purified by distillation under reduced argon atmosphere. Stannous octoate ($Sn(Oct)_2$), 1,6-hexanediol, methacrylic anhydride (MAAh), triethylamine (TEA), deuterated chloroform, trifluoroacetic anhydride (TFAA), ethylene carbonate (EC), polyethylene glycol with M_n = 4 kg/mol (PEG-4k) and PEG with M_n = 10 kg/mol (PEG-10k) were purchased from Sigma-Aldrich (U.S.A.). Dichloromethane (DCM) was obtained from Biosolve (The Netherlands), dried over ground CaH_2 and distilled before use. Ethanol was obtained from Assink Chemie (The Netherlands). Diethyl ether was obtained from Fisher Scientific (The Netherlands). Irgacure 2959 (2-hydroxy-4-(2-hydroxyethoxy)-2-methylpropiophenone) was obtained from Ciba (Switzerland).

Synthesis and characterization of dimethacrylate-functionalized PTMC, PDLLA, PCL and PEG oligomers

Linear hydroxy-terminated oligomers with molar masses of 4 and 10 kg/mol were prepared by ring-opening polymerization (ROP) of TMC, DLLA and CL monomers using calculated amounts of hexanediol as initiator and $Sn(Oct)_2$ as catalyst. The polymerizations were conducted in an inert argon atmosphere at 130 °C for two days. The synthesized oligomers, PEG-4k and PEG-10k were dried at 120 °C under vacuum for 2 h, then cooled to room temperature under argon. The oligomers were functionalized in DCM (3 mL g^{-1} oligomer), by reaction with MAAh (4 mol/mol oligomer) in the presence of TEA (4 mol/mol oligomer). The functionalization reaction proceeded at room temperature for five days. The dimethacrylate (dMA)-functionalized oligomers (macromers) were then purified by precipitation. PTMC-dMA, PDLLA-dMA and PCL-dMA were precipitated in cold ethanol (-25 °C), while PEG-dMA was precipitated in cold diethylether (-25 °C). The macromers were subsequently dried under vacuum at 40-50 °C for 3 days. The number average molecular weights (Mn) of the oligomers and the degrees of functionalization (f) of the macromers were determined using a Varian Inova 400 MHz NMR spectrometer in deuterated chloroform. The solubility of the macromers in EC (25 wt.% macromer in EC) was determined at a temperature of 50°C. Soluble macromers in EC yield clear solutions, while insoluble macromers remain turbid mixtures.

High throughput preparation and characterization of combinatorial porous network structures based on PTMC-dMA, PDLLA-dMA and PEG-dMA

Solutions of PTMC-dMA 4k, PDLLA-dMA 4k, PEG-dMA 4k, PTMC-dMA 10k, PDLLA-dMA 10k and PEG-dMA 10k macromers were prepared in EC at 50 °C. The concentration of the macromers in the solutions was 25 wt.%. To the macromer solutions, 1 wt.% (with respect to the macromers) of Irgacure 2959 was added. Combinatorial mixtures of the solutions were prepared in 48 wells polystyrene tissue culture plates using a binary approach: a macromer is either present or absent in a mixture of solutions. In Table 2 an overview is given of the prepared mixtures, macromers are marked grey when present (in equal weight fractions) or marked white when absent. The hot mixtures were then transferred into cylindrical

poly(tetrafluoro ethylene) (PTFE) molds (diameter 5mm, height 5 mm) by pipetting and cooled to 21 °C. The samples (n=3) were photo-crosslinked by illumination in an Ultralum (USA) crosslinking cabinet (365 nm, 10 mW/cm^2, 20 min). The intensity of the light was measured using a light detector (Newport Optical Power Meter, Model 1916-C, with a 818 series UV photodetector). Homogeneity of the light intensity at the site were the samples are crosslinked was confirmed. EC was extracted with distilled water during a period of three days, the water was changed every day. The samples were then rinsed with ethanol and dried in vacuum for 5 days. As ethanol evaporates faster than water, this is more efficient than evaporating water.

The porosity (expressed as a volume percentage, vol.%) of the dried porous structures was determined using the following equations.

$$\text{Porosity} = 1 - \frac{m_1}{\rho_m \cdot V} \qquad \rho_m = \frac{\sum \rho_s}{n}$$

In these equations (m_1) is the mass of the dried porous structures (g), (ϱ_m) is the density of the polymer matrix (g/cm^3), (V) is the volume of the porous structure (cm^3), (ϱ_s) is the density of a macromer present in the porous network structure (PTMC: 1.31 g/ml, PDLLA: 1.25 g/ml, PEG: 1.18 g/ml), and (n) is the number of different macromers that were combined in the porous network structure.

Water uptake (WU) of the cylindrical porous structures was assessed by submerging the dried scaffolds for 48 hours in distilled water at room temperature. Excess water was removed from the surface of the porous structures using blotting paper and the water uptake was determined as follows:

$$\text{WU} = \frac{m_s - m_1}{m_1} \times 100\%$$

Here (m_s) is the mass of the hydrated scaffold (g) and (m_1) is the mass of the dried scaffold (g).

The mechanical properties of the porous structures in the dried state and in the wet state were assessed by compression testing using a Zwick-Z020 tensile tester equipped with a 500 N load cell at a speed of 30%/min. The compression modulus (Ec) was determined at 8% compression.

The pore architecture of the different porous structures was analyzed using a scanning electron microscope (SEM) (Philips XL 30 ESEM-FEG). The cylindrical porous structures were gold sputtered prior to experiment.

Results

Characterization of dimethacrylate-functionalized PTMC, PDLLA, PCL and PEG oligomers

Linear dimethacrylate end-functionalized oligomers (macromers) based on TMC-, DLLA-, CL- and PEG oligomers with molar masses of approximately 4 kg/mol and 10 kg/mol were prepared as described. The molecular weights (M_n) of the oligomers and the degree of functionalization of the macromers was determined by ^{1}H-NMR. An overview is given in Table 1.

The M_n PTMC macromers was calculated using the peak integrals at δ 1.68 ppm (hexanediol, 4H) and δ 2.05 ppm (PTMC, 2n). The M_n of PDLLA macromers was calculated using the peak integrals at δ 4.12 ppm (hexanediol, 4H) and δ 5.16 ppm (PDLLA, 1n). The M_n of PCL macromers was calculated using the peak integrals at δ 1.68 ppm (hexanediol, 4H) and δ 4.06 ppm (PCL, 2n). The M_n of PEG macromers was calculated using the peak integrals at δ 4.31 ppm (methacrylate, 4H) and δ 3.7 ppm (PEG, 4n). Successful coupling of methacrylic anhydride was confirmed by the appearance of –C=CH_2 and–CH_3 peaks of the methacrylate endgroups at δ 6.11, δ 5,57 and δ 1.94 ppm. The degree of functionalization of PTMC macromers was determined using the integral values of the –CH_2– peak of hexanediol at δ 1.68 and the –C=CH_2 peaks at δ 6.11 and δ 5,57 ppm. For PDLLA, the integral value of the –O–CH_2– peak of hexanediol at δ 4.12 ppm was used. For PCL, the integral value of the HO–CH_2– peak of any residual oligomer at δ 3.64 ppm was used. The degree of functionalization of PEG macromers was determined after addition of TFAA. Non-functionalized –OH end-groups of the oligomer will react with this highly electronegative anhydride and show a peak in the NMR spectrum at δ 4.50 ppm. The integral values of this peak and that of the –CH_2 –O– peak of the macromer at δ 4.31 ppm was used to determine the degree of functionalization. For all

macromers conversions of at least 85 % were observed, suggesting that the functionalization reactions were essentially complete.

To be able to prepare scaffolds by this combinatorial phase separation, crystallization and extraction method, the macromers need to dissolve in EC. The solubility of the macromers in EC is also given in Table 1.

Table 1. Characteristics of the synthesized macromers. The number average molar mass (M_n) and the degree of functionalization (f) were determined by ^1H NMR as described in the text.

Macromer	**Mn** kg/mol	**f** %	**Solubility in EC (50°C)**
PTMC-dMA 4k	4.2	89	Soluble
PDLLA-dMA 4k	4.7	95	Soluble
PCL-dMA 4k	4.8	95	Not soluble
PEG-dMA 4k	4.2	100	Soluble
PTMC-dMA 10k	9.5	90	Soluble
PDLLA-dMA 10k	10.0	85	Soluble
PCL-dMA 10k	9.6	100	Not soluble
PEG-dMA 10k	11.5	100	Soluble

As only the PTMC-dMA, PDLLA-dMA and PEG-dMA macromers were found to soluble in EC, these macromers were used to prepare porous structures. The PCL-dMA macromers are insoluble in EC, porous structures could not be prepared from these macromers in this manner.

Preparation of combinatorial porous structures in high throughput using EC as a crystallizable solvent

By making combinatorial mixtures of the six different macromers, PTMC-dMA 4k, PDLLA-dMA 4k, PEG-dMA 4k, PTMC-dMA 10k, PDLLA-dMA 10k and PEG-dMA 10k, in EC, cooling to below the melting temperature of EC, subsequent network formation by photo-polymerization and extraction with water, a total of 63 different porous structures could simultaneously be prepared.

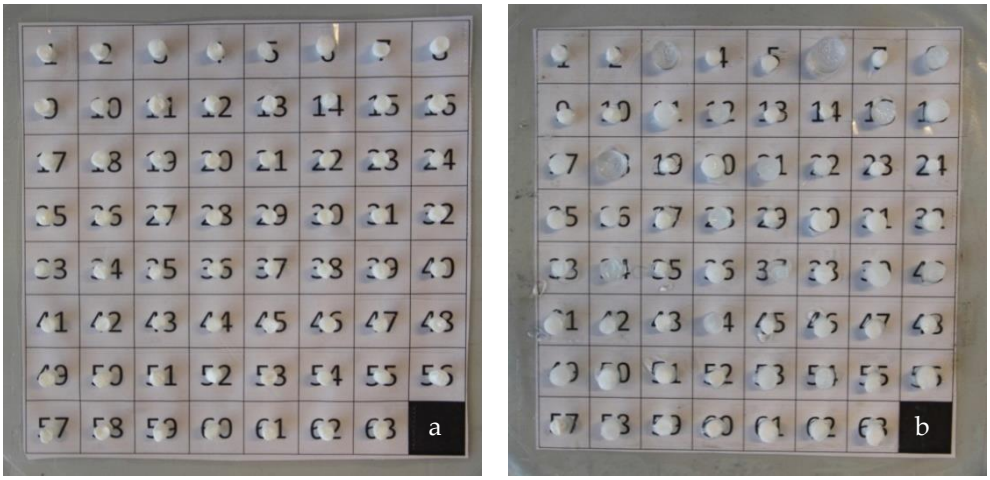

Figure 1. Photographic images of dried (a) and of hydrated (b) specimens that were prepared simultaneously. The dried porous structures had an average height of 3.9±0.22 mm and an average diameter of 4.0±0.15 mm. In several cases the hydrated specimens had become transparent and showed a very large increase in their diameter, indicating large differences in water uptake. The individual grids measured 1.0 x 1.0 cm.

In Figure 1 an overview of the different prepared porous structures in the dried state and in the hydrated state is given. The figure shows that upon hydration, the degree of swelling of the porous structures can differ significantly. Porous structures number 3, 6 and 18, for example, show very high swelling ratios due to the uptake of large amounts of water. These porous network structures are respectively prepared from only PEG-dMA 4k, only PEG-dMA 10k and a mixture of PEG-dMA 4k and PEG-dMA 10k macromers. See also Table 2. The preparation of porous structures from the many mixtures of these hydrophilic PEG macromers

and hydrophobic PTMC-dMA and PDLLA-dMA allows for the preparation of tissue engineering scaffolds with an enormous range of swelling ratios.

The results of this combinatorial approach in preparing 63 widely differing porous structures on porosity, on mechanical properties (dried and hydrated) and on water uptake is illustrated in Table 2. It can be seen that in the dried state, the average porosity is not affected by the composition of the network: their porosities were 50±4 vol.%. These values are much lower than could be expected from the amount of crystallizable EC that was used, indicating shrinkage of the scaffolds during their production. This is also reflected in the reduced dimensions of the specimens, which now measured approximately 4.0x4.0 mm (diameter x height). This shrinkage can be the result of the covalent network structure that is formed during photo-crosslinking [31]. When the crystallized EC is washed out during the extraction process, the amorphous network chains relax to less strained conformational states which leads to isotropic shrinkage of the porous structure.

Table 2. Overview of prepared combinatorial porous structures. The second to seventh columns indicate whether a macromer is present (grey) or absent (white) in the network from which the porous structure is prepared. Their porosities and compression modulus (Ec) in the dried state, the water uptake (WU) and compression modulus in the hydrated state are presented as well. Values are averages, with standard deviations in parentheses.

Number	PTMC-dMA 4k	PDLLA-dMA 4k	PEG-dMA 4k	PTMC-dMA 10k	PDLLA-dMA 10k	PEG-dMA 10k	Porosity [vol.%]	Ec (dried) [MPa]	WU [wt.%]	Ec (hydrated) [MPa]
1							55 (3)	0.32 (0.04)	22 (2)	0.26 (0.03)
2							51 (6)	30.03 (17.85)	12 (2)	21.13 (8.78)
3							45 (0)	3.42 (1.82)	634 (21)	0.03 (0.01)
4							51 (6)	0.23 (0.03)	19 (1)	0.28 (0.06)
5							41 (1)	16.32 (13.41)	16 (1)	29.47 (10.25)
6							54 (4)	3.84 (1.91)	1532 (204)	0.01 (0.00)
7							50 (4)	1.67 (0.7)	16 (1)	2.06 (0.49)
8							58 (3)	0.39 (0.21)	298 (11)	0.25 (0.01)
9							57 (3)	0.28 (0.04)	17 (1)	0.44 (0.01)
10							47 (4)	8.69 (7.46)	9 (4)	7.60 (3.58)
11							57 (1)	2.99 (1.02)	349 (67)	0.07 (0.02)
12							44 (2)	0.23 (0.03)	210 (8)	0.14 (0.02)
13							51 (5)	3.37 (1.83)	10 (1)	4.50 (1.85)
14							53 (3)	40.57 (15.63)	10 (2)	60.93 (24.76)
15							54 (2)	3.34 (0.76)	275 (9)	0.25 (0.02)
16							50 (2)	2.12 (0.68)	299 (17)	0.16 (0.07)
17							44 (3)	1.37 (0.15)	172 (20)	0.43 (0.12)
18							52 (2)	5.24 (0.42)	797 (18)	0.02 (0.01)
19							51 (5)	5.53 (2.09)	4 (1)	5.99 (1.72)
20							52 (2)	1.86 (0.84)	424 (40)	0.08 (0.02)
21							52 (3)	8.16 (1.72)	289 (58)	0.07 (0.03)
22							52 (1)	0.26 (0.09)	125 (15)	0.34 (0.05)
23							50 (5)	1.18 (0.28)	11 (6)	1.17 (0.26)
24							49 (9)	30.40 (5.67)	7 (3)	14.41 (8.56)
25							51 (4)	0.71 (0.13)	160 (23)	0.22 (0.05)
26							53 (1)	0.38 (0.03)	172 (15)	0.29 (0.14)
27							52 (2)	0.35 (0.07)	77 (12)	0.49 (0.10)
28							54 (2)	4.10 (0.99)	419 (17)	0.16 (0.05)
29							53 (3)	1.43 (0.55)	5 (0)	1.58 (0.16)
30							57 (2)	1.76 (0.36)	244 (71)	0.23 (0.04)

Table 2. (continued)

Number	PTMC-dMA 4k	PDLLA-dMA 4k	PEG-dMA 4k	PTMC-dMA 10k	PDLLA-dMA 10k	PEG-dMA 10k	Porosity [vol.%]	Ec (dried) [MPa]	WU [wt.%]	Ec (hydrated) [MPa]
31	■				■	■	55 (2)	1.76 (0.45)	165 (15)	0.20 (0.02)
32		■	■	■			53 (3)	0.22 (0.08)	137 (2)	0.20 (0.10)
33		■	■		■		43 (8)	0.27 (0.09)	88 (6)	1.07 (0.30)
34		■	■			■	53 (1)	2.87 (0.92)	451 (28)	0.05 (0.04)
35		■		■	■		57 (2)	11.44 (4.64)	11 (1)	24.40 (4.89)
36		■		■		■	53 (4)	2.11 (0.4)	191 (87)	0.13 (0.06)
37		■			■	■	40 (8)	2.70 (2.15)	129 (16)	2.06 (0.94)
38			■	■	■		40 (5)	0.86 (0.75)	98 (12)	0.34 (0.12)
39			■	■		■	52 (1)	2.83 (0.40)	438 (31)	0.16 (0.04)
40			■		■	■	43 (5)	5.59 (0.93)	317 (16)	0.12 (0.03)
41				■	■	■	55 (2)	2.12 (0.58)	195 (32)	0.23 (0.06)
42	■	■	■	■			56 (1)	0.28 (0.08)	75 (11)	0.20 (0.08)
43	■	■	■		■		48 (8)	0.24 (0.06)	60 (8)	0.34 (0.31)
44	■	■	■			■	50 (3)	1.78 (0.50)	259 (19)	0.12 (0.01)
45	■	■		■	■		49 (2)	3.17 (2.25)	6 (2)	4.12 (4.29)
46	■	■		■		■	53 (3)	0.93 (0.18)	156 (6)	0.19 (0.07)
47	■	■			■	■	52 (2)	0.80 (0.44)	116 (51)	1.39 (1.06)
48	■			■	■		51 (3)	0.37 (0.06)	48 (3)	0.54 (0.06)
49	■			■		■	53 (0)	1.90 (0.27)	296 (27)	0.20 (0.05)
50	■				■	■	51 (1)	2.43 (0.16)	200 (35)	0.22 (0.07)
51	■			■	■	■	54 (1)	1.08 (0.13)	99 (11)	0.18 (0.07)
52		■	■	■	■		41 (2)	0.22 (0.02)	60 (16)	0.58 (0.05)
53		■	■	■		■	52 (2)	2.68 (0.59)	291 (18)	0.11 (0.02)
54		■	■		■	■	47 (5)	3.93 (2.10)	178 (27)	0.33 (0.06)
55		■		■	■	■	48 (4)	2.27 (1.31)	94 (20)	1.86 (1.36)
56			■	■	■	■	49 (2)	1.45 (0.24)	219 (13)	0.12 (0.03)
57	■	■	■	■	■		45 (8)	0.37 (0.02)	38 (5)	0.60 (0.10)
58	■	■	■	■		■	51 (3)	0.91 (0.32)	199 (13)	0.17 (0.04)
59	■	■	■		■	■	47 (3)	1.21 (0.66)	140 (13)	0.30 (0.05)
60	■	■		■	■	■	50 (2)	1.80 (1.06)	73 (23)	0.45 (0.19)
61	■		■	■	■	■	48 (1)	1.71 (0.30)	180 (11)	0.23 (0.01)
62		■	■	■	■	■	47 (5)	2.18 (0.25)	140 (8)	0.30 (0.08)
63	■	■	■	■	■	■	49 (2)	1.19 (0.30)	132 (11)	0.37 (0.07)

The mechanical properties of all 63 porous structures prepared were assessed in compression. The compression modulus of porous structures with similar porosities depended on composition, and ranged from 0.22 to 40.57 MPa. The main effect of the presence of PDLLA-dMA macromers in the porous networks is the increase in their rigidity. In the dried state the compression modulus of a porous structure made from PTMC-dMA 10k (structure nr.4) is 0.23 MPa, while under the same conditions a porous structure made from 50 wt.% PTMC-dMA 10k and 50 wt.% PDLLA-dMA 10k (structure nr.19) has a compression modulus of 5.53 MPa. This is due to the relatively high glass transition of PDLLA polymers (approximately 60 ^{0}C). PTMC has a relatively low glass transition temperature of approximately -15 ^{o}C, therefore the presence of PTMC-dMA macromers decreases the rigidity of the porous structures. A dried porous structure made from PEG-dMA 4k (nr.3), for example, has a compression modulus of 3.42 MPa, while one made from 50 wt.% PTMC-dMA 4k and 50 wt.% PEG-dMA 4k (structure nr.8) has a modulus of 0.39 MPa.

The compression modulus of hydrated porous structures was markedly affected by the presence of PEG-dMA macromers in the network structure. The higher the PEG-dMA content, the higher the water uptake of the porous structure and the lower its compression modulus. Additionally, hydrated porous structures prepared from the higher molar mass PEG-dMA showed a much higher water uptake and lower compression modulus. The porous structure prepared from PEG-dMA 4k (structure nr.3) absorbed 634 wt.% of water and had a compression modulus of 0.03 MPa in the hydrated state. The porous structure prepared from PEG-dMA 10k (structure nr. 6) was found to absorb 1532 wt.% water and had a compression modulus of only 0.01 MPa in the hydrated state. An increase in PEG-dMA molar mass leads to an increase in the network mesh size which results in a higher the water absorption capacity. This greatly influences the mechanical properties of the porous networks.

For the prepared porous structures, the water uptake ranged from 3 to 1532 wt.%, while their compression modulus in the hydrated state ranged from 0.01 to 60 MPa. In tissue engineering, the hydrophilicity and mechanical properties are important parameters that determine the interaction of cells with biomaterials. The high throughput preparation of such arrays of porous structures, will allow for the

selection of a specific scaffolding structure for a desired tissue engineering application.

The characteristics of the internal pore network of the porous were assessed by SEM. A selection of SEM micrographs of the cross-sections of different porous structures is presented in Figure 2.

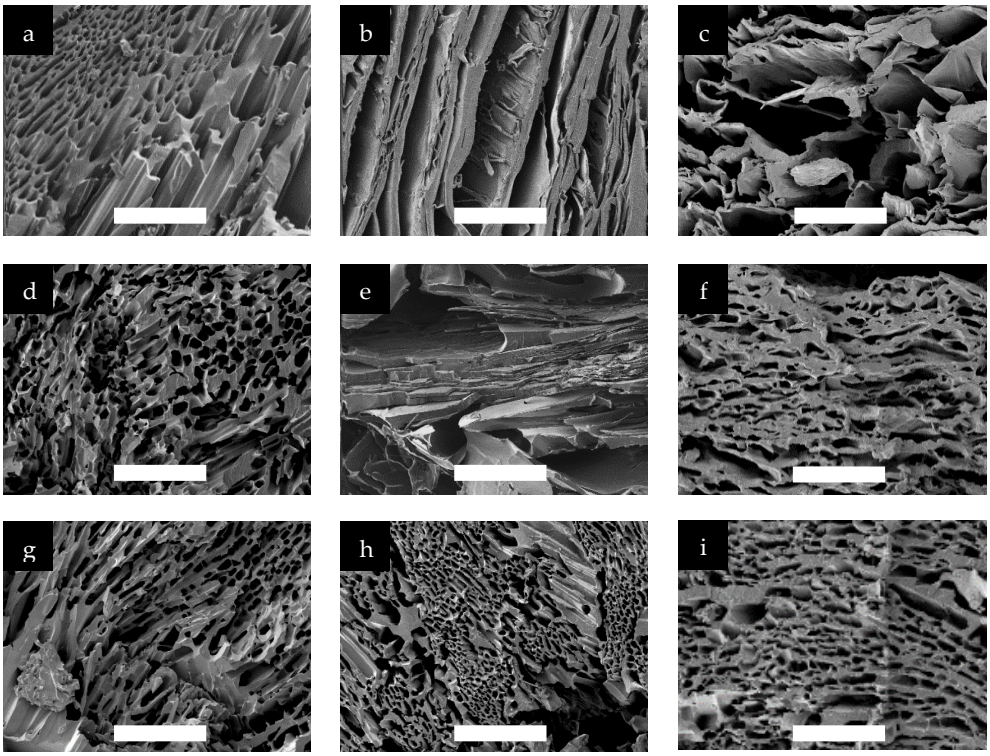

Figure 2. SEM micrographs of cross-sections of porous structures prepared using EC as a crystallizable solvent from PTMC-dMA 4k (a, structure nr 1), PDLLA-dMA 4k (b, structure nr 2), PEG-dMA 4k (c, structure nr 3), PTMC-dMA 10k (d, structure nr 4), PDLLA-dMA 10k (e, structure nr 5), PEG-dMA 10k (f, structure nr 6), PTMC-dMA 10k-PDLLA-dMA 10k (g, structure nr 19), PTMC-dMA 10k-PEG-dMA 10k (h, structure nr 20) and PTMC-dMA 10k-PDLLA-dMA 10k-PEG-dMA 10k (i, structure nr 41). Scale bars indicate 200 μm.

The micrographs show that different morphologies of the pore networks are obtained when the porous structures are prepared from different homomacromers or combinations of macromers (Figure 2a-f). In porous structures based on PTMC and PEG macromers, long hexagonal shaped pores were found, whereas structures based on PDLLA macromers showed a more lamellar-like morphology of the pores. The porous structures obtained from combinatorial macromer mixtures (Figure 2g-i) were found to have similar features. The diameters of the pores ranged from 20 to 100 μm.

As PCL-dMA macromers are not soluble in ethylene carbonate, it was possible to incorporate particles based on PCL into the porous structures. See the Supporting Information.

Conclusions

A new method for the simultaneous preparation of large numbers of porous polymeric structures, widely differing in their physical properties, has been developed. Using ethylene carbonate as a solvent, combinatorial mixtures of PTMC-dMA, PDLLA-dMA and PEG-dMA macromer solutions were prepared. Upon crystallization of the solvent, photo-crosslinking and extraction of the solvent, 63 different porous structures with a porosity of approximately 50 % were simultaneously prepared from only 6 different macromers. These porous structures, prepared in high throughput, had highly diverging physical properties. Their water uptake ranged from 3 to 1532 wt.%, while their compression modulus in the hydrated state ranged from 0.01 to 60 MPa.

Acknowledgement

This work was supported by a grant from the Dutch government to the Netherlands Institute for Regenerative Medicine (NIRM, grant No. FES0908).

References

1. Simon Jr CG, Yang Y, Dorsey SM, Ramalingam M, and Chatterjee K, 3D polymer scaffold arrays. Methods in molecular biology (Clifton, N.J.), 2011. 671: p. 161-174.
2. Simon CG, Stephens JS, Dorsey SM, and Becker ML, Fabrication of combinatorial polymer scaffold libraries. Review of Scientific Instruments, 2007. 78(7).
3. Chatterjee K, Sun L, Chow LC, Young MF, and Simon CG, Combinatorial screening of osteoblast response to 3D calcium phosphate/poly(ε-caprolactone) scaffolds using gradients and arrays. Biomaterials, 2011. 32(5): p. 1361-1369.
4. Chatterjee K, Lin-Gibson S, Wallace WE, Parekh SH, Lee YJ, Cicerone MT, Young MF, and Simon Jr CG, The effect of 3D hydrogel scaffold modulus on osteoblast differentiation and mineralization revealed by combinatorial screening. Biomaterials, 2010. 31(19): p. 5051-5062.
5. Khan F, Tare RS, Oreffo ROC, and Bradley M, Versatile Biocompatible Polymer Hydrogels: Scaffolds for Cell Growth. Angewandte Chemie International Edition, 2009. 48(5): p. 978-982.
6. Oliveira MB, Salgado CL, Song WL, and Mano JF, Combinatorial on-chip study of miniaturized 3D porous scaffolds using a patterned superhydrophobic platform. Small, 2013. 9(5): p. 768-778.
7. Anderson DG, Levenberg S, and Langer R, Nanoliter-scale synthesis of arrayed biomaterials and application to human embryonic stem cells. Nature Biotechnology, 2004. 22(7): p. 863-866.
8. de Gans BJ and Schubert US, Inkjet printing of polymer micro-arrays and libraries: Instrumentation, requirements, and perspectives. Macromolecular Rapid Communications, 2003. 24(11): p. 659-666.
9. Hansen A, McMillan L, Morrison A, Petrik J, and Bradley M, Polymers for the rapid and effective activation and aggregation of platelets. Biomaterials, 2011. 32(29): p. 7034-7041.
10. Webster DC, Combinatorial and high-throughput methods in macromolecular materials research and development. Macromolecular Chemistry and Physics, 2008. 209(3): p. 237-246.
11. Brocchini S, James K, Tangpasuthadol V, and Kohn J, A combinatorial approach for polymer design. Journal of the American Chemical Society, 1997. 119(19): p. 4553-4554.
12. Hook AL, Anderson DG, Langer R, Williams P, Davies MC, and Alexander MR, High throughput methods applied in biomaterial development and discovery. Biomaterials, 2010. 31(2): p. 187-198.

13. Meredith JC, Karim A, and Amis EJ, High-Throughput Measurement of Polymer Blend Phase Behavior. Macromolecules, 2000. 33(16): p. 5760-5762.
14. Meredith JC, Smith AP, Karim A, and Amis EJ, Combinatorial materials science for polymer thin-film dewetting. Macromolecules, 2000. 33(26): p. 9747-9756.
15. Meredith JC, Sormana JL, Keselowsky BG, Garcia AJ, Tona A, Karim A, and Amis EJ, Combinatorial characterization of cell interactions with polymer surfaces. Journal of Biomedical Materials Research Part A, 2003. 66A(3): p. 483-490.
16. Menger FM, Eliseev AV, and Migulin VA, Phosphatase catalysis developed via combinatorial organic chemistry. The Journal of Organic Chemistry, 1995. 60(21): p. 6666-6667.
17. Healey BG and Walt DR, Fast temporal response fiber-optic chemical sensors based on the photodeposition of micrometer-scale polymer arrays. Analytical Chemistry, 1997. 69(11): p. 2213-2216.
18. Khan F, Tare RS, Kanczler JM, Oreffo ROC, and Bradley M, Strategies for cell manipulation and skeletal tissue engineering using high-throughput polymer blend formulation and microarray techniques. Biomaterials, 2010. 31(8): p. 2216-2228.
19. Zant E, Bosman MJ, and Grijpma DW, Combinatorial synthesis of photo-crosslinked biodegradable networks. Journal of Applied Biomaterials & Functional Materials, 2012. 10(3): p. 197-202.
20. Aubert JH and Clough RL, Low-Density, Microcellular Polystyrene Foams. Polymer, 1985. 26(13): p. 2047-2054.
21. Claase MB, Grijpma DW, Mendes SC, de Bruijn JD, and Feijen J, Porous PEOT/PBT scaffolds for bone tissue engineering: Preparation, characterization, and in vitro bone marrow cell culturing. Journal of Biomedical Materials Research Part A, 2003. 64A(2): p. 291-300.
22. Hinrichs WL, Lommen EJ, Wildevuur CR, and Feijen J, Fabrication and characterization of an asymmetric polyurethane membrane for use as a wound dressing. Journal of applied biomaterials : an official journal of the Society for Biomaterials, 1992. 3(4): p. 287-303.
23. Ho M-H, Kuo P-Y, Hsieh H-J, Hsien T-Y, Hou L-T, Lai J-Y, and Wang D-M, Preparation of porous scaffolds by using freeze-extraction and freeze-gelation methods. Biomaterials, 2004. 25(1): p. 129-138.
24. Izal I, Aranda P, Sanz-Ramos P, Ripalda P, Mora G, Granero-Molto F, Deplaine H, Gomez-Ribelles JL, Ferrer GG, Acosta V, Ochoa I, Garcia-Aznar JM, Andreu EJ, Monleon-Pradas M, Doblare M, and Prosper F, Culture of human bone marrow-derived mesenchymal stem cells on of poly(L-lactic acid) scaffolds: potential application for the tissue engineering

of cartilage. Knee Surgery Sports Traumatology Arthroscopy, 2013. 21(8): p. 1737-1750.
25. Luk JZ, Cooper-White J, Rintoul L, Taran E, and Grondahl L, Functionalised polycaprolactone films and 3D scaffolds via gamma irradiation-induced grafting. Journal of Materials Chemistry B, 2013. 1(33): p. 4171-4181.
26. Mu C, Su Y, Sun M, Chen W, and Jiang Z, Fabrication of microporous membranes by a feasible freeze method. Journal of Membrane Science, 2010. 361(1-2): p. 15-21.
27. Groot JH, Nijenhuis AJ, Bruin P, Pennings AJ, Veth RPH, Klompmaker J, and Jansen HWB, Use of porous biodegradable polymer implants in meniscus reconstruction. 1) Preparation of porous biodegradable polyurethanes for the reconstruction of meniscus lesions. Colloid and Polymer Science, 1990. 268(12): p. 1073-1081.
28. Vaquette C and Cooper-White J, A simple method for fabricating 3-D multilayered composite scaffolds. Acta Biomaterialia, 2013. 9(1): p. 4599-4608.
29. Cao Y, Croll TI, O'Connor AJ, Stevens GW, and Cooper-White JJ, Systematic selection of solvents for the fabrication of 3D combined macro- and microporous polymeric scaffolds for soft tissue engineering. Journal of Biomaterials Science-Polymer Edition, 2006. 17(4): p. 369-402.
30. Bat E, Kothman BHM, Higuera GA, van Blitterswijk CA, Feijen J, and Grijpma DW, Ultraviolet light crosslinking of poly(trimethylene carbonate) for elastomeric tissue engineering scaffolds. Biomaterials, 2010. 31(33): p. 8696-8705.
31. Nawab Y, Casari P, Boyard N, and Jacquemin F, Characterization of the cure shrinkage, reaction kinetics, bulk modulus and thermal conductivity of thermoset resin from a single experiment. Journal of Materials Science, 2013. 48(6): p. 2394-2403.

Supporting Information

Preparation of porous structures containing dispersed PCL microparticles

As PCL-dMA macromers (and also PCL polymers) are not soluble in ethylene carbonate, it was not possible to prepare porous networks structures containing PCL moieties with the described combinatorial method. This does, however, allow us to incorporate particles based on PCL into the porous structures. This could be

of great interest in tissue engineering, as such microparticles could be employed for the release of drugs or growth factors to achieve a desired cell response. We prepared microparticles from PCL with a relatively low molar mass. The molar mass of the PCL, as determined by NMR, was 5.6 kg/mol. Use of PCL of this low molar mass is beneficial, as it degrades and resorbs *in vivo* within a reasonable time. High molecular weight PCL, in contrast, takes several years to be completely resorbed [1].

PCL with a molar mass of 5 kg/mol was synthesized by ROP of ε-Cl monomer as described earlier. From this polymer, microparticles were fabricated by membrane emulsification using a Nanomi Iris-20 microporous membranes [2]. The PCL solution (1 g/ml in DCM) was forced through the membrane at a rate of 4 ml/h using a syringe pump (ProSense NE-300), the microparticles then formed in an aqueous polyvinyl alcohol (PVA) solution (concentration 2 wt.%) flowing at a rate of 88 ml/h with use of peristaltic pump (Spetec Perimax-12). The microparticles were collected, washed with distilled water and freeze-dried for 24h.

Porous PTMC-dMA 10k network structures containing PCL microparticles were prepared by suspending 0.1 g PCL microparticles in 1.0 ml of a solution of 10 wt.% PTMC -dMA 10k in EC at 50°C. The specimens were cooled to room temperature, photocrosslinked and extracted as described earlier. SEM was used for analysis of the PCL microparticle sizes and for visualization of the microparticles in the porous structures.

Figure S1a shows an SEM image of the prepared PCL microparticles. It can be seen that the microparticles are smooth and spherical, their diameter is 39.9±2.3 μm. These microparticles could be dispersed into solutions of macromers in EC. Then, upon cooling, crystallization and photo-crosslinking, and subsequent extraction of the solvent, porous microparticle-containing porous structures could be obtained. In Figure S1b an SEM image is shown where the PCL particles are embedded in a porous structure prepared from PTMC-dMA 10k. It can be seen that the PCL particles are physically well-attached to the PTMC matrix, without voids or spaces between the particles and the matrix. Furthermore, it can be seen that the PCL microparticles are homogeneously distributed throughout the porous polymer

matrix. The microparticles remained smooth and spherical in shape, and seemed not to be affected by the ethylene carbonate.

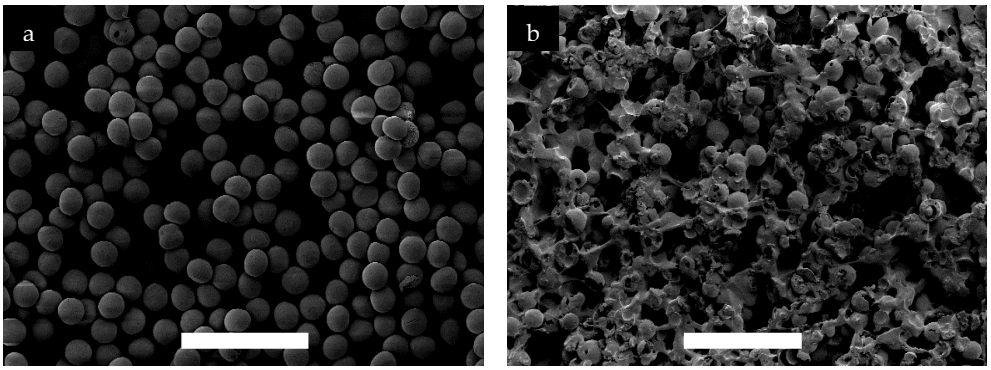

Figure S1. SEM micrographs of the prepared PCL microparticles (a) and a porous structure prepared from PTMC-dMA 10k into which these particles were incorporated. The porous structure was prepared by dispersing 0.1 g of PCL microspheres into 1 ml PTMC-dMA 10k solution (10 wt.% in EC) at 50°C, crystallization at 21 °C, photo-crosslinking and extraction of the EC with water. Scale bars indicate 200 μm.

In conclusion, the method also allowed the dispersion of PCL microparticles in the solvent, and porous structures containing PCL microparticles suitable for drug- and growth factor delivery could readily be prepared. The high throughput preparation of these arrays of porous structures, will allow for the selection of a specific scaffolding structure for a desired tissue engineering application.

References

[1] Sun H, Mei L, Song C, Cui X, and Wang P, Biomaterials, 2006. 27 (9): p. 1735-1740.

[2] Wissink J, van Rijn CJM, Nijdam W, Goeting CH, Heskamp IR, and Veldhuis GJ (Nanomi B.V.), US8100348B2, 2012.

Chapter 7 - Drug-loaded low molecular weight PCL microparticles prepared by a w/o/w double emulsion and solvent evaporation technique

Erwin Zant, Kamila J. Szafulera, Dirk W. Grijpma

Abstract

Poly(ε-caprolactone) (PCL) of low molecular weight (Mn=6.2 kg/mol) was used to prepare vitamin B12 loaded microparticles. A water-in-oil-in-water (w/o/w) double emulsion and solvent evaporation method was used to prepare the particles. High encapsulation efficiencies (EE) of 61% were obtained by using high polymer concentrations (0.20 g/ml) and adding NaCl (0.10 g/ml) to the external water phase. In vitro vitamin B12 release characteristics were determined in PBS and in lipase buffer. Release rates in lipase buffer were significantly higher than in PBS, likely the result of enzymatic PCL degradation.

Introduction

Poly(ε-caprolactone) (PCL) has often been used for the preparation of biodegradable microparticles for drug delivery applications [1-4]. Various techniques to prepare the microparticles exist: solvent evaporation, spray-drying, ultrasonication or membrane emulsification. The drugs are loaded by single- or double emulsification techniques to respectively encapsulate lipophilic and hydrophilic drugs [5, 6]. Most studies concern the fabrication of microparticles from high molecular weight PCL (40 kg/mol or higher). High molecular weight PCL, however, barely degrades *in vivo* [7, 8]. In order to use PCL microparticles as true biodegradable drug delivery vehicles, it would be advantageous to prepare these particles using low molecular weight PCL since its degradation is much faster than that of high molecular weight PCL [9, 10].

Here, the encapsulation and release of vitamin B12, a hydrophilic model drug from low molecular weight PCL microparticles prepared by a double emulsion and solvent evaporation method is described.

Materials and methods

Materials

Stannous octanoate ($SnOct_2$), 1,6-hexanediol, poly(vinyl alcohol) (PVA) (80% hydrolyzed, MW = 9-10 kg/mol), ethylene carbonate (EC), sodium chloride (NaCl), phosphate buffer saline (PBS), lipase from Thermomyces lanuginosus, vitamin B12 (cyanocobalamine) and ε-caprolactone (CL) were purchased from Sigma Aldrich (The Netherlands). CL was dried over ground calcium hydride (Merck, Germany) and purified by distillation under reduced argon atmosphere. PCL (MW=50 kg/mol) CAPA® 650 was purchased from Perstorp (Sweden).

Synthesis and characterization of PCL

Low molecular weight PCL, with targeted molecular weight of the polymer was 6 kg/mol, was synthesized by ring opening polymerization (ROP) of CL in the presence of $SnOct_2$ (0.02 mmol/g monomer) as catalyst and hexanediol (0.16 mmol/g monomer) as initiator. The polymerization conducted in an argon atmosphere at 130 °C for 2 days. PCL was purified by dissolution in dichloromethane (0.3 g/ml), followed by precipitation in ethanol. The oligomer was then dried in a vacuum oven at 40 °C for three days. ^{1}H-NMR was used to determine M_n and conversion in deuterated chloroform.

Preparation of vitamin B12 loaded PCL microparticles

PCL microparticles loaded with vitamin B12 were obtained by a double emulsion and solvent evaporation method. This method was previously used for the encapsulation of lysozyme in poly(ethylene glycol)-poly(butylene teraphthalate) block copolymers [11]. A scheme of the method is shown in Figure 1.

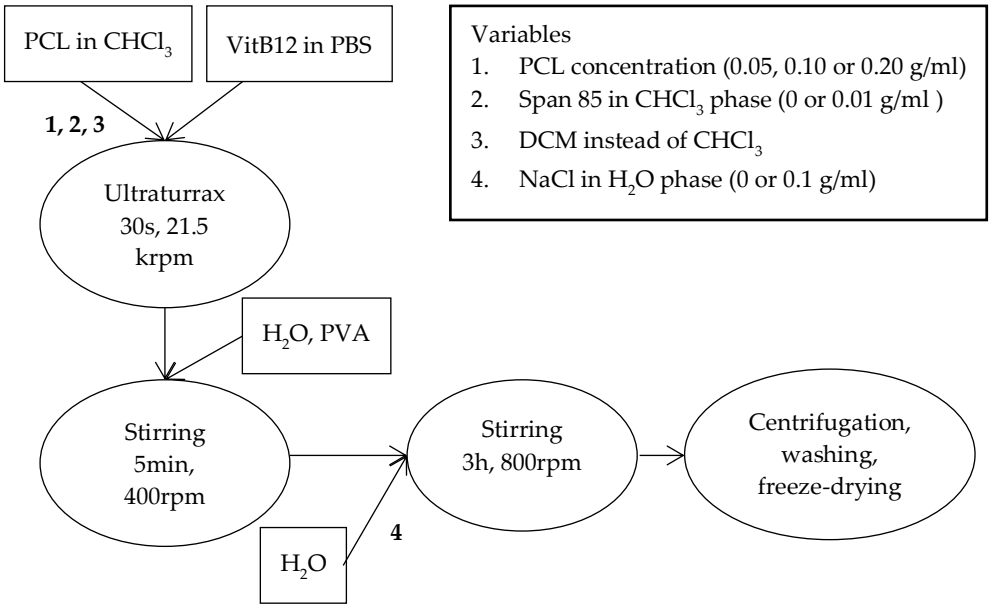

Figure 1: Scheme illustrating the w/o/w emulsification procedure to prepare low molecular weight PCL microspheres loaded with vitamin B12. The experimental variables are listed in the text box.

Vitamin B12 was dissolved in PBS and then dispersed in low molecular weight PCL solutions in chloroform using an ultra-high-speed homogenizer (Ultra-Turrax T25) at 21.5 krpm for 30 seconds to obtain the first emulsions (w/o). This first emulsion was then added to a stirred PVA solution (0.04 g/ml in water) to obtain the second emulsion (w/o/w). Stirring of the water phase was done using a mechanical stirrer equipped with a four bladed rotor at a speed of 400 rpm for 5 min. Then 200 ml ultrapure MilliQ water was added and stirring was continued for another 3h at 800 rpm to obtain the hardened PCL microparticles. The PCL microparticles were isolated by centrifugation, washed (3x) and subsequently freeze dried.

To maximize the loading of the microparticles, the concentration of the PCL solution was in chloroform was varied (0.05, 0.10 or 0.20 g/ml). At PCL concentrations of 0.05 g/ml, microparticles were also prepared using DCM as a solvent, using Span 85 (0.01 g/ml) in the PCL/chloroform phase and dissolving 0.10 g/ml NaCl in the water phase.

As a control, loaded microparticles were prepared using high molecular weight PCL dissolved at 0.05 g/ml in $CHCl_3$.

Characterization of the microparticles

The amount of encapsulated vitamin B12 was determined by dissolving 30 mg of the obtained microparticles in 2 ml chloroform. Then, 1 ml PBS was added and the two phases were thoroughly mixed by a vortex mixer for 2 minutes to allow the vitamin B12 to dissolve in the PBS phase. After centrifugation (2400 rpm, 4 minutes), the water phase was pipetted (3 x 200 µl) into the wells of a 96 wells plate and the absorbance at 361 nm was measured using a SLT 340 ATCC microplate reader. The loading capacity (LC) and encapsulation efficiency (EE) were calculated using the following equations:

$$LC = \frac{W_{ed}}{W_{mp}} \times 100\% \qquad EE = \frac{W_{ed}}{W_{tad}} \times 100\%$$

Here, W_{ed} is the total weight of encapsulated vitamin B12, W_{mp} the mass of the microparticles and W_{tad} the total amount of drug added at the start of the process.

Scanning electron microscope (SEM, FEI ESEM XL30) was used to analyze the morphology of the microspheres. The samples were gold sputtered before analysis.

Particle sizes and particle size distributions were determined microscopically by dispersing the microparticles in demineralized water and pipetting them onto a microscope slide. The samples were visualized using an AMG EVOS fl LED fluorescence microscope, and the recorded images were analyzed with ImageJ software. The average diameters and particle size distributions of microspheres prepared under the different experimental conditions were calculated using 100 microspheres per specimen.

Release of vitamin B12 from low molecular weight PCL particles

Vitamin B12 release experiments were conducted using the low molecular weight PCL microparticles that had the highest encapsulation efficiencies. The microparticles (50 mg) were dispersed in 1.5 ml PBS (pH 7.4, containing 0.02 % w/v NaN_3 bactericide) and in a lipase solution in PBS (the lipase was diluted to 1 mg lipase buffer solution per ml PBS) at 37°C for a period of up to 18 days. Lipase is an enzyme often used in the accelerated degradation of PCL [12]. The tubes were shaken periodically, and after centrifugation of the particle suspensions (3500 rpm, 3 minutes) samples were taken at various time points, allowing the concentration of the released vitamin B12 to be determined as shown above.

Results

Synthesis and characterization of PCL

Low molecular weight PCL was prepared by ROP of ε-CL using bifunctional hexanediol as an intiator. The monomer conversion and number average molecular weight of the obtained polymer as determined from the ^{1}H-NMR spectra were 99% and 6.2 kg/mol , respectively.

Preparation of PCL microparticles loaded with vitamin B12

In order to prepare low molecular weight PCL microparticles efficiently loaded with vitamin B12, several parameters in the preparation procedure were varied. It was found in literature, that these parameters improved the encapsulation efficiency of a hydrophilic compounds in poly(D,L-lactide) microspheres [13]. The different conditions applied and the characteristics of the resulting microspheres are given in Table 1.

Table 1: The preparation of the PCL microparticle loaded with vitamin B12 under different experimental conditions. Sample 1 is prepared from high molecular weight PCL (52 kg/mol), samples 2-8 are prepared using low molecular weight PCL (Mn=6.2 kg/ml).

Sample #	**Mn of PCL** kg/mol	**Concentration** g/ml	**Span 85** 0.01 g/ml	**Solvent**	**NaCl** 0.1 g/ml	**LC** %	**EE** %
1	52	0.05	-	CHCl3	-	0.33	12.4
2	6	0.05	-	CHCl3	-	0.05	1.8
3	6	0.05	+	CHCl3	-	0.04	1.9
4	6	0.05	-	DCM	-	0.04	1.4
5	6	0.05	-	CHCl3	+	0.17	6.5
6	6	0.10	-	CHCl3	-	0.03	2.5
7	6	0.20	-	CHCl3	-	0.25	37.1
8	6	0.20	-	CHCl3	+	0.42	60.3

It is clear from the table that the encapsulation efficiency of vitamin B12 in low molecular weight (sample 2, 1.81 %) microparticles is much lower than in PCL microparticles of high molecular weight PCL (sample 1, 12.4 %). However, by variation of the experimental parameters (increasing the concentration of the PCL and adding NaCl into the water phase), the EE of vitamin B12 in the low molecular weight PCL microparticles could be improved from 1.81 to 60.32 %.

Sample 3 was prepared with the addition of Span 85 to the PCL solution in the first emulsion. Span 85 is an emulsifier which belongs to the group of lipophilic detergents, these were shown to increase the encapsulation efficiency of hydrophilic drugs [13]. Although the particles contained much smaller holes (Figure 2b) as compared to PCL particles prepared without Span 85 (sample 2, Figure 2a), there was no significant improvement of the vitamin B12 encapsulation efficiency (EE = 1.90 %) upon addition of Span 85 to the PCL phase. Therefore, it was not used in further formulation experiments.

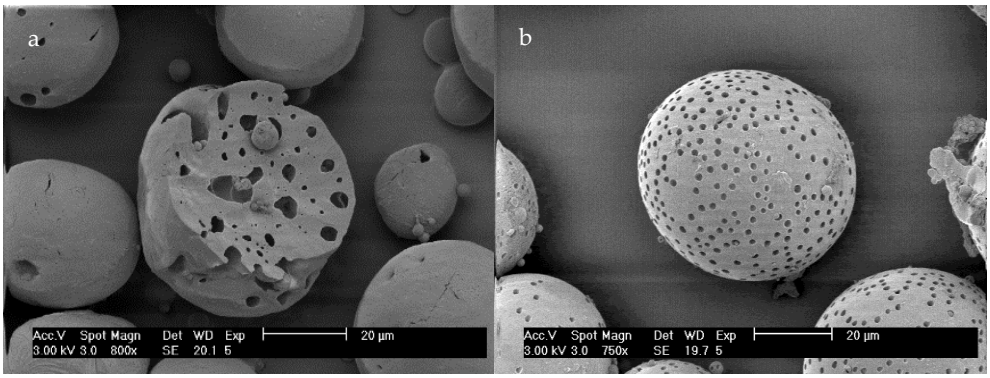

Figure 2: Microparticles loaded with vitamin B12 obtained using low molecular weight PCL dissolved at a concentration of 0.05 g/ml with (a, sample 2) and without (b, sample 3) the addition of Span 85 to the $CHCl_3$ phase. Noticeable are the smaller holes in the microparticles produced in the presence of Span 85. The scale bar indicates 20 µm.

Dichloromethane was used in preparing sample 4, because it is a more volatile solvent than chloroform. As the rate of evaporation should be faster, this could increase the rate of particle solidification. The faster the particles solidify, the less

vitamin B12 will diffuse into the aqueous phase. It was observed, however, that the EE of sample 4 was lower than that of sample 2. Apparently, vitamin B12 could still diffuse into the aqueous phase during the process of solidification.

Addition of 0.1 g/ml NaCl to the external water phase in sample 5 significantly improved the EE (up to 6.5 %). Addition of NaCl to the water may decrease the solubility of both the vitamin B12 and the organic solvent [13], leading to less diffusion of vitamin B12 into the aqueous phase.

The EE could also be improved using higher concentrations of PCL. The EE increased up to 37.1 % in sample 7 when the particles were prepared from a PCL solution of 0.20 g/ml (Figure 3a). Most probably the higher viscosity of the organic phase attributed to the higher EE. The vitamin B12 dissolved in water in the first emulsion droplets are less mobile and therefore more stable during the microparticle formation process. Moreover, diffusion of vitamin B12 is hindered by the higher viscosity resulting in a much higher EE. Addition of NaCl to the water phase, in combination with the higher PCL concentration, was found to yield microparticles loaded with vitamin B12 at an EE of 60.3 % (sample 8, Figure 3b).

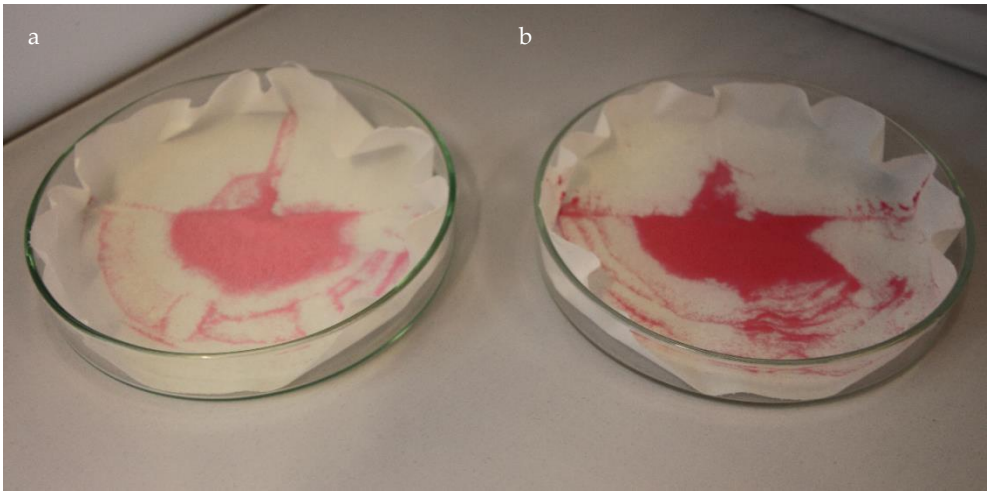

Figure 3: Microparticles loaded with vitamin B12 obtained using low molecular weight PCL dissolved at a concentration of 0.20 g/ml (a, sample 7) (LC: 0.25 %, EE: 37.1 %) and microparticles loaded with vitamin B12 obtained using low molecular weight PCL dissolved at a concentration of 0.20 g/ml and NaCl (0.10 g/ml) in the water phase (b, sample 8) (LC: 0.42 %, EE: 60.3 %).

Particle size and particle size distribution

The size (mean diameter) of the vitamin B12 loaded microparticles prepared at different PCL concentrations ranged from approximately 42 to 149 μm. The average particle size depended on the PCL concentration and on the presence of NaCl in the external water phase. The microparticle size distributions are given in Figure 4. Particles with a narrow size distribution were obtained using 0.05 g/ml PCL solutions (sample 2), with an average diameter of 42±10 μm. Microparticles obtained from 0.10 g/ml PCL solutions (sample 6) had an average diameter of 82±24 μm, and particles obtained using 0.20 g/ml PCL solutions (sample 7) had an average diameter of 127±47 μm. Using 0.20 g/ml PCL solutions and adding NaCl to the external water phase (sample 8) increased the average particle size to 149±44 μm.

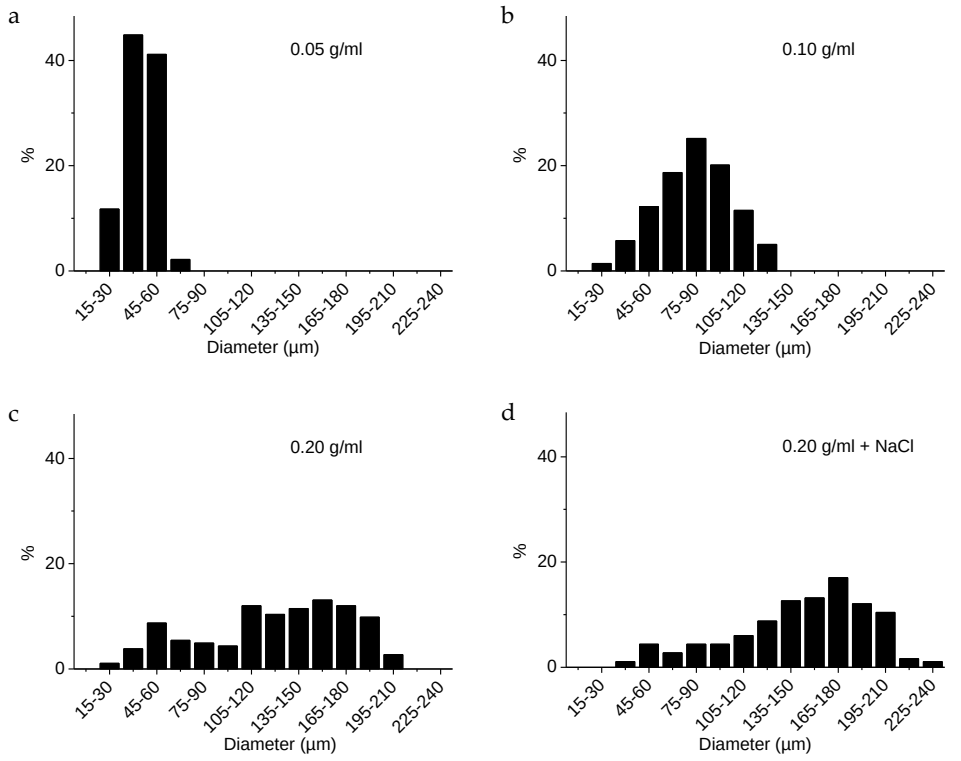

Figure 4: Particle size distributions of vitamin B12 loaded low molecular weight PCL microspheres obtained using 0.05 (a), 0.10 (b) and 0.20 (c) g/ml PCL solutions and a 0.20 g/ml PCL solution containing 0.10 g/ml NaCl in the external water phase (d).

The effect of polymer concentration on particle size is the result of an increase in viscosity of the dispersed phase, which leads to less efficient disruption of the w/o droplets by the acting shear forces [14]. The size distribution of the microparticles also increased with polymer concentration. This can be due to non-uniform reduction of the droplet size. A variable content of the aqueous protein phase within the polymer droplets can result in non-uniform shrinkage of the microparticles and a broader particle size distribution [15].

Release of vitamin B12

To assess potential drug delivery applications, an *in vitro* release study of vitamin B12 from the low molecular weight PCL microparticles with the highest LC and EE (sample 8) was conducted. The release study was performed using two different media: PBS and lipase buffer solution. The release profiles are presented in Figure 5. It can be seen that in PBS release does not exceed 10 % of the total amount of vitamin B12 present in the microspheres. This suggests almost complete encapsulation of the compound within the PCL microparticle and release into the medium of only the small amounts of vitamin B12 present on the surface of the particles. When the release experiment is conducted in lipase buffer, the PCL matrix will degrade much more rapidly than in PBS and accelerated release of vitamin B12 is observed.

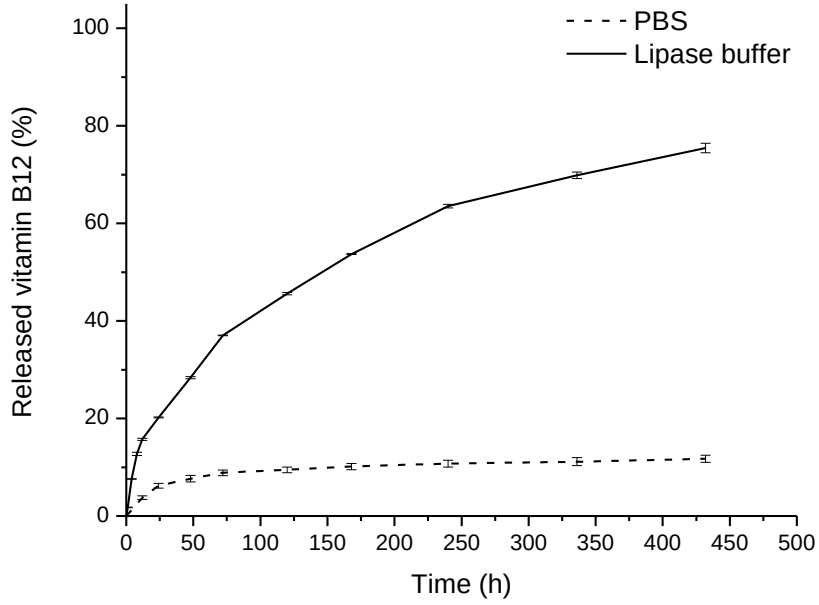

Figure 5: Cumulative release of vitamin B12 from low molecular weight PCL particles prepared from using 0.20 g/ml polymer solution and 0.10 g.ml NaCl in the external water phase. The release experiments were conducted in PBS (dashed line) and in lipase buffer (solid line).

Conclusions

Using a w/o/w double emulsion and solvent evaporation method, we successfully prepared low molecular weight PCL microparticles loaded with vitamin B12 as a hydrophilic model drug at high encapsulation efficiencies (61%). An *in vitro* release study showed that the vitamin B12 was only released upon degradation of the PCL matrix.

References

1. Jameela SR, Suma N, and Jayakrishnan A, Protein release from poly(epsilon-caprolactone) microspheres prepared by melt encapsulation and solvent evaporation techniques: A comparative study. Journal of Biomaterials Science-Polymer Edition, 1997. 8(6): p. 457-466.
2. Mundargi RC, Srirangarajan S, Agnihotri SA, Patil SA, Ravindra S, Setty SB, and Aminabhavi TM, Development and evaluation of novel biodegradable microspheres based on poly(D,L-lactide-co-glycolide) and poly(epsilon-caprolactone) for controlled delivery of doxycycline in the treatment of human periodontal pocket: In vitro and in vivo studies. Journal of Controlled Release, 2007. 119(1): p. 59-68.
3. Perez MH, Zinutti C, Lamprecht A, Ubrich N, Astier A, Hoffman M, Bodmeier R, and Maincent P, The preparation and evaluation of poly(epsilon-caprolactone) microparticles containing both a lipophilic and a hydrophilic drug. Journal of Controlled Release, 2000. 65(3): p. 429-438.
4. Sinha VR, Bansal K, Kaushik R, Kumria R, and Trehan A, Poly-ϵ-caprolactone microspheres and nanospheres: an overview. International Journal of Pharmaceutics, 2004. 278(1): p. 1-23.
5. van der Graaf S, Schroën CGPH, and Boom RM, Preparation of double emulsions by membrane emulsification—a review. Journal of Membrane Science, 2005. 251(1–2): p. 7-15.
6. Dash TK and Konkimalla VB, Poly-ϵ-caprolactone based formulations for drug delivery and tissue engineering: A review. Journal of Controlled Release, 2012. 158(1): p. 15-33.
7. Sun HF, Mei L, Song CX, Cui XM, and Wang PY, The in vivo degradation, absorption and excretion of PCL-based implant. Biomaterials, 2006. 27(9): p. 1735-1740.
8. Lam CXF, Hutmacher DW, Schantz JT, Woodruff MA, and Teoh SH, Evaluation of polycaprolactone scaffold degradation for 6 months in vitro

and in vivo. Journal of Biomedical Materials Research Part A, 2009. 90A(3): p. 906-919.
9. Hoglund A, Hakkarainen M, and Albertsson AC, Degradation profile of poly(epsilon-caprolactone) - the influence of macroscopic and macromolecular biomaterial design. Journal of Macromolecular Science Part a-Pure and Applied Chemistry, 2007. 44(7-9): p. 1041-1046.
10. Kulkarni A, Reiche J, Hartmann J, Kratz K, and Lendlein A, Selective enzymatic degradation of poly(ε-caprolactone) containing multiblock copolymers. European Journal of Pharmaceutics and Biopharmaceutics, 2008. 68(1): p. 46-56.
11. Bezemer JM, Radersma R, Grijpma DW, Dijkstra PJ, van Blitterswijk CA, and Feijen J, Microspheres for protein delivery prepared from amphiphilic multiblock copolymers 1. Influence of preparation techniques on particle characteristics and protein delivery. Journal of Controlled Release, 2000. 67(2-3): p. 233-248.
12. Bat E, Plantinga JA, Harmsen MC, van Luyn MJA, Zhang Z, Grijpma DW, and Feijen J, Trimethylene carbonate and epsilon-caprolactone based (co)polymer networks: mechanical properties and enzymatic degradation. Biomacromolecules, 2008. 9(11): p. 3208-3215.
13. Dinarvand R, Moghadam SH, Sheikhi A, and Atyabi F, Effect of surfactant HLB and different formulation variables on the properties of poly-D,L-lactide microspheres of naltrexone prepared by double emulsion technique. Journal of Microencapsulation, 2005. 22(2): p. 139-151.
14. Bezemer JM, Radersma R, Grijpma DW, Dijkstra PJ, van Blitterswijk CA, and Feijen J, Microspheres for protein delivery prepared from amphiphilic multiblock copolymers 2. Modulation of release rate. Journal of Controlled Release, 2000. 67(2-3): p. 249-260.
15. Crotts G and Park TG, Preparation of porous and nonporous biodegradable polymeric hollow microspheres. Journal of Controlled Release, 1995. 35(2-3): p. 91-105.

Appendix A - Seeding and culturing of C2C12 cells on mixed-macromer scaffolds produced by a combinatorial photo-crosslinking method

Erwin Zant, Ana Sofia de Carvalho Pimentel, Dirk Grijpma

Abstract

First cell culturing experiments were conducted to assess the adhesion and infiltration characteristics of C2C12 cells on mixed-macromer scaffolds. The scaffolds were obtained from the combinatorial mixing of PTMC-dMA 4k, PDLLA-dMA 4k and PEG-dMA 4k macromers and photo-crosslinking in ethylene carbonate. The pore structure is determined by the crystallization characteristics of the solvent. Under the conditions chosen, the pore structure was suboptimal for cell seeding. In general, adhesion of the cells to the surface of the scaffolds was the highest for scaffolds with the lowest water uptake. A scaffold prepared from a mixture of all three macromers, surprisingly showed both a very high water uptake of 125 wt.% and a high number of adhering cells comparable to that of the most hydrophobic samples.

Introduction

Recently, we showed the simultaneous preparation of large numbers of porous polymeric structures with a very wide range of physical properties. This was achieved through the preparation of combinatorial mixtures of poly(trimethylene) (PTMC-dMA), poly(D,L-lactide) (PDLLA-dMA) and polyethylene glycol (PEG-dMA) dimethacrylate functionalized macromers in solution in ethylene carbonate (EC), followed by photo-crosslinking and subsequent extraction of the crystallized solvent with water [1]. It was also shown that combinatorial mixing of macromers and the resulting photo-crosslinked mixed-macromer networks can have unexpected positive effects on the adhesion of C2C12 myoblasts [2] and human mesenchymal stem cells (hMSCs) [3].

In this work, we prepared 7 different mixed-macromer porous structures from PTMC-dMA, PDLLA-dMA and PEG-dMA macromers with molar masses of approximately 4 kg/mol and assessed their ability to allow C2C12 myoblast cell adhesion and proliferation.

Materials and methods

Mixed-macromer scaffold preparation

Porous scaffolds were prepared by making combinatorial mixtures of macromers PTMC-dMA 4k, PDLLA-dMA 4k and PEG-dMA 4k solutions in EC, cooling to room temperature, subsequently photo-crosslinking and extracting EC with water. The experimental details have previously been described in detail [1]. The total concentration of the macromers in the solutions was 25 wt.%. A total of 7 different mixed-macromer scaffolds measuring 6 x 10 mm were prepared, their detailed compositions are given in Table 1.

Cell culturing

The mixed-macromer scaffolds were disinfected with ethanol (75 vol.%) for 30 minutes and dried under atmospheric conditions overnight. To extract any remains of ethanol, the specimens were washed once with PBS and then kept in DMEM containing 1% PenStrep (Gibco®, USA)) for 48h at 37 °C. C2C12 myoblast cells were cultured and expanded in 175 cm^2 T-flasks. The cells were seeded onto the scaffolds at a concentration of 68,000 cells per scaffold. The medium was refreshed three times per week.

Table 1. Overview of prepared mixed-macromer scaffolds. The second to fourth columns indicate whether a macromer is present (grey) or absent (white) in the network from which the porous structure is prepared. Their water uptake, pore size and porosities in the dried state are presented as well [1]. Values are averages, with standard deviations in parentheses.

	Scaffold composition			**Water uptake[a]**	**Pore size[a]**	**Porosity[a]**
Scaffold number	**PTMC-dMA 4k**	**PDLLA-dMA 4k**	**PEG-dMA 4k**	wt.%	μm	vol.%
1				634 (21)	50-100	45 (0)
2				12 (2)	50-100	51 (6)
3				22 (2)	50-100	55 (3)
4				210 (8)	50-100	44 (2)
5				298 (11)	50-100	58 (3)
6				16 (1)	50-100	50 (4)
7				125 (15)	50-100	52 (1)

a data from [1]

On day 7, the scaffolds were washed in warm PBS (37 °C) to remove excess medium and non-adhering cells. The adhering cells were fixed using 4.7% paraformaldehyde (Sigma, USA) for 10 minutes. The samples were washed with PBS, and methylene blue solution (1%, Fluka, Germany) was added to stain the adhering cells. To visualize cell penetration into the scaffolds, cross-sections were observed under a stereoscopic lightmicroscope (Nikon SMZ-10A).

On day 1 and day 7, the scaffolds were washed in warm PBS (37 °C) to remove excess medium and non-adhering cells. The scaffolds were transferred to new 48 wells plates in order to avoid measurement of the metabolic activity of cells adhering to the bottom and walls of the culture wells. The scaffolds were incubated with MTS solution (CellTiter 96® AQueous One Solution Cell Proliferation Assay protocol, Promega, WI, USA) for 3 hours at 37 °C. The number of cells was determined by measurement of the absorbance of converted MTS at 490 nm using a Tecan, Infinite M200 Pro plate reader.

Results and discussion

To show the penetration of the cells into the scaffolds after seeding and culturing, cross-sections of the scaffolds were made and visualized by microscopy. Images of the cross-sections are shown in Figure 1. It is evident that while the cells have spread over the surface of the scaffolds, in most cases penetration of the cells is limited. Only in the images of scaffold number 3 the presence of cells in the middle of the scaffold can be observed.

In these first cell seeding experiments, the pore network characteristics of the mixed-macromer scaffolds were not optimized. The limited penetration of the cells might be affected by shrinkage of the scaffolds during production [1]. As can be seen in Table 1, the obtained porosities were much lower than the intended 75 vol.%. Also the pore size of 50 to 100 μm might have been too small,. Although cell penetration into the scaffolds was limited, cell adhesion and proliferation were very good in several cases.

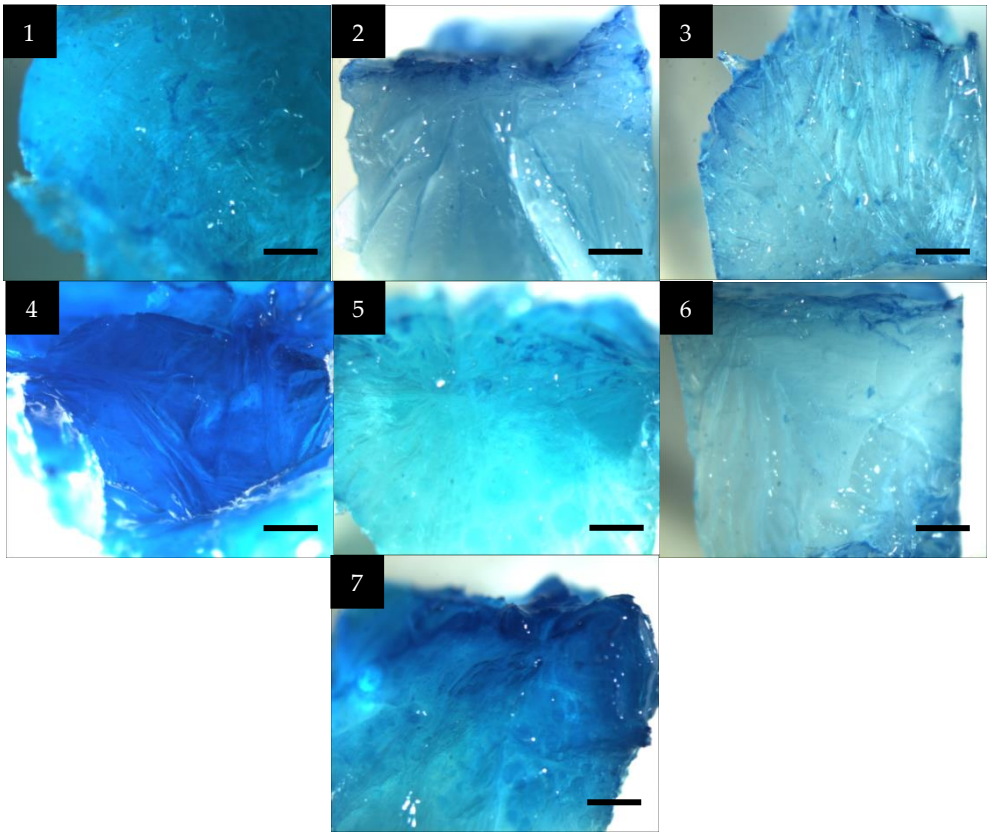

Figure 1: Light microscopy images of methylene blue stained C2C12 cells seeded and cultured for 7 days on mixed-macromer scaffolds. For each scaffold, a cross-section was made to show the penetration of cells into the scaffold. The numbers in the figure correspond to the scaffold numbers in Table 1. Scale bars indicate 1 mm.

For each scaffold the number of adhering cells was determined using an MTS assay. In Figure 2 the number of adhering cells at 1 and 7 days, as well as the water uptake (see Table 1) is presented. The most hydrophilic scaffold, scaffold 1, did not show any cells attaching at 1 day and very low numbers of cells at day 7. The more hydrophobic scaffolds numbers 2 and 3 were found to support the attachment and proliferation much better. By preparing scaffolds from mixtures of the three macromers, cell attachment and proliferation was much improved. Most remarkably, a scaffold prepared from all three components (scaffold 7) showed a water uptake of 125 wt.% while at the same time allowing large numbers of cells to

adhere. This scaffold allowed equal or better cell attachment and proliferation than the hydrophobic scaffolds.

In recent work we discussed that the extraordinary cell adhesion characteristics of these highly hydrated materials can be due to the microscopic phase separation phenomena occuring in these materials [3]. Detailed thermal analysis of the hydrated materials needs to be performed to give insight into these phenomena.

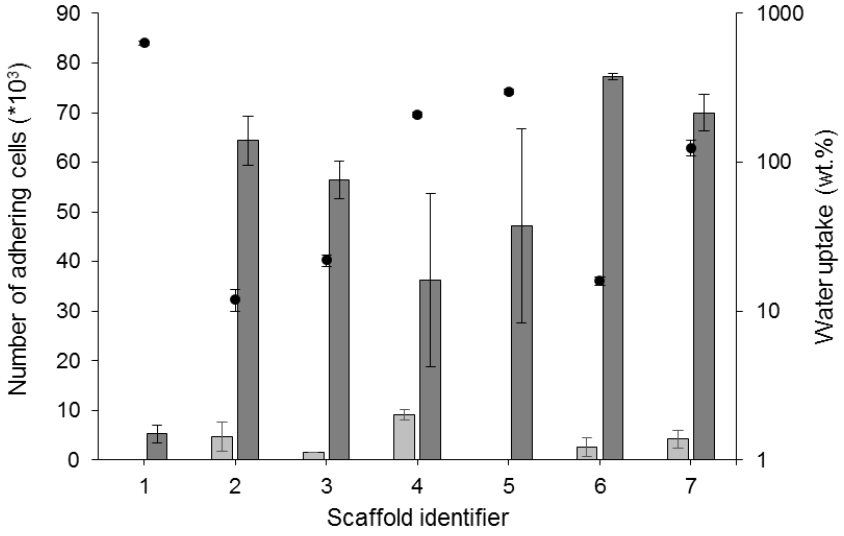

Figure 2: The total number of adhering cells per scaffold (6x10mm) as determined using an MTS assay. The number of the scaffold corresponds to the numbers in Table 1. The light grey columns indicate the cell numbers at day 1, the dark grey bars indicate the cell numbers at day 7. Water uptake values are indicated with (●).

Conclusions

We have described first C2C12 cell seeding and culturing experiments on mixed-macromer scaffolds prepared by making combinatorial mixtures of macromers solutions in EC, cooling the solvent to below its melting temperature, photo-crosslinking the macromers and subsequent extraction of the crystallized solvent with water. Methylene blue staining and light microscopic analysis of cross-sections of the cell seeded scaffolds revealed that most cells only occupied the

surface of the porous structures and that only a limited number of cells penetrated into the interior of the scaffolds. Nevertheless, very good cell attachment and proliferation was shown for most of scaffolds. Surprisingly, a scaffold prepared by photo-crosslinking a mixture of PTMC-dMA, PDLLA-dMA and PEG-dMA showed a high water uptake of 125 wt.%, while at the same time allowed abundant cell adhesion and proliferation.

References

1. Zant E, Blokzijl MM, and Grijpma DW, A combinatorial photocrosslinking method for the preparation of porous structures with widely differing properties. Macromolecular Rapid Communications, 2015. 36 (21): p. 1902-1909. Chapter 6 of this thesis.
2. Zant E, Bosman MJ, and Grijpma DW, Combinatorial synthesis of photo-crosslinked biodegradable networks. Journal of Applied Biomaterials & Functional Materials, 2012. 10(3): p. 197-202. Chapter 2 of this thesis.
3. Zant E and Grijpma DW, Synthetic biodegradable hydrogels with excellent mechanical properties and good cell adhesion characteristics obtained by the combinatorial synthesis of photo-crosslinked networks. Biomacromolecules, submitted. Chapter 5 of this thesis.

Appendix B - High throughput mechanical analysis of porous polymeric structures prepared using combinatorial chemistry

Erwin Zant, Maarten M. Blokzijl, Dirk W. Grijpma

Abstract submitted to European Society for Biomaterials, 2014, Liverpool, UK

Abstract

Here, a novel high throughput mechanical testing apparatus was used to analyze the compression modulus of the many hydrated porous polymeric structures described in Chapter 6. The compression moduli determined correlated well with those determined by conventional testing.

Introduction

In Chapter 6 it was shown that porous polymeric structures with a very wide range of physical properties can be prepared [1]. Recently it was also shown that a newly developed HT mechanical screening (HTMS) device can simultaneously assess the mechanical properties of multiple samples [2]. In this paper, hydrated mixed-macromer porous structures prepared from PTMC-dMA, PDLLA-dMA, and PEG-dMA 4k and 10k were mechanically evaluated by HTMS and compared to compression moduli determined in a conventional manner.

Materials and methods

Mixed-macromer scaffolds were prepared from PTMC-dMA, PDLLA-dMA and PEG-dMA 4 and 10k macromers as is described in Chapter 6 [1]. The samples were dried and swollen in distilled water for 48h. The compression modulus (E_c) of the specimens was determined at 8% compression in a conventional manner (sequential testing of single specimens) using a Zwick Z100 tensile tester. In a HT manner, the equilibrium compression modulus of the hydrated samples was simultaneously measured using a HTMS device [2].

Results

The compression moduli of the porous structures in the hydrated state were determined in a conventional manner by sequentially conducting single compression tests on network specimens and in HT by simultaneously carrying out compression tests on a large number of different specimens using the HTMS device. The results for the porous structures with E_c < 1MPa are presented in Figure 1. It is shown that the compressive modulus values determined in the different ways agree very well.

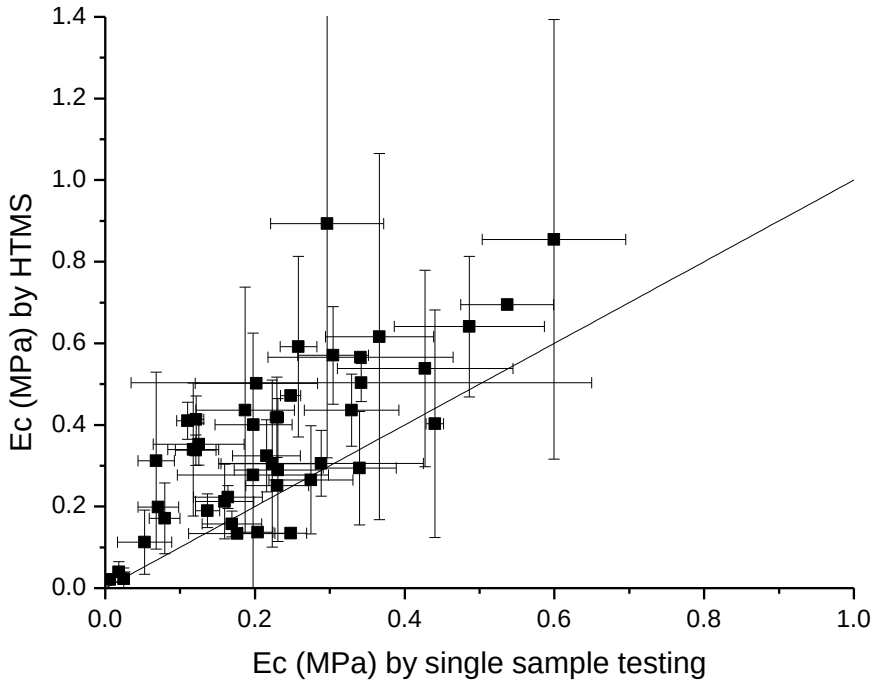

Figure 1: Comparison of the compression modulus (E_c) values of hydrated scaffolds determined by single specimen testing and by HTMS testing. The plotted line represents the relation x=y.

Conclusions

A combinatorial HT approach was used to produce numerous scaffolds with widely differing water uptake and mechanical characteristics. It was shown that a HT mechanical screening device could successfully be used to determine the compression modulus of these scaffolds in high throughput.

Acknowledgements

We would like to thank Bhavana Mohanraj and Robert Mauck (University of Pennsylvania, PA, USA) for the HTMS measurements. The funding by the Netherlands Institute for Regenerative Medicine (NIRM) is gratefully acknowledged.

References

1. Zant E, Blokzijl MM, and Grijpma DW, A combinatorial photocrosslinking method for the preparation of porous structures with widely differing properties. Macromolecular Rapid Communications, 2015. 36 (21): p. 1902-1909. Chapter 6 of this thesis
2. Mohanraj B, Hou C, Meloni GR, Cosgrove BD, Dodge GR, and Mauck RL, A high throughput mechanical screening device for cartilage tissue engineering. Journal of Biomechanics, 2014. 47(9): p. 2130-2136.

Appendix C - Tough biodegradable hydrogel scaffolds prepared by stereolithography.

Bas van Bochove, Erwin Zant, Dirk W. Grijpma

Abstract submitted to World Biomaterials Congress, 2016, Montreal, Canada

Introduction

Combinatorial chemistry allows for simultaneous preparation of a large number of different synthetic polymeric materials. Using mixtures of poly(trimethylene carbonate) (PTMC)-, poly(D,L-lactide) (PDLLA)-, poly(ethylene glycol) (PEG)- and poly(ε-caprolactone) (PCL)- dimethacrylate (dMA) functionalized macromers we prepared 255 different networks with widely differing properties at the same time. Of these networks, several hydrogels with high water-uptake, excellent mechanical properties and very good cell adhesion and proliferation were identified [1].

Stereolithography (SLA) is a rapid-prototyping technique that allows the manufacturing of designed 3D structures using photo-crosslinkable macromers.

Here we prepared mixed-macromer hydrogel network films with excellent mechanical properties as well as designed hydrogel scaffolds by SLA.

Materials and Methods

Linear TMC- or DLLA- oligomers (molar mass 4 or 10 kg/mol) were prepared by ring-opening polymerization of TMC- or DLLA monomers. dMA-functionalized TMC-, DLLA- and PEG macromers were prepared by functionalization of their respective oligomers with methacrylic anhydride.

For mechanical testing, equal amounts of PTMC-dMA 4k, PDLLA-dMA 4k, PEG-dMA 4k, PTMC-dMA 10k and PEG-dMA 10k were dissolved in propylene carbonate (PC) containing 1 wt% Irgacure 2959 photoinitiator. Specimens of 5mm in height and 5mm in diameter and network films were prepared by casting, followed by photo-crosslinking, extraction and drying. Prior to mechanical testing, the specimens were equilibrated in water for 48h.

For SLA, equal amounts of PTMC-dMA 4k, PDLLA-dMA 4k, PEG-dMA 4k, PTMC-dMA 10k and PEG-dMA 10k were dissolved in PC containing 5 wt% TPO-L photoinitiator and 0.15 wt% Orasol Orange dye. After building, the scaffolds were extracted and dried.

Results and Discussion

The water uptake of the photo-crosslinked networks was 197 ± 18 wt%. The water-swollen hydrogels showed excellent compressive properties and did not fail during the compression test, the compressive modulus was 0.7 MPa. Interestingly, the hydrogels obtained their original dimensions after testing when placed in water.

Furthermore, the hydrogels showed very good tensile properties: the tensile modulus was 1.27 MPa, the maximum tensile strength 0.72 MPa and the elongation at break 186%. These values are extraordinarily high for synthetic hydrogel networks with such a high water content.

We also prepared designed mixed-macromer hydrogel scaffolds by SLA. See Figure 1. The scaffolds were prepared with very high control over the pore-size, porosity and architecture.

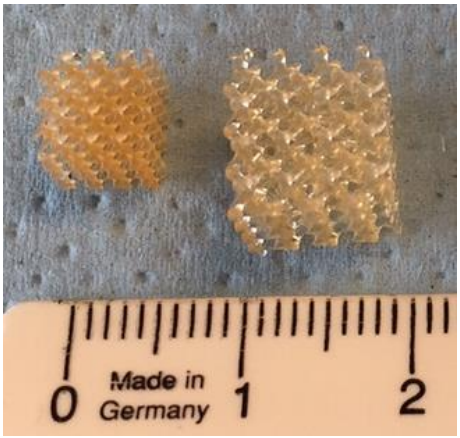

Figure 1: Porous hydrogel networks with designed pore structures prepared by stereolithography in the dry (left) and hydrated (right) state.

Conclusions

Tough, synthetic photo-crosslinked mixed-macromer hydrogels were prepared and their mechanical properties were evaluated. The structures showed high water uptake and had excellent mechanical properties. Porous hydrogel structures could readily be built by SLA, allowing the preparation of designed hydrogel scaffolds with extraordinary properties for biomedical applications and tissue engineering.

References

1. Zant E and Grijpma DW, Synthetic biodegradable hydrogels with excellent mechanical properties and good cell adhesion characteristics obtained by the combinatorial synthesis of photo-crosslinked networks. Biomacromolecules, submitted. Chapter 5 of this thesis

Summary

Regenerative medicine aims at replacing, engineering or regenerating human cells and tissues. There is a need for novel biomaterials to function as a temporal replacement of damaged tissues or organs. Synthetic biodegradable polymer networks can be such materials, since they offer benefits such as superior mechanical properties and the ease of tailoring physical properties when compared to natural materials. The selection of new polymeric biomaterial candidates can be accelerated by combinatorial chemistry, a very efficient strategy to obtain new materials with desired characteristics that could never be designed using conventional synthesis methods.

This thesis presents the results of research on the photo-crosslinking of combinatorial mixtures of di-methacrylate functionalized PTMC, PDLLA, PCL and PEG oligomers.

In **Chapter 2** an introduction to the development of polymer biomaterials by combinatorial methods is presented. This development is significantly facilitated by the use of discrete microarrays and continuous gradient libraries. Moreover, photo-crosslinking of combinatorial functional-monomer mixtures was found to be very efficient in the parallel synthesis of numerous different materials. An introduction on the physical properties which determine the surface-interactions of materials with cells and the high throughput analysis thereof is given.

In **Chapter 3** a first study on photo-crosslinked mixed-macromer networks is presented. The networks were synthesized by dissolving and mixing macromers in dichloromethane (DCM), photo-crosslinking then proceeded in polypropylene 96 wells plates yielding 255 mixed-macromer networks. A cell seeding study using C2C12 myoblasts cells revealed some hydrogels with the ability to allow cell adhesion while also showing high water uptakes. In this first experiment material characteristics of the mixed-macromer networks such as phase separation and mechanical properties were not qualified.

The preparation of mixed-macromer networks using DCM as the diluent was found to be difficult since DCM evaporates during the mixing process and photo-

crosslinking. Better mixing and high quality networks were obtained using a solvent with a high boiling point, propylene carbonate (PC).

New mixed-macromer networks were produced using PC, the properties of these materials are presented in **Chapter 4**. Crosslinking PTMC-dMA 10k in PC yielded networks with incredibly high toughness in both tensile testing and tear propagation experiments. Crosslinking mixtures of PTMC-dMA 10k, PDLLA-dMA 10k, PCL-dMA 4k and PEG-dMA 10k in PC yielded very high quality mixed-macromer networks with microphase-separated structures. The toughest mixed-macromer networks had a high maximum tensile strength of 8 MPa, a maximum elongation at break of 680% and a very high tearing energy of 47 kJ/m^2 after extraction and drying. Mixed-macromer networks that contained a PEG-dMA component could take up 74 to 303 wt.% water. It was found that in the hydrated state, most of these mixed-macromer hydrogel networks were also extremely tough. The toughest mixed-macromer hydrogel was prepared from PTMC-dMA, PCL-dMA and PEG-dMA macromers and had a maximum tensile strength of 0.94 MPa, a maximum elongation at break of 200% and a very high tearing energy of 0.81 kJ/m^2. These values are significantly higher than for any other synthetic hydrogel and comparable to the tearing energy of articular cartilage (1 kJ/m^2).

In **Chapter 5** it was assessed whether synthetic hydrogels with good cell adhesive properties prepared using the same synthesis principles could be found. 255 mixed-macromer networks crosslinked in PC were screened for their ability to allow the adhesion of human mesenchymal stem cells (hMSCs). Of these networks, several hydrogels could be identified that were able to take up large amounts of water, while at the same time allowed the adhesion and proliferation of cells. By synthesizing these hydrogel networks anew and analyzing the cell adhesion and proliferation behavior of human mesenchymal stem cells to these synthetic hydrogels in more detail, it was confirmed that mixed-macromer hydrogel networks prepared from equal amounts of PTMC-dMA 4k, PDLLA-dMA 4k, PCL-dMA 4k, PEG-dMA 4k and PEG-dMA 10k and hydrogel networks prepared from PTMC-dMA 4k, PDLLA-dMA 4k, PEG-dMA 4k, PTMC-dMA 10k and PEG-dMA 10k were highly hydrophilic (water uptake was 181 ± 2 and 197 ± 18 wt.% water respectively) and allowed very good cell adhesion and proliferation. Furthermore,

these networks were extremely resilient in the hydrated state, with tearing energies of 0.64 ± 0.34 and 0.27 ± 0.04 kJ/m^2 respectively.

A straightforward method to produce three dimensional porous structures with highly diverse physical properties is presented in **Chapter 6**. Ethylene carbonate (EC) is a benign, water-soluble compound with a low melting point of approximately 35°C. The preparation of combinatorial mixtures of PTMC, PDLLA and PEG macromers in solution in EC, followed by photo-crosslinking and subsequent extraction of the solvent with water, allowed us to simultaneously prepare large numbers of porous polymeric structures with a very wide range of physical properties. In this manner, we were able to prepare 63 different porous polymeric structures with a very wide range of physical properties at the same time. In the hydrated state the compressive moduli of the prepared structures ranged from 0.01 to 60 MPa, as water uptake ranged between 3 and 1500 wt.%. As PCL was found to be insoluble in EC, PCL microspheres could be incorporated into the porous structures. In this manner, tissue engineering scaffolds that include a drug- or growth factor delivery system can be prepared.

In **Chapter 7** low molecular weight PCL microparticles loaded with the hydrophilic model drug vitamin B12 were prepared by a double emulsion evaporation technique. Several parameters, such as the addition of a lipophilic emulsifier, sodium chloride and the increase in polymer concentration, were varied to prepare microparticles with optimized loading and encapsulation efficiencies. The addition of sodium chloride in the external water phase, as well as the increase in polymer concentration, were found to have the most beneficial effect on the encapsulation efficiency of vitamin B12 which increased from 2 to 61 %.

In **Appendix A** culturing of C2C12 cells was done on porous polymeric structures obtained by the method presented in **Chapter 6**. The scaffolds were obtained from the combinatorial mixing of PTMC-dMA 4k, PDLLA-dMA 4k and PEG-dMA 4k. A total number of 7 structures was assessed for their ability allow cell adhesion over a period of 7 days. In general, the samples with the lowest water uptake allowed the highest numbers of cells to adhere. However, a sample prepared from all three macromers, surprisingly showed a very high water uptake of 125 wt.% and a high

number of adhering cells which was comparable to that of the most hydrophobic samples.

In **Appendix B** a novel high throughput mechanical testing apparatus was used to analyze the compression modulus of the many hydrated porous polymeric structures described in **Chapter 6**. The compression moduli determined correlated well with those determined by conventional testing.

In **Appendix C** porous hydrogel structures were built by stereolithography. The used resin was prepared from PTMC-dMA 4k, PDLLA-dMA 4k, PEG-dMA 4k, PTMC-dMA 10k and PEG-dMA 10k, a formulation developed in **Chapter 5**. There it was found to yield a tough hydrogel which allowed the adhesion and proliferation of stem cells and it showed a high value of water uptake (197 wt.%).

This work presents some very promising properties of synthetic biodegradable polymer networks. By photo-crosslinking mixtures of different macromers, a wide range of mixed-macromer networks with highly diverging physical properties could be synthesized simultaneously. Crosslinking in solution leads to materials with highly advantageous properties, such as extremely tough micro-phase separated rubbers and hydrogels. Most interesting, hydrogels that showed both high water uptake and allowed the adhesion of stem cells were found. It is anticipated that in these materials phase separation phenomena play a crucial role in this ability, this needs to be investigated in more detail. The use of PC as a solvent allowed the synthesis of high quality mixed-macromer network films, while the use of crystallizable EC as a solvent offered the possibility of fabricating mixed-macromer porous polymeric structures. By dispersing insoluble PCL microparticles into the macromer solutions in EC, a very practical method to prepare microsphere-loaded scaffolds with drug delivery potential was developed.

Samenvatting

Het doel van regeneratieve geneeskunde is het vervangen, ontwerpen of herstellen van menselijke cellen en weefsels. Hiervoor is er een vraag naar nieuwe biomaterialen die kunnen dienen als tijdelijke vervanging voor beschadigde weefsels of organen. Synthetische, biologisch afbreekbare polymere netwerken zouden hiervoor geschikt kunnen zijn, omdat deze zeer hoogwaardige mechanische eigenschappen hebben. Daarnaast zijn ze, in tegenstelling tot natuurlijke materialen, eenvoudig te modificeren zodat zij de gewenste fysische eigenschappen hebben. Het vinden van zulke nieuwe polymere biomaterialen kan versneld worden wanneer gebruik wordt gemaakt van zogenaamde *combinatorische* chemie; een (in tegenstelling tot conventionele synthese routes) zeer efficiënte strategie om nieuwe materialen met optimale eigenschappen te vinden.

In dit proefschrift staan de onderzoeksresultaten van gefoto-crosslinkte combinatorische mengsels van di-methacrylaat gefunctionaliseerde PTMC, PDLLA, PCL en PEG oligomeren.

De ontwikkeling van polymere biomaterialen door middel van combinatorische chemie wordt geïntroduceerd in **Hoofdstuk 2**. Een ontwikkeling die veelvuldig wordt gefaciliteerd door het gebruik van discrete microarrays en continue gradiënt materiaal bibliotheken. Foto-crosslinking van combinatorische functionele monomeer mengsels is een zeer efficiënte manier om veel verschillende materialen parallel te synthetiseren. Daarnaast is er in dit hoofdstuk ingegaan op de fysische eigenschappen die de materiaal grensvlak interacties met cellen bepalen en technieken die deze eigenschappen kunnen meten in high-throughput.

Een eerste studie met gefoto-crosslinkte gemixte-macromere netwerken is gepresenteerd in **Hoofdstuk 3**. In dit onderzoek zijn 255 gemixte-macromere netwerken gesynthetiseerd door macromeren te mengen in dichloormethaan (DCM) en te foto-crosslinken in 96 wells platen van polypropyleen. In een cel studie waarbij gebruik werd gemaakt van C2C12 myoblasten zijn sommige hydrogelen aan het licht gekomen die zowel een hoge cel adhesie als water opname lieten zien. In dit eerste experiment zijn karakteristieken zoals fase scheiding en mechanische eigenschappen van de gemixte-macromere netwerken niet gekwalificeerd.

Doordat DCM snel verdampt tijdens het meng- en het crosslink-proces bleek het maken van gemixte-macromere netwerken in dit oplosmiddel erg lastig. Betere mengsels en netwerken van hoge kwaliteit werden verkregen door gebruik te maken van een oplosmiddel met een hoog kookpunt: propyleen carbonaat (PC).

Nieuwe gemixte-macromere netwerken zijn gemaakt in PC, de eigenschappen van deze materialen zijn beschreven in **Hoofdstuk 4**. Het crosslinken van PTMC-dMA 10k in PC bracht netwerken op met onwaarschijnlijk hoge taaiheid in zowel trek- als scheurpropagatie proeven. Het crosslinken van mengsels van PTMC-dMA 10k, PDLLA-dMA 10k, PCL-dMA 4k en PEG-dMA 10k in PC bracht netwerken op van een zeer hoge kwaliteit met microscopisch fase-gescheiden structuren. Het taaiste gemixte-macromere netwerk had een hoge treksterkte van 8 MPa, een maximale rek bij breuk van 680% en een zeer hoge scheurpropagatie energie van 47 kJ/m^2 na extractie en drogen. Gemixte-macromere netwerken die een PEG-dMA component hadden konden 74 tot 303 wt.% water opnemen. Daarnaast bleken veel van deze in water gezwollen gemixte-macromere hydrogelen erg taai. De taaiste gemixte-macromere hydrogel was samengesteld uit PTMC-dMA, PCL-dMA en PEG-dMA en had een maximale treksterkte van 0.94 MPa, een rek bij breuk van 200% en een zeer hoge scheur propagatie energie van 0.81 kJ/m^2. Deze waarden zijn significant hoger dan die voor andere synthetische hydrogelen en zijn vergelijkbaar met articulair kraakbeen (1 kJ/m^2).

In **Hoofdstuk 5** staat de vraag centraal of synthetische hydrogelen gemaakt volgens hetzelfde principe met goede cel adhesieve eigenschappen konden worden verkregen. Voor dit onderzoek zijn 255 in PC gesynthetiseerde gemixte-macromere netwerken gescreend op hun mogelijkheid om human mesenchymal stem cells (hMSCs) te kunnen hechten. Van deze netwerken, lieten sommige hydrogelen zowel een hoge wateropname zien alsmede een hoge celhechting en proliferatie. Deze hydrogelen zijn volledig opnieuw gesynthetiseerd en in detail geanalyseerd ten aanzien van hMSC adhesie en proliferatie. Hieruit bleek dat gemixte-macromere hydrogelen samengesteld uit gelijke hoeveelheden PTMC-dMA 4k, PDLLA-dMA 4k, PCL-dMA 4k, PEG-dMA 4k en PEG-dMA 10k en hydrogelen samengesteld uit PTMC-dMA 4k, PDLLA-dMA 4k, PEG-dMA 4k, PTMC-dMA 10k en PEG-dMA 10k sterk hydrofiel zijn (water opname is respectievelijk 181 ± 2 en 197 ± 18 wt.% water) en ze lieten een goede cell adhesie en proliferatie zien.

Daarnaast waren de hydrogelen zeer rekbaar in de gehydrateerde toestand, met scheurpropagatie-energieën van respectievelijk 0.64 ± 0.34 en 0.27 ± 0.04 kJ/m^2.

Een zeer eenvoudige manier om driedimensionale poreuze structuren met uiteenlopende fysische eigenschappen te produceren is gepresenteerd in **Hoofdstuk 6**. Ethyleen carbonaat (EC) is een vriendelijke, water oplosbare stof met een laag smeltpunt van ongeveer 35°C. Uit de experimenten blijkt dat door combinatorische mengsels van PTMC, PDLLA en PEG macromeren in een EC oplossing te maken, deze te foto-crosslinken en vervolgens het oplosmiddel met water uit te wassen, simultaan grote hoeveelheden poreuze structuren kunnen worden geprepareerd. Via deze methode hebben we tegelijkertijd 63 verschillende poreuze polymere structuren met uiteenlopende fysische eigenschappen gemaakt. In gehydrateerde toestand varieerde de compressie modulus van 0.01 MPa tot 60 MPa, wanneer de water opname varieerde van 3 tot 1500 wt.%. Omdat PCL onoplosbaar bleek te zijn in EC, konden PCL microdeeltjes in de poreuze structuren worden geïntegreerd. Op deze manier kunnen tissue engineering drager structuren met een medicijn- of groei factor afgifte systeem worden geprepareerd.

Hoofdstuk 7 gaat in op het prepareren van microdeeltjes gemaakt van laag moleculair gewicht PCL. Deze zijn beladen met het hydrofiele model medicijn vitamine B12, waarbij gebruik is gemaakt van een dubbele emulsie verdampings-techniek. Een aantal parameters, waaronder het toevoegen van een lipofiele emulgator, natrium chloride en het verhogen van de polymeer concentratie, zijn veranderd om microdeeltjes te maken met een zo hoog mogelijke ladings- en inkapselings-efficiëntie. Het toevoegen van natrium chloride in de externe water fase, alsmede het verhogen van de polymeer concentratie bleken het beste effect op te leveren en de inkapselings-efficiëntie van vitamine B12 werd verhoogd van 2 naar 61%.

In **Appendix A** is een studie beschreven waar C2C12 cellen gezaaid zijn op poreuze structuren. De structuren zijn gefabriceerd op de manier gepresenteerd in **Hoofdstuk 6**. De structuren zijn verkregen uit het combinatorisch mengen van PTMC-dMA 4k, PDLLA-dMA 4k en PEG-dMA 4k. In totaal zijn er 7 structuren geanalyseerd voor hun mogelijkheid cellen te hechten over een periode van 7 dagen. Over het algemeen lieten de minst hydrofiele structuren de hoogste cel

adhesie zien. Hoewel een sample samengesteld uit alle componenten een hoge water opname van 125 wt.% en een verrassend hoge cel adhesie liet zien die vergelijkbaar was met die van de meest hydrofobe samples.

In **Appendix B** is een studie beschreven waarbij een nieuw high throughput mechanisch test apparaat gebruikt om de compressie moduli van een groot aantal structuren uit **Hoofdstuk 6** te meten. De gemeten compressie moduli correleren goed met de moduli die zijn gemeten op een conventionele manier.

In **Appendix C** is beschreven hoe poreuze structuren op een stereolithograaf zijn gemaakt. De gebruikte hars was samengesteld uit PTMC-dMA 4k, PDLLA-dMA 4k, PEG-dMA 4k, PTMC-dMA 10k en PEG-dMA 10k, een formulering die is ontwikkeld in **Hoofdstuk 5**. In dit onderzoek werd gevonden dat een taaie hydrogel kan worden verkregen met een hoge water opname (197 wt.%) alsmede een goede cel adhesie en proliferatie.

Dit werk laat een aantal veelbelovende eigenschappen van synthetische bioafbreekbare netwerken zien. Door het foto-crosslinken van diverse macromeren kan een groot bereik aan gemixte-macromere netwerken met uiteenlopende fysische eigenschappen simultaan gesynthetiseerd worden. Het crosslinken in oplossing geeft materialen met erg gunstige eigenschappen, zoals extreem taaie micro-fase gescheiden rubbers en hydrogelen. Het meest interessant zijn hydrogelen die een hoge wateropname hebben en het hechten van stamcellen toelaten. Verwacht wordt dat fase scheiding in deze materialen een cruciale rol speelt, maar dit zou in meer detail moeten worden onderzocht. Het gebruik van PC als een oplosmiddel maakte het mogelijk om gemixte-macromere netwerken van hoge kwaliteit te fabriceren, terwijl met het kristalliseerbare EC als oplosmiddel gemixte-macromere poreuze structuren verkregen konden worden. Het dispergeren van onoplosbare PCL microdeeltjes in deze macromeer oplossingen in EC bleek een praktische manier om poreuze structuren met microdeeltjes te fabriceren. Deze structuren hebben een grote potentie in de medicijn afgifte.

Dankwoord

De jaren tijdens een promotie lijken voorbij te vliegen en je beseft je bij het schrijven van een proefschrift pas dat er ontzettend veel gedaan is. Het voelt dan ook heerlijk om alles tot een geheel te zien. Eén van de belangrijkste hoofdstukken van een proefschrift is zonder meer het dankwoord, want van een groot aantal mensen heb ik veel steun gehad en zonder hen was het nooit gelukt.

Allereerst wil ik mijn promotor en direct begeleider Dirk Grijpma bedanken. Dirk, jij hebt mij ontzettend veel geholpen bij het samenstellen van het onderzoek en het begrijpelijk maken van de resultaten. Ondanks dat je het de afgelopen jaren erg druk hebt gehad met je eigen oratie, het fuseren met andere groepen en congresbezoeken over de hele wereld, was er altijd de mogelijkheid je om raad te vragen. Het was voor mij soms moeilijk door de combinatorische bomen het spreekwoordelijke lineaire bos te zien, maar jij gaf er op z'n tijd weer een zinnige draai aan. Het was dan ook niet zelden dat ik met een zwaar hoofd je kantoor binnenstapte en met een opgewekt humeur mij weer naar het lab spoedde om te starten aan frisse ideeën. Je ideeën werden dikwijls ondersteund met resultaten uit papers van vroeger. Auteur, datum en pagina wist je uit het hoofd, maar waar op de computer stond dat ook alweer verstopt? Ook vond ik het erg leuk dat er af en toe eens zo'n vergeeld proefschrift uit 1990 bij werd gepakt voor een korte cursus Grunniger Polymeer Chemie.

Een grote steun heb ik gehad van de vakgroep BST. Het was een mooie tijd. Naast nuttige discussies heb ik heb veel plezier met jullie beleefd bij pubquizzen en op congres locaties ver van huis. Aga, it was great having you back in the group as a PhD student. You have shown that a work-week has 7 instead of 5 days. Shahriar, thank you for sharing your tremendous knowledge on everything and telling me great stories about your home country Iran. Marlon, ik had de eer jou als paranimf te mogen bijstaan. Ik heb erg veel plezier beleefd aan het maken van een biografisch filmpje voor op je promotiefeest. Sébastien, monsieur, you brought a lot of good spirit in the group. Of course, born in France always brings its language issues, but after some time we spoke about the same thing while having a conversation. I wish you all the best for the future with Hailey and Marilyne. Gert-Jan, je bent hier als master student begonnen en later gestart als promovendus in Davos Zwitserland. Bedankt voor je mooie verhalen aan de koffie en de schitterende Engelse grappen. Suvi, you took care of all the social skills at BST.

Have fun in the future and I wish you all the best with Leo and Jonas. Ook bedank ik Mark, Denys, Natalia, Jos P, Nick, Aysun, Iris, Ilaria, Kasia, Xiaolin, Karin, Tony, Gijs, Sandra, Vincent, Sanne, Karin, Niels, Rene en alle studenten die in ZH247 hebben gehokt voor de goede sfeer op het lab, aan de koffietafel en daarbuiten. Ondanks dat je officieel nooit in de BST groep zat, was je onlosmakelijk verbonden met ons: Jos W, voor lange tijd onze quizmaster, triatleet en regelneef van gezellige avondjes in de vestingbar en pubquizzes in de stad. Deze memorabele avondjes duurden al gauw tot in de kleine uurtjes en de ochtenden erna waren erg vroeg, maar het was het zeker waard om zo nu en dan eens leven in de (bier)brouwerij te houden. Een korte stedentrip in Hongkong met Piet en Janny mag natuurlijk niet ontbreken in dit lijstje.

Karin, je hebt me door de papierwinkel heen geloodst. Ook was je nooit te beroerd voor een gezellige babbel. Hetty, het grootste deel van mijn computerperikelen werden door jou opgelost, hoewel je zelf ook af en toe met de handen in het haar zat. Marc, jij moest je af en toe opstellen als de lab-uitsmijter, maar hierdoor werd ons werk een stuk veiliger. Anita, bedankt voor de GPC resultaten en de mooie bruiloft. Ik hoop dat je het naar je zin gaat hebben op je nieuwe werkplek. Lydia, je voelde je na de fusie met de membranen-groep helemaal thuis. Bedankt voor de hulp op het biologisch lab en je altijd opgewekte humeur. Dimitrios en André, bedankt voor jullie zeer nuttige discussies bij presentaties en overleggen.

Ook wil ik een aantal studenten bedanken die mij hebben geholpen met het onderzoek. Mijn eerste bachelor student, Evelien. Mijn eerste master student, Mirjam. Mijn eerste mannelijke bachelor student, Robbert. Mijn eerste Erasmus student, Ana. Mijn eerste mannelijke master student, Maarten en mijn eerste Poolse student Kamila. Het was erg leuk om jullie te begeleiden en ik ben blij met alle resultaten die op tafel kwamen. Succes met het invullen van jullie toekomstplannen, in het onderzoek of daarbuiten. For Ana and Kamila: it was great to work with you and I am very happy with all the results. Good luck in the future!

Tijdens een promotie is een kantoor met een goede sfeer, muziek en koffie belangrijk. Ik mocht me gelukkig prijzen met dit alles in ZH248. Bas, Frits en Mike: jullie hebben invulling gegeven aan een waardig mannen-kantoor. Het installeren van een 2.1-muziekinstallatie, lekkere koffie en een schaarsgeklede-vrouwen-kalender hebben daaraan zeker bijgedragen.

Het kantoor brengt me ook meteen naar de paranimfen, Bas en Frits. Bas, we hebben al een aantal kilometers op de racefiets gesleten en die zullen er na mijn promotie hopelijk weer bijkomen. Onze gedeelde passie voor whisky mag dan soms wat ver gaan, maar langzaamaan beginnen ook anderen het te snappen. Frits, je Tukkerse nuchterheid bracht je door de winter en mij door de cel-experimenten. Ook jij bent nu aan het werk aan het afronden, daarmee heel veel succes en alle geluk gewenst samen met Taiga en je volgende baan.

Naast de mensen op de UT heb ik ook veel gehad aan de ontspannen momenten met vrienden daar buiten. De vrienden van Club 9-2 hebben een belangrijke rol gespeeld. Josse, Kees, Paul, Robin, Groen en Leroy, een regelmatige borrel voelt alsof we nooit anders gedaan hebben. Een jaarlijkse burgervakantie met de vrouwtjes mag natuurlijk niet ontbreken. Ook bedank ik mijn studievrienden, Janine, Jetty, Maarten, Theun, Bart en Roeland. Jullie wonen inmiddels niet allemaal meer binnen fietsbereik, maar wij vinden altijd wel een gelegenheid voor een bakkie koffie of een klein biertje. Verder bedank ik nog Le Metropolitain. Hoewel ik met jullie niet de volle 15 jaar heb meegekregen, kan ik toch spreken van een dubbel lustrum. De Wie-Kentjes zijn memorabel en ik hoop de er nog vele gaan komen.

Zeer gelukkig ben ik met mijn schoonfamilie. Hans, Emmy, Renske, Marjolein en Thomas, bedankt voor jullie interesse en leuke momenten in Zutphen, Amsterdam en Utrecht.

Een grote steun heb ik gekregen van mijn ouders. Pap en mam, bedankt voor jullie vertrouwen en luisterend oor. Eext ligt niet om de hoek, maar het was heerlijk om er af en toe stoom af te blazen en de batterijen weer op te laden. Mijn huidige baan ligt zowaar nóg verder weg en sinds maart mag ik mij twee avonden per week gelukkig prijzen met een zorgzame moeder, bedankt mam.

Kirsten, Peter, Birgit, Han, Maysie, Davis en Laurinda, ook aan jullie heb ik veel steun gehad. De reisafstand tussen Assen en Enschede heeft onze familiebezoekjes soms in de weg gestaan, maar jullie zijn straks van harte welkom in Zwolle.

Joppie, zoals jij al hebt gezegd in je proefschrift; wat hebben we ons op de hals gehaald? Onze beide promoties, een koophuis, een rondrennende peuter en twee banen op 150 km afstand van elkaar geeft ons voorlopig nog geen rust. Laat het een goede motivatie zijn om er over een paar weken eens een fijne vakantie

achteraan te plakken. Jij hebt mij erg veel geholpen en gaf mij de duwtjes in de goede richting. Dankje moppie, ik hou van je!

Ik mag dit boek afsluiten met onze lieve dochter. Esmé, je geeft me elke dag weer nieuwe energie en laat mij zien dat het super fijn is om papa te zijn. Ik ben gelukkig met ons gezinnetje en verheug me op de toekomst!

Erwin